Addis Ababa University

Addis Ababa Institute of Technology

School of Mechanical and Industrial Engineering

Analysis and Optimization of Process Parameters for Friction Stir Welding of Dissimilar Aluminum 6061 and Commercial pure Titanium Metal

---

A Thesis Submitted to the Graduate School of Addis Ababa University in Partial Fulfillment of the Requirement for the Degree of Masters of Science in Mechanical Engineering (Manufacturing Engineering)

By: Dawit Gebeyehu GSE/4697/13

Advisor: Henok Zewdu (PhD Candidate)

Addis Ababa, Ethiopia
June, 2024

Declaration

I hereby declare that the work, which is being presented in this thesis entitled "**Analysis and Optimization of Process Parameters for Friction Stir Welding of Dissimilar Aluminum 6061 and Commercial pure Titanium Metal''** submitted to the School of Mechanical and Industrial Engineering is an authentic record of my original work. The proposal has not been formed the basis for the award of any degree or diploma or any other similar titles. All applicable resources of information used in this thesis have been accordingly, acknowledged.

Dawit Gebeyehu _____ _____

Student Name Signature Date

This is to endorse that the above declaration made by the candidate is correct to the best of my knowledge and certainty. This thesis has been submitted for examination with my approval.

Mr. Henok Zewdu (PhD Candidate) _____ _____

Advisor Signature Date

Addis Ababa University

Addis Ababa Institute of Technology

School of Mechanical and Industrial Engineering

Analysis and Optimization of Process Parameters for Friction Stir Welding of Dissimilar Aluminum 6061 and Commercial pure Titanium Metal

By: Dawit Gebeyehu

Submitted by the requirements for the degree

Master of Science (M.Sc.)

Approved by: Board of Examiners

Henok Zewdu (PhD Candidate)	_____	_____
Advisor	Signature	Date
Dr. Desalegn Wogaso	_____	_____
Internal examiner	Signature	Date
Dr. Solomon Bayu	_____	_____
External examiner	Signature	Date
Dr. Araya Abera	_____	_____
Dean of the School	Signature	Date
Dr.Sosina Mengistu	_____	_____
Associate Director for PG program	Signature	Date

ABSTRACT

Friction stir welding (FSW) is a solid-state weld process were invented in 1991 that broadly used by industries and preferred rather than other weld process due to its capability to weld similar and dissimilar materials under high quality. FSW offers a number of advantages over other weld methods, including being automatic, suitable for most materials, able to be performed in any position, having minimal distortion, and not requiring filler or shielding gas., can be employed under water, and environmentally friendly.

In this research, a joint between 6061 aluminium alloy and commercially pure titanium Gr-1 was butt welded by using friction stir welding. at a speed of rotation (1100, 1400, 1600) rpm , a transfer (welding) speed at (50, 60, 80) mm×min-1, a tool pin profile (cylindrical, square, conical), and a dwell time of (5, 10, 15) sec. welded material microstructure and mechanical properties were assessed using the tensile test, the hardness test, and optical microscopy (OM), respectively. Tensile testing, hardness testing, and optical microscopy (OM) were used, respectively; to assess the mechanical characteristics and interfacial microstructure. The numbers of welding experiments were determined using both of the Taguchi and Grey relation analysis approaches. The strength of friction welded dissimilar joints and effect of parameters were analysed using ANOVA (analysis of variance) on Minitab 20 software.

After the materials are welded successfully, their tensile strength and hardness were evaluated at room temperature. According to the results, the cylindrical pin profile, 1100-rpm rotational speed, 80 mm/min transverse speed and 15 sec dwell time are the optimal conditions for combining these different joints. In the stir zone, strengthening precipitates were distributed finely and uniformly.

Keywords: Friction Stir Welding (FSW), Dissimilar Materials, Aluminium, Titanium, Butts Welding, Taguchi Method, Orthogonal Array Grey Analysis.

Table of Contents

List of Abbreviations

Al	Aluminum
B	Boron
Ti	Titanium
CMM	Convectional Milling Machine
CNC	Computer Numerical Control
DOE	Design of Experiment
FSWP	Friction Stir Welding Process
GMAW	Gas Metal Arc Welding
GRA	Grey Relation Analysis
HRC	Rockwell Hardness
HSS	High Speed Steel
OA	Orthogonal Array
PCA	Principal Component Analysis
SEM	Scanning Electron Microscope
HV	Vickers Hardness
BCC	Body-Centered Cubic
C	Carbon
Co	Cobalt
CP	Commercially Pure
Cr	Chromium
Cu	Copper
PCBN	Polycrystalline Cubic Boron Nitride
Fe	Iron
FEA	Finite-Element Analysis
FSW	Friction Stir Welding
Mo	Molybdenum
Cp-W	Commercial Pure Tungsten

BM	Base Metal
UTM	Universal Testing Machine
WS	Welding Speed
HSS	High-Strength Steel
HAZ	Heat Affected Zone
α	Alpha
TMAZ	Thermo Mechanically Affected Zone
WN	Welding Nugget
TWI	The Welding Institute

List of figures

List of Table

CHAPTER ONE

1. INTRODUCTION

1.1.Background

Welding is a manufacturing or sculptural technique that goes back to the time of Bronze Age. Evidence of pressure welding is found in gold circular boxes that were made about 2000 years ago. Three millennia year ago, people living in the Eastern Mediterranean region particularly the Egyptians learned how to fuse iron fragments. In addition to the numerous weapons and equipment they left behind, artifacts made of iron and bronze that show evidence of forging and forge welding have been found in the Egyptian pyramids. While at the time middle Ages, a great deal of iron was created using hammer welding. Almost 1700 years old, the Iron Pillar in Delhi, India, is one of the great examples of a weld from this era.[1]

Friction-stir welding (FSW) was patented by Thomas. et.al in 1991. The Institute of Welding (TWI) at United Kingdom did experiments initially on aluminum and its alloys. Titanium and its alloys were later performed with FSW. Since Aluminium materials have low melting points the FSW is easier to perform and being lightweight in advantage they have been widely used in many industries such as automobile and aeronautical industries.[2] The tool is made up of a shoulder and pin. As illustrated in Fig.1, the revolving tool is plunged along the junction of two metal plates that are firmly fastened on a backing plate. Friction is created when the shoulder surface and welding plate's top surface makes contact. Metal undergoes plastic deformation along the weld direction at the joint location. The joint movement of the shoulder and pin affects this. Metal is transferred from the advancing side to the retreating side and vice versa as a result of the pin's stirring action at the intersection zone [2].

The advancing side of the half plate is the side facing the tool's clockwise rotation along the welding direction, and the retreating side is the opposite side. It was discovered that the retreating side's hardness is typically lower than the advancing side's. This is because the repetitive material transfers to the advancing side of the heat cycle, resulting in more refined grains [2]. The major types of joints are the butt joint, lap joint, and fillet joint.The schematic illustration of the welding by friction stir process shown in Fig.1 is a butt type of joint, while the other type of joints is square butt, edge butt, T butt joint, lap joint, multiple lap joint, T lap joint, and fillet joint as shown in Fig.2. The most widely used type of joints is butt joint and

lap joint. In a butt weld the half plates are placed adjacent to each other while in a lap joint the plates are arranged the one above the other whereas in a fillet joint, the plates are arranged at right angles to each other.

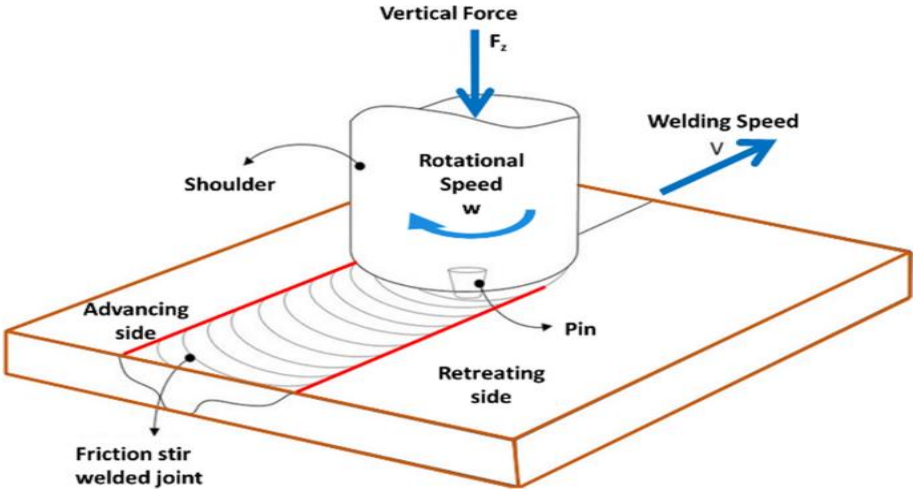

Figure 1.1: Butt type of joint [2]

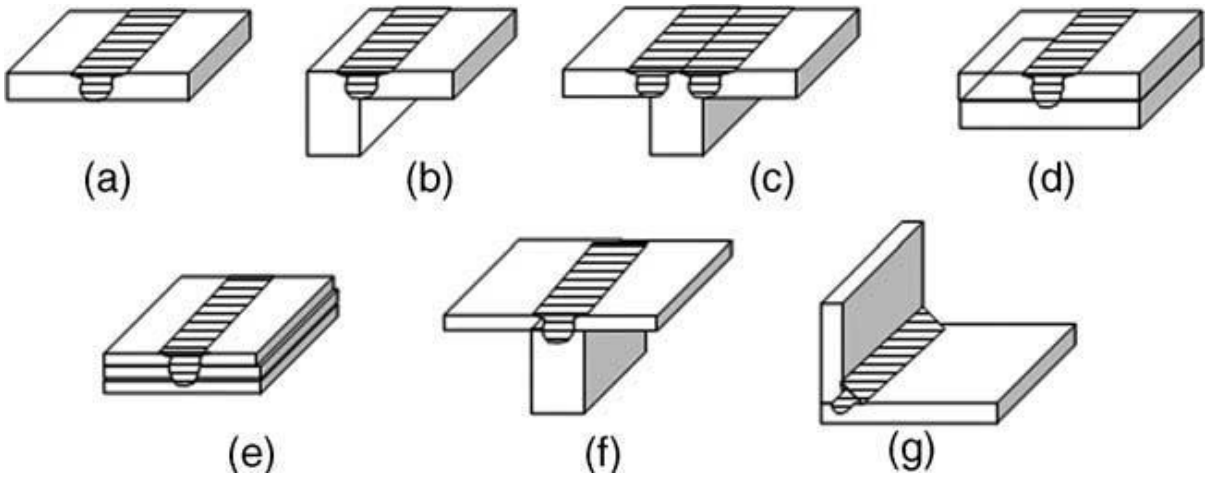

Figure 1-2: kinds of joints Square butt, edge butt, T butt joint, lap joint, multiple lap joint, T lap joint, fillet joint, and (a) lap joint [2]

This FSW approach is useful for combining metals with differing melting points, such as titanium and aluminum, because it can combine metals in a semisolid condition. FSW is currently one of the most widely used joining techniques in the industry for titanium, magnesium, and aluminum alloys [3-5].When it comes to joining dissimilar metals, friction stir welding offers a lot of benefits over traditional fusion welding techniques. Some of them are as follows:

Fusion welding has several drawbacks: (a) it produces a large heat-affected zone that eventually reduces the quality of welding strength; (b) it requires additional filler metal to weld the base metals, whereas in case of FSW additional filler metals are not totally require at all; and (c) it requires shielding gas to remove defects like porosity or hydrogen embrittlement.

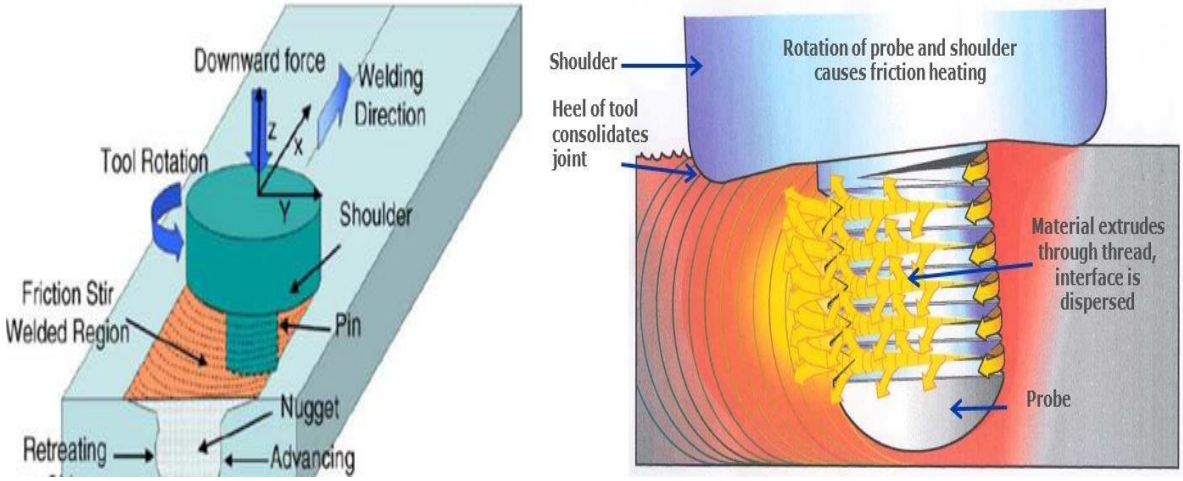

Figure 1-3. Schematic drawing of stir welding with friction [6]

Table 1.1 Key benefits of FSW

Metallurgical benefits	Environmental benefits	Energy benefits
• Solid phase process • Low distortion of work piece • Good dimensional stability and repeatability • No loss of Alloying elements • Fine microstructure • Absence of cracking	• No shielding gas required • No surface cleaning required • Eliminate grinding wastes • Consumable materials saving, such as rugs, wire or any other gases	• Improved materials use (e.g., joining different thickness) allows reduction in weight • Decreased fuel consumption in light weight aircraft automotive and ship applications

These days, because of their low weight, increased strength, and ease of machining, AA6061& titanium are the most prevalent and widely used materials in the automotive, marine, and aviation industries. Nevertheless, it needs appropriate process control parameters is a recent point of interest. Therefore, the goal of this research deals with finding optimum process parameters for the tensile and hardness strength of the dissimilar FSW of the above materials.

1.2.Problem statement

The friction stir welding method are involves various parameters that have a direct impact of the whole process and joining quality. Nowadays High performance and concurrent weight and cost reduction become more important in almost all industries. Therefore, the demand for dissimilar metal joining has increased in numerous industrial areas, such as transportation systems and the aerospace industry. The diverse physical and chemical characteristics of these joints, including as their mechanical qualities, melting temperature, crystal structure, thermal expansion coefficient, and heat conductivity, make them challenging to manufacture. The production of brittle intermetallic compounds (IMC) and incorrect material mixing at the interface are caused by these variations in characteristics [7]. It follows that a welding technique that enables the connecting of incompatible materials with the qualities of high strength, low weight, and low cost is required. Examples of these materials are Ti and Al. When it comes to the aircraft industry, the combination of titanium and aluminum alloys may find significant use in the body construction, since both high strength and lightweight are desired. In particular, titanium and aluminum alloys are widely used because of their superior corrosion resistance and enormous specific strength. The fusion of titanium and aluminum has been attempted numerous times in the past. Scholars have conducted trials utilizing conventional fusion welding methods such as laser and arc welding. Unfortunately, sound connections with the proper strength have not been achieved due to the existence of intermetallic compounds in the weld region and/or weld interface. Additionally, every one of these case studies illustrated problems including the need for shielding gas, sophisticated equipment, and geometric limitations at the welding interface [8]. As a result, it is evident that joining Al and Ti is difficult due to their very dissimilar mechanical, physical, thermal, and chemical characteristics as well as their increased dependence at high joining temperatures. FSW was discovered to have a greater effect in reducing flaws and offering a solid union for dissimilar Al-Ti welding, but it still has flaws. In the nugget zone, brittle IMC production is more frequent, and it is noted that mechanical testing typically results in joint failure. Therefore, the objective of this research project is to investigate the optimal FSW process parameters for the distinct metals titanium and Al6061, as well as to select appropriate welding techniques that significantly affect the overall performance of the weld joint and the possibility of defect formation.

1.3 Objective of the Study

1.3.1 General Objective

The main objective of this thesis work is to optimize proper process parameters and analyse the mechanical property of joining dissimilar material by friction stir welding of 6061 aluminum and commercially pure Titanium Gr-1.

1.3.2 Specific objective

The most specific objectives are:

- Perform tensile test and hardness test of FSW of dissimilar metal (Ti and Al6061)
- Analyze mechanical properties and microstructural of friction stir dissimilar Ti and Al 6061metals.
- Assess how process parameters affect the appropriate friction stir welding of different metals (such as Ti and Al6061).
- To investigate the optimum parameter for FSW of dissimilar Al-alloys by combining Taguchi and Grey relation analysis method.
- What are welding defects when friction stirs welding dissimilar material with a selection of different process parameters?

1.4 Significance of the Research

Today's scientists and engineers are very interested in connecting dissimilar materials. In many sectors, there is a constant need to create machine parts or structures that are strong, lightweight, have better electrical characteristics, and are economical. Al-Ti components are utilized extensively in the automotive, aerospace, defense, transportation, and other industries where integrated lightweight structures with excellent corrosion resistance are required. Al-Ti is joined to create skin-stringer joints in the aircraft manufacturing process, which replace fuselage sections that are riveted. Aluminum to titanium welding has become commercially interesting due to the manufacturing industries' ever-increasing demands. Therefore this research paper shares proper data regarding the selection of welding parameters for friction stir joining of dissimilar materials (Al and Ti) for future studies.

1.5 Scope of the Research

The solid-state joining method will be the main focus of this research project, with a special emphasis on friction-stir welding of titanium and aluminum alloys that differ in composition. The sole focus of the thesis is on process parameter optimization, including rotating speed, transvers speed, tool pin profile, dwell duration, tool material geometry, mechanical property, and macrostructure analysis of welded titanium and aluminum. The study will broaden the field of investigation into the present and future states, analyzing the field through experimentation to support the cost-effective and high-quality usage of friction stir welding for dissimilar metals.

1.6 Limitation of the study

This research is performed by adapting a CNC milling machine as a friction stir welding machine due to the lack of FSW machines in the country. Therefore some parameters like tool tilt angle are difficult to consider in CNC milling machine. An additional limitation of the study has not investigated the microstructure of the weld metal, by lack of access to SEM in the town. Also, the study targeted only dissimilar pure Ti and Al6061 materials based on the demand of the current aerospace, aviation, and maritime industries.

1.7 Research Questions

The study enables us to answer

a) What are the effects of process parameters on proper friction stir welding of Ti and Al 6061 metals?
b) What are the mechanical properties (tensile strength and hardness) of friction stir welded Aluminium and Titanium metals?
c) How to analyse the microstructural property of welded material in nugget zone
d) How can we get minimum defect based on different process parameter considerations in dissimilar friction stir welded Al6061-Ti metals?

So answering those questions will lead directly to the right action implementation

1.8 Thesis layout

This thesis work contains five chapters, which are an introduction, literature review, experimental work and methodology, results and discussions, and lastly conclusion and recommendations.

Chapter 1 begins with an introduction, which consists of the background of FSW, and its process parameters as well as FSW tools. Finally, the problem of the statement, objective, scope, and significance of the study is clearly shown in this chapter.

Chapter 2 presents a literature review of dissimilar FSW, literature on process parameters of FSW, and literature on FSW tool geometry.

Chapter 3 gives detailed information on the working materials, specifications, and experimental procedures used and optimizing the FSW parameters. Aluminum 6061 and pure Titanium using FSW

Chapter 4 explains the results found from lab results i.e. hardness, microstructure, and tensile of the joints formed by FSW of Al6061 and Ti.

Chapter 5 which is the final chapter of the paper, presents the general summary by making sound conclusions and recommendations as well as future scope.

CHAPTER TWO

2. LITERATURE REVIEW

2.1 Introduction

Friction stir welding is a solid-state joining process using a rotating tool moving along the joint interface, generating heat and resulting in a re-circulating plasticized material flow near the tool surface. A stir zone is created when the tool probe's linear and rotational movements extrude this plasticized material. The material flow behavior under the influence of the rotating tool affects the creation of this stir zone. The Welding Institute (TWI) created it in England in 1991 [9]. An intriguing engineering method that offers several benefits, including reduced weight, cost, hybrid structures and qualities, enhanced performance, and more, is the welding of disparate materials [10–12].

The manufacturing of cars and airplanes puts pressure on requirements to reduce costs and improve safety. Furthermore, distinct connecting of titanium with other light alloys was gradually researched for automotive applications and airplane manufacture, since environmental concerns and reduced fuel efficiency issues have been addressed recently. In particular, both the aerospace and automotive sectors have expressed interest in the welding of titanium and aluminum alloys due to their potential to reduce weight and boost mechanical and thermal qualities while also reducing cost [10].

Conventional fusion welding techniques for dissimilar materials are considered a difficult process due to the different melting points. Furthermore, the high temperature at which fusion welding processes work causes thick, brittle layers of Ti-Al intermetallic compound (IMC) to form at the interface, degrading the perfection of the dissimilar junction. There have been numerous attempts recently to weld titanium and aluminum alloys dissimilarly utilizing the laser welding method, which can prevent the formation of brittle intermetallic compounds (IMCs) between dissimilar materials by controlling the input of heat during the welding process. Nonetheless, substantial IMC layers continue to grow, worsening the brittleness of the joint and leading to fractures at the weld interface. [10]

The basic principle of FSW is having a non-consumable rotating tool, made of materials stronger than the workpiece and a specially designed tool shoulder and pin profile. The tool pin is plunged into the faying faces of the workpiece to a pre-programmed depth and the shoulder surface contacts with the workpiece. At this time, the workpieces are heated below the melting point and the softened materials move from the front to the backside, as well as

from top to bottom. It also provides stirring action in the nugget zone during the process. The tool rotates in a clockwise direction (Figure 2.1) and translates from front to back. The left side where the direction of tool rotation is the same as the tool travel direction is termed as advancing side. The side opposite to the advancing side where the tool rotation is reverse of the direction of tool travel is termed as a retreating side [11].

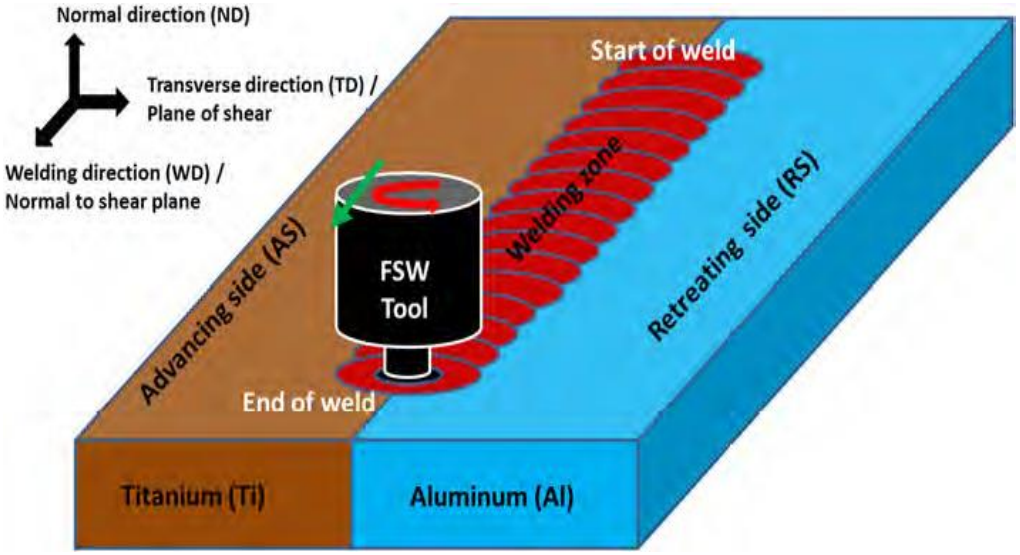

Figure 2.1 Schematic of the friction stir welding process (a) Friction stir butt-welding [12]

2.2. Benefits of FSW

FSW is the most major advancement in metal joining in a decade, and it is considered a green technology because of its energy efficiency, environmental friendliness, and adaptability.

Applications for dissimilar welding of Al-Ti components are numerous and include transportation, aerospace, defense, automotive, and any other field where there is a need for integrated lightweight structures with strong corrosion resistance. For instance, Al-Ti is joined to create skin-stringer connections in the production of aircraft (a replacement for riveted fuselage sections). Aluminum to titanium welding has become commercially interesting due to the manufacturing industries' ever-increasing demands. Combining Al and Ti could result in low-cost, high-strength structures, but the diverse physical and chemical characteristics of these joints such as their melting temperature, crystal structure, thermal expansion coefficient, and heat conductivity make them challenging to manufacture. The production of brittle intermetallic compounds (IMC) and incorrect material mixing at the contact are caused by these variations in characteristics. Friction stir welding (FSW) is an advanced solid-state joining process developed by TWI in the 1990s and from then it has progressed rapidly into a viable joining technology for welding a variety of metals and alloys.

In order to create the FSW joint, a non-consumable rotating tool was inserted into the plate edges. This created frictional heat, which softened the material around and under the tool and caused a localized movement of the plasticized component. High structural integrity of long length continuous welds and joins ,are produced by the transverse motion of the tool along the welding line [13].

Table 2.1 Metallurgical and environmental benefits of FSW [12]

Metallurgical benefits	Environmental benefits
• Solid phase process • Low distortion • Good dimensional stability and repeatability • No loss of alloying elements • Excellent mechanical properties in the joint area • Fine recrystallized microstructure • Absence of solidification cracking • Post FSW formability	• No shielding gas required • Minimal surface cleaning • No harmful emission • Eliminate the solvent requirement • Consumable material savings such as rugs, wire, or any other gases • Only 2.5 % of the energy needed compared with a laser weld.

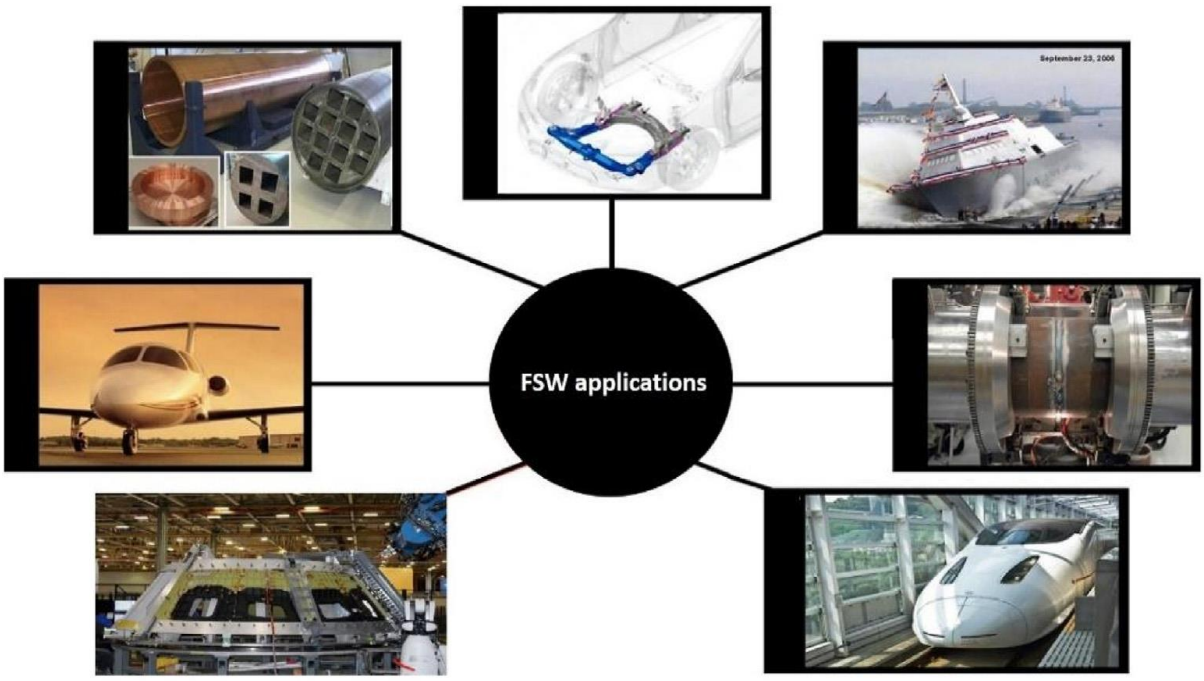

Figure 2.2 Industrial application of FSW [14]

2.2.1 Aerospace applications

In aerospace applications, a material that is lightweight and durable is essential. Henceforth, Aluminium &Titanium (Al-Ti) alloys are the most commonly used and applied in aerospace applications. These metals are efficient in critical applications of aerospace due to their lightweight, good strength and toughness, excellent corrosion resistance, and compatibility with standard manufacturing techniques. Figure 2.8 shows it is applicable in several aircraft parts such as the engine, seat track, leading and trailing edges, wing skin, and many other parts. Currently, the aircraft and aerospace industry improves their structure by double folding the raw material, which will ensure a stronger sheet metal. However, this will thicken the structure and increase the cost of the materials required. Henceforth, aircraft manufacturers came up with a cost reduction program for their existing aircraft version, which led to the application of new material solutions. This new and advanced material will help in facing the new challenges in the future involving mass air transportation. With the cost reduction programs, the once large assemblies and build-up structures consisting of riveted and joined parts were changed with a single integrated structure, which reduced the need for rivets and joints. This has proven advantageous in cost savings, weight reduction, simplifying storage systems, and improved production logistics [13].

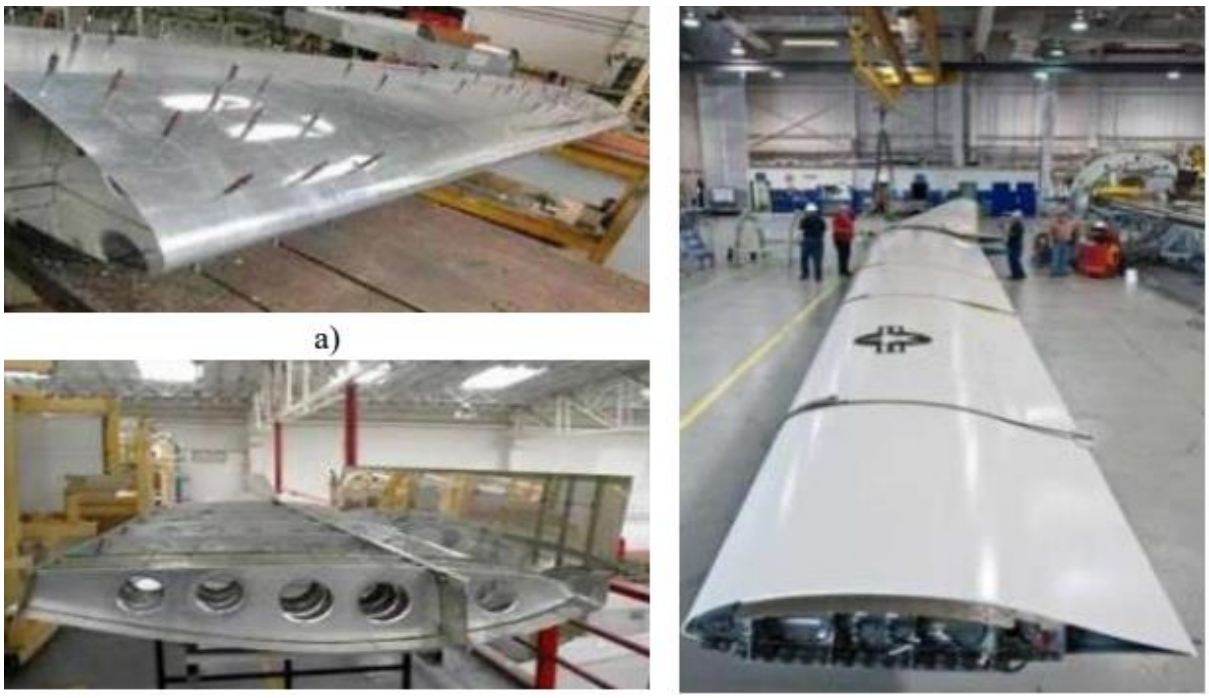

Figure 2.3: (a) aluminum alloys are used to make the following: (a) wing skin; (b) wing ribs; and (c) the final wing, upper skin, and ribs. [13]

FSW is the quite promising technique for joining different metals together. A number of researchers have investigated the FSW of dissimilar titanium and aluminum materials, with particular attention paid to numerical simulations, the joint microstructure, welding process, joint mechanical properties, and material flow pattern. Furthermore, the most fundamental step during the procedure of FSW is the welding process, which also controls how well welding joints form and function. The literature that are now available suggests that the present investigation into the FSW procedure of dissimilar Ti and Al materials can be classified into four categories: tool study, Ti/Al configuration study, tool offset study, and welding parameter selection.

2.3. Friction Stir Welding Defects

Weld quality, microstructural, and mechanical properties in friction stir welding are affected by various defects produced during the welding process. Low heat generation is one of the most prominent causes of defect formation in FSW. By using the right tool geometry in conjunction with process parameter optimization, defects can be reduced. Crack, cavity/groove, void/wormhole, tunnel, flash, kissing bond, and groove flaws are examples of friction stir welding flaws [15]. The table below shows the common flaws in FSW along with their corresponding causes.

Table 2.2: Defects along with their location and causes during FSW [15]

No	Defect	Location	Causes
1	Tunneling	On AS between the TMAZ and the stir zone under the surface of the weld	• Low plunge depth, • Too high welding speed, • Inappropriate pin offset, • Too low rotational speed, • Improper tool geometry
2	Kissing bond	At the interface in the stir zone	• Improper removal of the oxide layer from the faying surface, • High welding speed, • Inadequate material movement
3	Void	On AS of the weld, or beneath the weld surface	• Too high welding speed, • Improper forging pressure, • Improper tool tilt angle.
4	Joint line remnant	At the root of the weld or in the stir zone in the remnant of the original faying surface	Inadequate removal of oxide, • Poor tool joint alignment.
5	Incomplete root penetration	Below the stir zone at the interface of the faying surface	Local variations in the plate thickness, • Improper tool design, • Inappropriate plunge depth, • Too short pin length.
6	Hooking	TMAZ of AS and RS in lap joint welding	Low welding speed, • High rotational speed, • Improper tool design, • Inadequate tool tilt angle

2.4. Process parameter for FSW of Al and Ti joints

It is crucial to comprehend how various FSW factors, including the FSW tool, rotating speed, welding speed, tool tilt angle, and tool insertion depth, affect the attributes of the welded joint. To produce a high quality, flawless weld with FSW, these primary process parameters need to be thoroughly investigated. The importance of each FSW parameter on the weld physical appearance, the microstructure in the area of the weld, the thermal and electrical characteristics, and, most crucially, the joint strength has been studied through a variety of studies [16].Taguchi classified factors/parameters as controllable and fixed factors. Those controllable factors a factors whose levels can be specified and controlled during the experiment and in the final design of the product or process. On the other hand, fixed factors are factors that have an influence on the product or process results but generally are not maintained at specific levels during the production process or application period [17]. In the FSW process, the joint configuration is dominated by the effect associated with the material flow and large mechanical deformation. Many parameters will be considered in FSW for getting a high weld quality. In this study, parameters are classified into controllable and fixed parameters based on the availability of materials and tools.

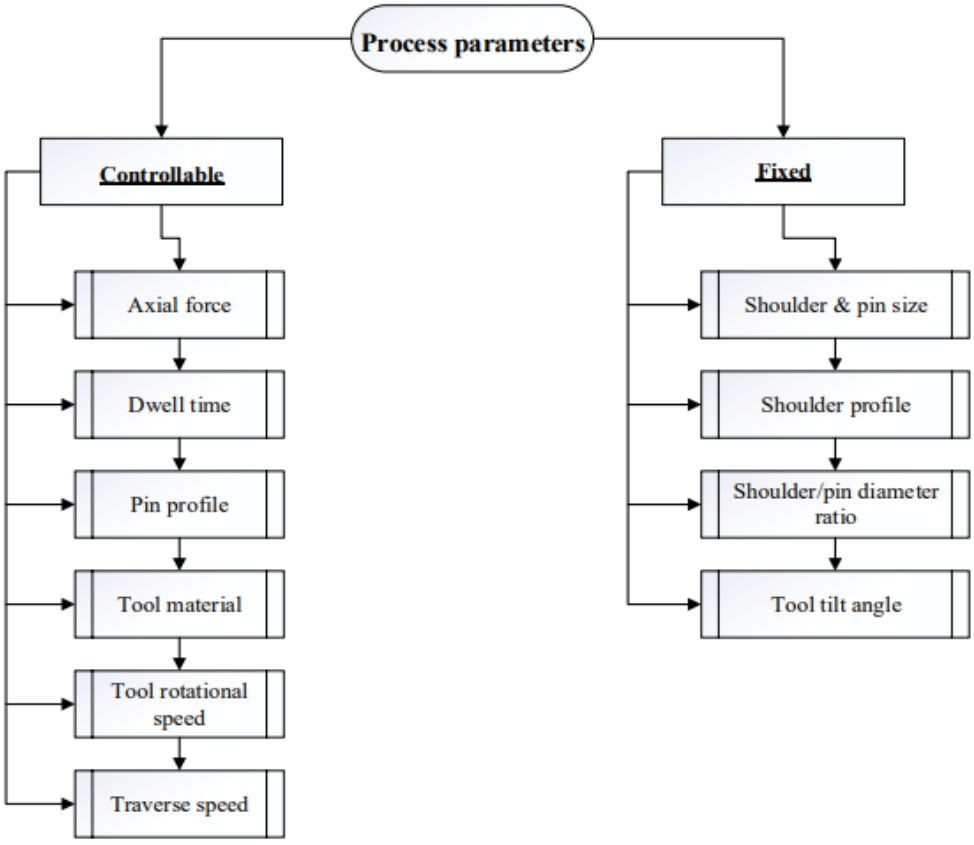

Figure 2.4 FSW process parameters [18]

Process parameters need to be carefully chosen within an appropriate operating range in the case of FSW of dissimilar aluminum and titanium in order to supply adequate heat and melt the materials of the workpiece, enabling proper material flows inside the stir zone in both horizontal and vertical orientations, ultimately, forming a high-quality weld joint between two dissimilar metals. The following section discusses the main process parameters that are utilized to fuse aluminum and titanium using FSW and how they affect the joint qualities. The two most crucial welding parameters in the FSW process are travel speed and rotation speed, which are referred to as TS and RS in this work, respectively. These two welding parameters are important to create enough shear stress and heat of friction. According to reports, the Rotational speed produces 40% of the heat produced during welding [19]. The joint's mechanical characteristics and appearance are highly influenced by the selection of Rotational speed and transfer speed. Additionally, the creation of IMCs would be eliminated and the choice of R and TS should satisfy the requirements of the plastic flow of materials surrounding the tool as well as the thickness direction [19]. Thus, in every experiment, the R and TS are issues that need to be examined. In previous years, researchers have favored to analyze and investigate the R and TS as a whole, but in earlier literature, they chose to separate the R and TS for separate investigations.

2.4.1 Travel or Welding Speed

The pace at which the tool moves through the workpiece's linked line is known as the welding speed or travel speed. Achieving high-quality dissimilar Ti–Al FSW requires a similar level of welding speed [20–22]. It has an impact on the mixing and metallurgical bonding of Ti and Al materials. Because there is insufficient heat input at extremely high welding speeds, joints with incompletely welded interfaces result [20]. Reduced welding speed results in increased heat input and increased IMC production [20, 21, 22]. The material is greatly softened by high heat input, which causes the plasticized material to move erratically. This causes the stir zone to fill with the turbulent Al matrix flow and a varied distribution of Ti particles, resulting in a significant quantity of IMCs. The joint strength is subsequently decreased as a result of these IMCs forming more cracks [22]. Increased welding speed results in reduced heat input, which leads to incorrect Ti–Al material mixing and flaws such as voids [21, 22].The variations in the flow stresses of the Ti and Al materials are another cause of these flaws. Therefore, in order to control the flow stress of different materials, the ideal welding speed is needed. A similar tendency was observed when the welding speed was decreased at constant rotational speeds as when the welding speed was

increased at constant rotational speeds [23]. Because it affects the heat input, it is well known that the ideal ratio between the rotating and welding speeds regulates the development of IMCs in different Ti–Al FSW systems [24]. The heat input directly impacts the ratio of rotating speed to welding speed, which in turn influences the mechanical properties of different Ti–Al FSW systems and the development of IMCs [25].

2.4.2. Speed of Rotation

Rotational speed is the rate of rotation of the FSW tool. In different Ti–Al FSW systems, rotational speed makes for an overall 40% of the contribution. The formation of IMCs, material flow, defect generation, the size of the stirred zone, and tool wear in the dissimilar FSW system are all influenced by the rotational speed, making it a crucial process parameter in FSW. It also affects the material's plastic deformation and forces applied to the tool. The creation of IMCs in different Ti–Al FSW is likewise impacted by a mutation in a frictional heat generation. Due of the increased heat input, a greater number of IMCs are formed at higher rotational speeds. Larger Ti particles, on the other hand, are separated from the Ti base material by a stronger stirring action at high rotating speed. Defects like cracks and gaps are caused by these particles because they are unable to properly bind with the Al matrix [26, 27]. Furthermore, because of the increased heat input at the joint interface, an increase in rotational speed is correlated with the thickening of the interfacial IMC layer [27]. In the case of high-strength alloys like brass and AA7XXX, the high rotating speed also results in increased tool wear due to the intense rubbing action, which shortens tool life (for tool steel alloys). Conversely, because of the minimal heat input, extremely low rotational speed leads to defective joints [28]. Slow rotation prevents the joint area from reaching a temperature that allows for adequate plastic deformation because it does not produce enough heat. As such, an inappropriate flow leads to defects, particularly macro-cracks and channel defects in dissimilar Ti–Al FSW, and the stir zone is unable to plasticize suitably [27]. Lower tensile strength and higher hardness values are the outcomes of extremely low or high rotational speed [26].

2.4.3. Tool Pin Profile

The primary function of the tool pin profile is guiding the material movement. The type of tool pin profile significantly influences the flow of softened material. The effect of different tool pin profiles on a 4.75 mm thickness of 6063 -T6 AA material with butt joint configurations. The experiment was conducted with a heavy-duty vertical milling machine

and used five different pin-profiled tools namely tapered cylindrical, straight cylindrical, straight square, hexagonal, and triangular tools[29]. The process parameters are taken at a constant rotational speed of 900 rpm, traverse speed of 50 mm/min, and tool tilt angle of 1.5^{o}. The researchers obtained the welded joints fabricated with tapered cylindrical tools bestow the maximum tensile and impact strength of 162 MPa and 26 joules respectively. The lowest strength of tensile 115.6 MPa was detected on the triangular tool and also, tunnel defect is found in the advancing side of the linking fabricated using this pin profile due to the inadequate flow of material and ineffective consolidation. Elangovan et.al has studied the impacts of tool pin profile and tool shoulder diameter on a 6 mm thickness of 6061 AA materials with butt joint configurations. Five distinct profiles for tool pins are used, such as square, triangle, tapering, threaded, straight, and cylindrical shapes pins with three different shoulder diameters such as 15, 18, and 21 mm have been used to fabricate the joints. The tool rotational speed, traverse speed, and axial force are 1200 rpm, 75 mm/min, and 7 KN respectively. The result of the paper showed that square pin profiled tools with 18 mm shoulder diameter bestow the maximum tensile strength of around 190 MPa and defect-free joint that is compared to other tool pin profiles [30].

2.4.4. Angle of Tool Tilt

"The angle at which the FSW tool is positioned relative to the workpiece surface, i.e., no or 00 tilted tool is positioned perpendicular to the workpiece surface" is the definition of tool tilt angle. A appropriate tilt angle guarantees that the material stirred by the tool pin is properly held by the shoulders and moved under the FSW tool from front to rear and from top to bottom [31]. The plastically deformed material beneath the FSW tool is likewise compressed by the tool tilt angle. Tilt angle therefore affects both the vertical and horizontal material movement within the stir zone. A range of 20 to 40 tilt degrees is advised for different Ti-AA6061-T651 FSW systems. Increased tilt angle causes the material to be forced downward, filling up the faults rather than spreading out above the top surface (also known as the flake effect). Furthermore, improved metallurgical bonding between Ti and Al is achieved when a higher tilt angle permits Ti particles to freely flow in the Al matrix at a larger axial plunge force. The volume and variety of IMCs grow as a result of the stir zone's temperature rising due to an increase in tilt angle. Therefore, when the tilt angle increases, the joint region gets stiffer. [31].

2.4.5 Base Material Position

In a similar material FSW system, the position of the base weld component is not a determining factor; however, in a dissimilar Ti–Al FSW system, it is. This parameter affects the configurations of the lap joint and butt joint. The advancing and retreating sides have a significant impact on material flow in the joint area [32]. For butt joint configuration, it is advised that Ti and Al be positioned on the advancing and retreating sides, respectively. In contrast, Al and Ti must be positioned top and bottom, respectively, for the configuration of the lap joint. Nune's kinematic model states that material flows from the receding side of the current flow straight through, whereas material flows from the advancing side follow a whirlpool pattern [32]. Therefore, by maintaining Ti on the advancing side, it is possible to enhance the flow path of Ti particles through the creation of a whirlpool pattern, which in turn results in a uniform distribution of Ti particles within the Al matrix and sound bonding. Furthermore, if the harder material Ti is positioned on the retreating side, it will be difficult to transport it to the advancing side, resulting in an uneven material flow. Because of insufficient mixing, this non-uniform dissimilar material flow results in visible volume defects like voids and tunnels. When Ti is kept on the retreating side, the surface tunnel is created most of the time, but when Ti is kept on the advancing side, defect-free surface morphologies are described [33]. However, for different Ti–Al lap junctions, the location of the base materials is also thought to be a significant factor influencing the joint quality. the impact of the position of the base material (Ti and Al) in the lap FSW. They came to the conclusion that when Al must be maintained at the top and Ti at the bottom, a defect-free joint can be created. When Al is retained on top, a lot of heat is produced in the nugget due to Al's low thermal conductivity compared to Ti. This causes a grained stir zone to form without any defects. Additionally, by retaining it on top, more stirring can be provided in the Al matrix, which can aid in the production of sound metallurgical bonding between the Al matrix and Ti particles that are likely to separate from the bottom Ti material [33].

2.4.6 Axial force, Plunge force, or downward force

Downward force, plunge force, or axial force is terms used to describe the force acting perpendicular to the spindle axis direction. Plunge force aids in keeping the tool in contact with or below the material. It takes a sufficient plunge force to reach the stir zone's full penetration. Higher plunge forces thin the deformed material and provide a flash-out effect, while insufficient plunge forces generate an improper vertical flow of the deformed material.

Because of the higher hardness of Ti compared to Al, a larger axial plunge load (more than 600 kg) is needed for dissimilar Ti–Al FSW systems in order to obtain sound joints. Process parameters like welding speed and tilt angle are studied in relation to plunge force, which is increased when there is a higher axial force. This higher axial force causes the base metal to melt and extrude as a flash, which causes a tunnel defect in the middle of the weld zone. because of inadequate material flow and moreover, the The nugget zone widens toward the top of the surface because to the close contact between the tool shoulder and the upper surface of the plates that need to be connected. In friction stir welding, there is a substantial correlation between the axial force and the plunge depth and temperature of the tool. The FSW procedure and tool settings on 7075-T6 AA materials welded with butt joint configurations at a thickness of 5 mm. Six, seven, eight, nine, and ten KN of axial forces were employed. For the joint that was manufactured with a tool rotation speed of 1400 rpm, traverse speed of 60 mm/min, axial force of 8 KN, and tool parameters of 15 mm for the shoulder diameter and 5 mm for the pin diameter, they were able to obtain a higher tensile strength of 373 MPa with a hardness of 203 Hv. As seen in the 7075-T6 aluminum alloy, the study indicates that axial force is significant in the FSW process [34]. the impact of three distinct axial force values, such as 1, 2, and 3 KN, on the mechanical characteristics of AZ80A Mg materials. They found that the welded connections were free of defects and that the 3 KN axial force, 750 rpm tool rotation speed, and 75 mm/min feed rate resulted in a greater tensile strength of 234 MPa [35]. It was investigated how welding parameters affected the materials made of aluminum alloy RDE-40. Axial forces of 4, 6, and 8 KN were employed, together with feed rates of 22, 45, and 75 mm/min and tool rotational speeds of 1200, 1400, and 1600 rpm. They were able to achieve a greater tensile strength of 303.16 MPa at a rotational speed of 1400 rpm, a traversal speed of 45 mm/min, and an axial force of 6 KN. Furthermore, the tensile strength of welded joints is influenced by the axial force to the tune of 21%. After tool rotation speed and traverse speed, it is the third most important characteristic [36].

2.4.7. Tool Pin Offset

The most important factor in the similar Ti-Al FSW system is the tool pin offset. The FSW tool's displacement toward a specific base material is known as the tool pin offset. When the FSW tool is precisely at the center of the joint line, Figure 6 shows no pin offset, meaning it is zero. In contrast, Figure 8(a) shows 0.5 mm displacement toward the Al side, meaning pin offset is 1 mm. Due to variations in melting points and thermal conductivities, it is not possible to induce plastic deformation in Ti and Al combined when the tool pin offset is set to 0 mm, or without any offset at all. The goal of the tool pin offset is to distribute and generate heat in both materials as efficiently as possible, which is challenging to achieve with a

standard tool pin offset of 0 mm. More heat is produced at the Al side and less at the Ti side as the tool is moved toward the Al material. Consequently, Ti's greater coefficient of thermal expansion allows it to disperse heat more effectively than Al, which in turn aids in the ideal distribution of thermal stresses. The joint's weld strength is reduced because of the larger quantity of IMCs produced in the weld area by the smaller pin offset [37].

Standard tool pin insertion (0 mm) results in numerous flaws and poor joints [37]. Additionally, when the pin offset is too tiny, the surface morphology deteriorates. The tool pin for the Ti-Al FSW system needs to be moved toward the Al side so that only a small number of particles can separate from the Ti base material and readily flow and mix with the Al matrix. Therefore, the tool pin offset setting maintains the sizes of the Ti particles. Additionally, greater stirring at the Al side is produced by the larger tool pin offset toward an Al material, which forms an Al matrix that offers a better route for the smaller Ti particles.

By lowering the quantity of IMCs, these smaller Ti particles aid in the formation of strong metallurgical bonding with an Al matrix. Additionally, by arranging an additional sheet of Al next to Ti, the tool pin offset in a lap joint configuration can be modified. Additionally, they demonstrated that adding pin offset to the dissimilar lap joint configuration can boost joint strength [37]. Furthermore, they asserted that by taking the pin offset toward softer (meaning Al) material, uniform mixing between Al and Ti can be accomplished. Thus, for the different system, this is also the reason why butt FSW is preferable to lap welding. According to the literature, a 1.5 to 2 mm pin offset is ideal for producing a high-quality dissimilar Ti–Al FSW connection. Nonetheless, the thickness of the work-piece to be welded and the tool design determine the ideal tool pin offset.

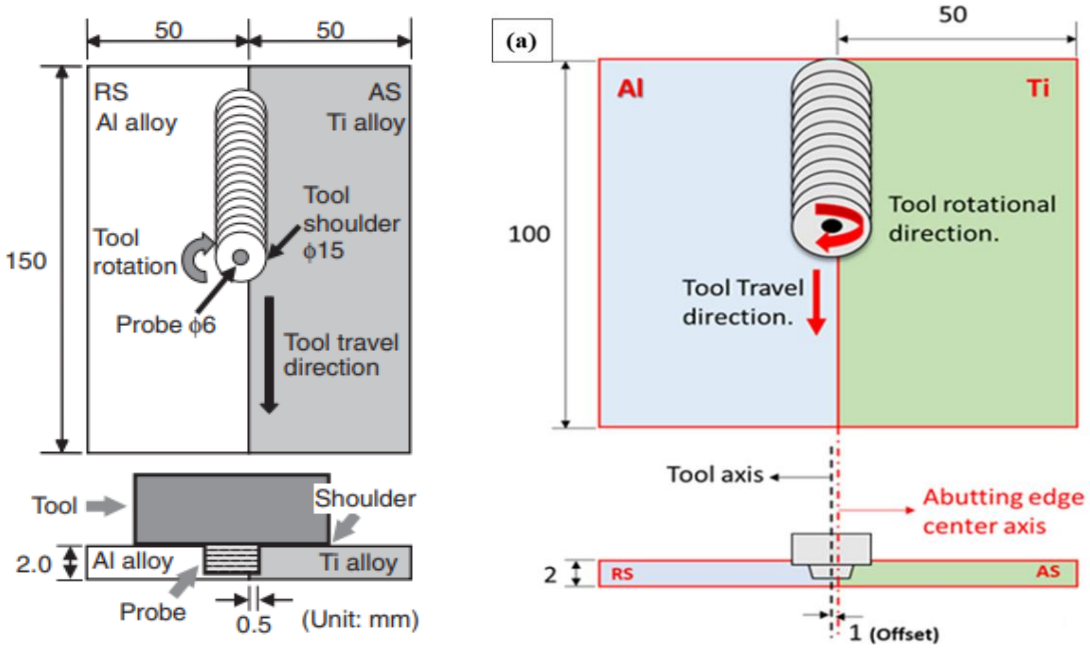

Figure 2.5: Concept of tool pin offset [38,39]

2.4.8. Dwell time

The amount of time that tools are submerged in the weld material at the intended depth and rotational speed without experiencing translational motion is known as the dwell time. After rotational speed, it is the most important welding parameter for weld strength [65]. Dwell time has a direct impact on the mechanical characteristics and microstructure development of dissimilar friction stir spot welding.The longer dwell time can lead to a higher peak temperature and vice versa. Researchers look into how process variables affect friction stir spot welding of aluminum alloy materials with dwell times of 1, 5, and 10 seconds with plunge speeds of 5, 10, and 15 mm/min. The researchers are concluding that dwell time is to be a more influential factor in determining joint strength compared with plunge speed [66].

2.5. Dissimilar materials joining of FSW

FSW could be used for the joining of dissimilar Al alloys and stainless steel. The observation showed that seven different zones of the microstructure in the welding were parent stainless steel, HAZ, and TMAZ on the stainless steel on the advancing side of the weld, parent stainless steel, weld nugget, TMAZ and HAZ on the Al alloy at the retreating side of weld and parent Al alloy. Additionally, microstructure revealed that the presence of finely or coarsely scattered stainless steel particles on the weld nugget caused the hardness of the nugget to exhibit varying values [40]. A solid-state welding technique called friction stir

welding (FSW) is used to fuse both similar and dissimilar materials together. Due to the process of producing sound welds and not having typical issues with fusion welding procedures, including as solidification and liquefaction cracking it was widely used. The commercialization of aluminum and its alloys' FSW led to a recent focus on connecting disparate materials. The study examined the current status of FSW between copper and aluminum, included mechanical testing, the instruments used to create the welds, and offered suggestions for further research in the area of study [41]. Microstructure-property characterisation of a friction-stir welded connection using various joint designs and welding conditions between high-density polyethylene and aluminum alloy AA5059. Scholars note Using the butt joint arrangement, With AA5059 on the advancing side, a 1.4 mm pin offset, a speed of rotational 710 rpm, and a welding velocity of 63 mm/min, the investigation produced an FSW weld that was free of defects and had an excellent look. They also demonstrated the presence of trapped aluminum pieces in a solidified polymer matrix inside the microstructural characteristics of the FSW joint cross-section.

According to the results of the tensile test, which was conducted from a mixed zone/AA5059 interface, the aluminum surface wettability of the SZ contributed to a significantly higher tensile strength than that of the AA5059/HDPE interface [42].

A new solid-state joining method called friction stir welding was extensively used in a variety of industrial domains to fuse various metallic alloys that are difficult to fuse together using traditional fusion welding. Since friction stir welding is a very complicated process that involves a number of intricately coupled physical phenomena, creating a comprehensive system of governing equations to theoretically analyze the behavior of friction stir-welded joints is challenging due to the complicated geometry and three-dimensional nature of some types of joints.

The most recent advancements in numerical analysis of microstructures, welded joints, and friction stir welded structures were covered in this study. Numerical problems were also covered [42], including materials flow modeling, meshing techniques, and failure criteria.

Al-Li alloys played a significant role in aerospace components due to their exceptional strength and stiffness-to-density ratios and were most competitive or superior to a composite-based design in an aircraft or space launcher. Aerospace industries requires very large size sheets, it is not available commercially, the known Al & Li alloys fusion welding was not

possible due to lithium low melting temperature, which causes low joint efficiency porosity and cracking. Therefore, another solid-state joining process is needed, like friction stir welding, it was generally appropriate for joining Al-Li alloys, and experimental investigation provided the influence of rotating and welding speed on microstructure, mechanical properties, and joint efficiency. In addition, recommended effective information about processing parameters which results in a successful friction-welded joining of those alloys [43]. The mechanical and morphological properties of friction-assisted joints made by PVC and aluminum sheets are investigated to know the impact of the main process parameters. The outcome shown that using the maximum axial force with an interaction period of 20 seconds allowed for the achievement of the ultimate shear strength (16 MPa), or 75% of the base material's shear strength. Increased dwell time caused material deterioration, which in turn decreased the strength of the weld. The dimensions of the joined area, the degree to which the teeth created on the aluminum penetrate the softened PVC substrate, and the polymer degradation are the primary determinants of the success and strength of these joints [44].Aluminum matrix composites (AMCs) are joined via friction stir welding (FSW). The negative impacts of the traditional fusion welding technique are eliminated by the solid-state welding of the FSW process, which occurs much below the melting temperature of the material. By examining the effects of welding process variables on the microstructural characteristics and the joints mechanical properties , the behaviour of reinforcing materials during welding, and the impact of tool profiles on the joint strength, their work provided an outline for the friction stir welding technique used to join AMCs. and provided some enhancements as well as guidance for next studies [45]. Via friction stir lap welding (FSLW) using a tapered thread pin with triple facets, a suitable combination of 6061-T6 aluminum (Al) alloy and polyether ether ketone (PEEK) was used to create the hybrid joint. The high-quality joining is attributed to the adhesion bonding and mechanical interlocking, which are achieved by carefully considering the process conditions. According to the findings, mechanical interlocking deteriorated as welding speed increased due to a decrease in the adhesion area and the size of the Al anchor [46].

2.6. FSW tool for joining of Al-Ti

The focal point of the procedure is the FSW tool. The FSW tool is used to heat and soften base materials, extrude them from the tool's front to rear and from its top to bottom, and then bond the softened material to create solid state joints [47]. The geometry and characteristics of the tool material should not change while the process is being done. For work-piece materials with higher melting points, the necessity for tool material is essential. To be successful in the FSW process, a tool material must have certain important properties, including uniformity in microstructure, density, wear resistance, fracture toughness, machinability, elevated temperature stability, and availability of materials [48].

First, the welding tool's material selection is crucial. Strength, high melting points, hardness, and wear resistance are important for the tool material. The friction stir welding technique requires the tool material to be able to bear heat loads, force loads, and friction wear.The tool material should withstand the heat load, force load, and friction wear at the friction stir welding process. Table 2.3 lists several typical materials used in welding tools along with their properties and uses. There will be sufficient material flow and higher heat input during the welding process if a welding material with a significant difference in the friction coefficient between titanium and aluminum is chosen as the tool material. Nowadays, common tool materials for welding of dissimilar materials are include stainless steel, HSS steel, nickel alloy, tool steel and carbon steel. Second, the impact of shoulder shape and diameter on welded joints has also been investigated by several academics. According to reports, the shoulder generates between 70 and 87 % of the heat during the FSW process [49, 50]. The shoulder can help in weld forming by preventing the outflow of melted materials in addition to producing heat [50]. The shoulder geometry is also crucial for the process of welding; the shoulder is often concave, which might cause the material to be subjected to inward force during the FSW process and fill the cavity that is generated behind the pin when the pin rotates. Although there are many different shoulder shapes that can be used for FSW, most studies employ the typical concave annular shoulder for FSW involving Ti–Al dissimilar materials.

Table 2.3 Common materials for the friction stir welding tool and their applications [50].

№	Tool materials	Materials welded	Characteristics
1	HCHCr	AA5083-H111 Al alloy and Magnesium alloy	High wear resistance.
2	SS310	Commercial grade Al-alloy 6 mm thick and Magnesium alloy	Very high corrosion resistance.
3	H13	AA5754 and C11000 copper 3.175 mm thick	-
4	HSS	AA2011, AA6063 alloys10 mm thick and Magnesium alloy	High wear-resistant.
5	C40	AA6082 and AA2024 are 4 mm thick	-
6	H13	6061-T6 Al and AISI 1018 mild steel 6 mm thickness and Magnesium alloy	Shock and abrasion resistance combined with red hardness.
7	Tungsten alloy	Aluminum alloy; magnesium alloy; titanium alloy; steel	High strength; high temperature resistance
8	PCBN	Wear-resistant material	Good high-temperature stability; high hardness

The two biggest benefits of different Ti–Al FSW systems are their inexpensive tool material and straightforward tool design. According to the literature that is currently available, tool steel—which is typically hardened between 45 and 62 HRC and has been tempered and quenched—is frequently utilized as a tool material for different Ti–Al FSW systems. The alloys and workpiece thickness determine the necessary hardness of the tool material. Table 1 displays a summary of the literature on various suggested tool materials for dissimilar Ti–Al FSW systems. Esmaeilia claims that the H13 grade of tool steel corroded off at a faster rotating speed in different brass AA1050H16 FSW systems [51, 52]. The Cu-AA6063 FSW system receives consistent results [53]. Lower wear resistance and increased temperature stability at greater rotational speeds could be the cause of this. The tool may get worn down by rubbing against high-strength alloys like brass and AA6063 materials at a faster rotating

speed. The Ti-Al mixed material sticking to the tool's surface after each welding session is another significant issue that causes flaws.

However, this problem can be overcome by inserting the FSW tool into the fresh Al material after every experiment. Tool pin cleaning and defect prevention are achieved by reacting Ti–Al mixed material with new Al material when the tool is inserted into fresh material [51]. The two most crucial parts of the FSW tool are the material and geometry of the tool. The FSW process requires the welding tool, which consists of a pin and a shoulder. The properties of the joint are impacted by the FSW tool's impacts on heat generation and material flow during the FSW operation [54]. Therefore, effective FSW tool design influences improved Al-Ti FSW joint performance, improved FSW performance, and a wider range of FSW process parameters. For FSW of various Al and Ti, the tool material and its inherent properties are therefore crucial.

2.6.1 Tool Design and Geometry

The two primary parts of the FSW tool are the (I) pin and (II) shoulder. Important elements of these items include pin geometry, shoulder surface angle, and shoulder diameter, including size, shape, and tool surface composition. In FSW technology, the heat input, force, torque fluctuations, and flow of plasticized material are influenced by the shape and design of the tool [55]. The following discusses several tool designs and geometry for distinct Ti–Al FSW systems.

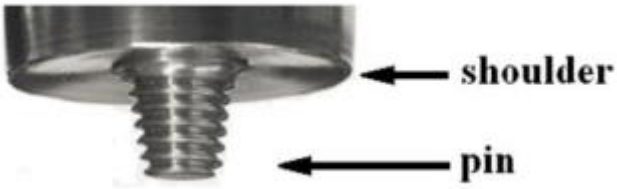

Figure 2.5: Parts of FSW tool [55]

2.6.2 Tool shoulder

The greatest area in FSW that produces heat is the shoulder diameter. It is found that approximately 87% of the heat is produced by the shoulder due to the rubbing action between the shoulder surface and the workpiece. Because they contribute to maximal heat generation, tool shoulder diameter and geometrical surface features have an impact on the quality of the weld in FSW. One of the crucial factors to take into account before welding is the ideal shoulder diameter in order to achieve a high-quality FSW joint [56]. The tool shoulder

diameter affects material deformation, peak temperature variation, microstructural variation, mechanical properties, and the development of IMCs in various Ti–Al FSW systems.

Three shoulder geometries—concave, convex, and flat—as well as special profile elements like scrolling, ridges, grooves, and focusing circles can be added to improve material deformation and homogenous mixing in FSW (Fig. 2.6). The thickness of the workpiece, the materials of the workpiece and the tool all influence the choice of appropriate shoulder geometry features. In various Ti–Al FSW systems, the tool shoulder geometries and profile affect material flow, the development of IMCs, and the mechanical qualities of the joint. [57] According to Akinlambiet, the Ti–Al mixed material is forced downward by a scrolling shoulder, which results in good surface morphology. However, using the scrolling profile results in a significant number of IMCs. Defects are also caused by these IMCs because they make the stir zone harder and more brittle. Therefore, it is not advised to use a scroll surface profile to create a sound, defect-free dissimilar Ti–Al FSW junction. For different Ti–Al FSW systems, conical and flat surface shoulder characteristics are advantageous profiles. The cavity's conical shape aids in the proper material flow for joint development by forcing the material downward by centrifugal force. The conical angle is determined by the shoulder diameter and the thickness of the workpieces. The best shoulder design for various Ti–Al FSW systems may still be seriously considered despite the paucity of research articles in this area.

2.6.3 Tool pin

The plasticized material flow in the joint area is caused by the stirring action of the tool pin. The tool pin's length, surface shape, and pin diameter are all crucial components. The nugget-stir zone's plasticized material penetration depth is influenced by pin length. In order to allow the shoulder to make proper contact with the workpiece by applying an acceptable axial plunge load, the tool pin length is typically kept 0.2 to 0.3 mm smaller than the thickness of the workpiece [57]. The material flow, microstructure, and stir zone size are influenced by surface profile characteristics and pin diameter.

A pin, or probe, and a shoulder make up the friction stirring instrument, as seen in Fig. 2.6. The workpiece material becomes softer when the pin and workpiece come into touch. Conversely, when the shoulder and workpiece come into contact, the workpiece becomes hotter, the softened material's zone is larger, and the deformed material is constrained. Naturally, abrasive wear, high temperatures, and dynamic impacts have a significant impact on the tool throughout the welding process.

Thus, desirable tool materials should have good hardness, temper resistance, high-temperature strength, and wear resistance. Therefore, tool material and shape are two crucial components of tool design in friction stir welding [58]. The most challenging parts of friction stir welding include the utilization of high-temperature materials, tool material development, tool design, complex geometries, and dissimilar materials. Better FSW joint performance, a wider range of FSW process parameters, and enhanced FSW performance are all influenced by appropriate FSW tool design. Therefore, the tool material and its intrinsic qualities are critical for FSW of different Al and Ti.

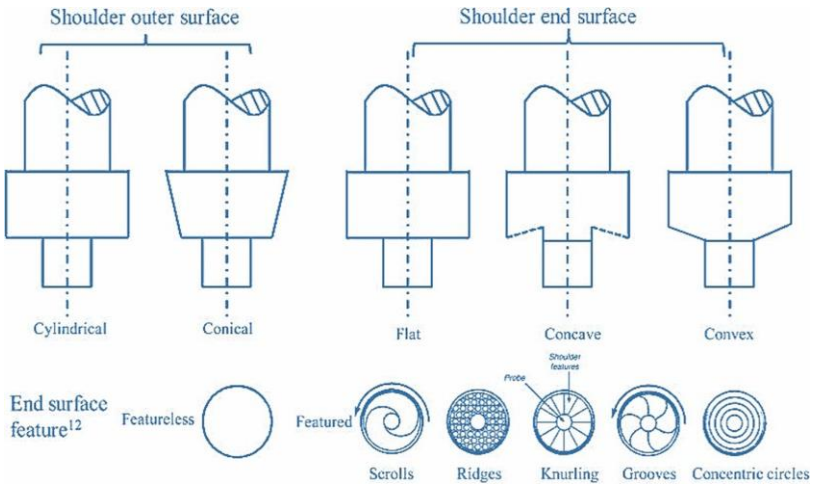

Figure 2.6 FSW welding tool shoulder features [59].

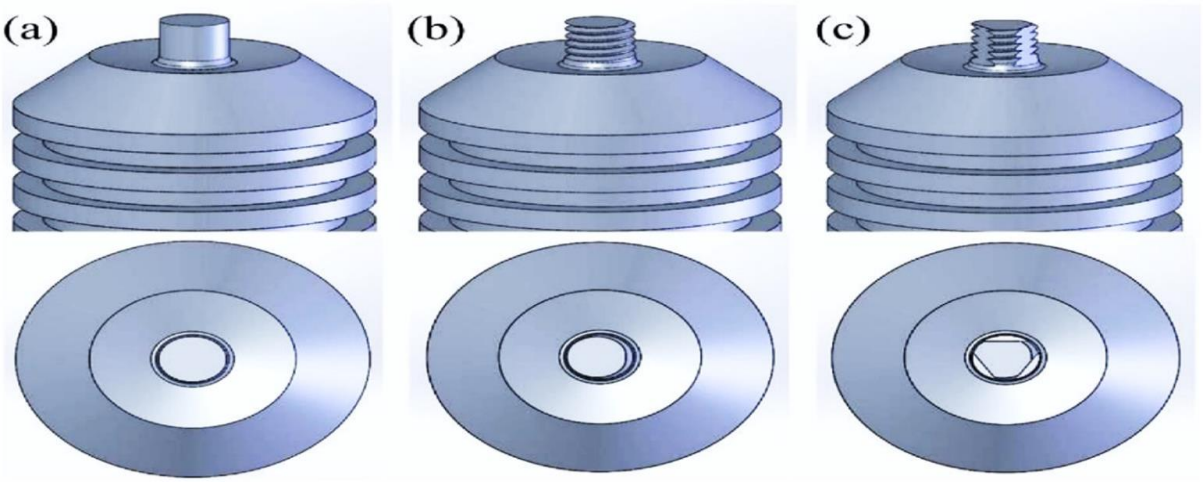

Figure 2.7: Illustration of the welding tool with different pin shapes: (a) featureless pin, (b) threaded pin, (c) threaded pin with flutes [59].

2.6.4. Tool design

The two important characteristics of FSW tool geometry are as follows:

- Its shape should be as simple as possible to reduce the cost and time and
- It should be able to produce an adequate stirring effect to produce sufficient material movement. Tool design is a critical factor during FSW and plays a vital role in plasticized material flow and localized heating at the stirring zone (SZ) that significantly affects defect formation and post-weld mechanical properties. FSW tools are designed to generate sufficient heat due to friction between the tool and BM and plastic deformation of BM and to obtain effective material flow [59].

2.7. Intermetallic Compounds and Microstructures

Four sections make up the microstructures of similar materials in the FSW system: the parent metal microstructure and the heat affected zone are located outside the shoulder, while the two microstructures under the shoulder are the stir zone and the thermo mechanically affected zone (TMAZ). Similarly, these zones comprise the dissimilar materials FSW system. The mechanical properties are thus influenced by these diverse microstructures. Three distinct zones can be observed in the weld nugget (WN) in the dissimilar FSW of Al6061 to Ti6Al4V:

a. Shoulder affected zone,

b. Pin affected zone, and

c. Mechanically mixed zone

As depicted in Figure 2.8a. The macrographs presented in Fig. 2.8b demonstrate the lamellar stacking of layers, with the thickness decreasing towards the as a result of material shearing caused by the tool's transverse and rotational motion in the weld pool. Severe friction is produced beneath the plunged shoulder as it moves in the direction of the weld, shattering the lamellae into particles.

Due to the stirring action of the tool, these particles get dispersed over the Al matrix as shown in the SEM micrographs Fig. 2.8 d. When the EDS line scan was conducted on a single fragment as shown in Fig. 2.8 e, the results concluded that these particles contained average amount of Ti (85.55), Al (7.91), V (5.02), Si (0.09) and Mg (0.23). So, these particles are identified as Ti which are embedded as reinforcement in the Al matrix leading to composite strengthening. As demonstrated in Fig. 2.9 a, the softened Al will attempt to flow along the

deformed Ti at the Al junction during this process, creating a hook-like structure that allows these two different materials to interlock. This zone is also known as a mechanically mixed zone (Fig. 2.9b). As seen in Fig. 2.9a, the BM's average grain size was 6.74 lm for Al and 3.96 lm for Ti. It then decreased to 1.005 lm at the advancing side (AS) and 0.6130 lm in the center of the stir zone (CSZ). The degree of recrystallization is directly influenced by the grain boundary distribution [60], which also has an impact on the grain size. Therefore, more research is done on the grain boundary distribution at the AS and CSZ to have a better understanding.

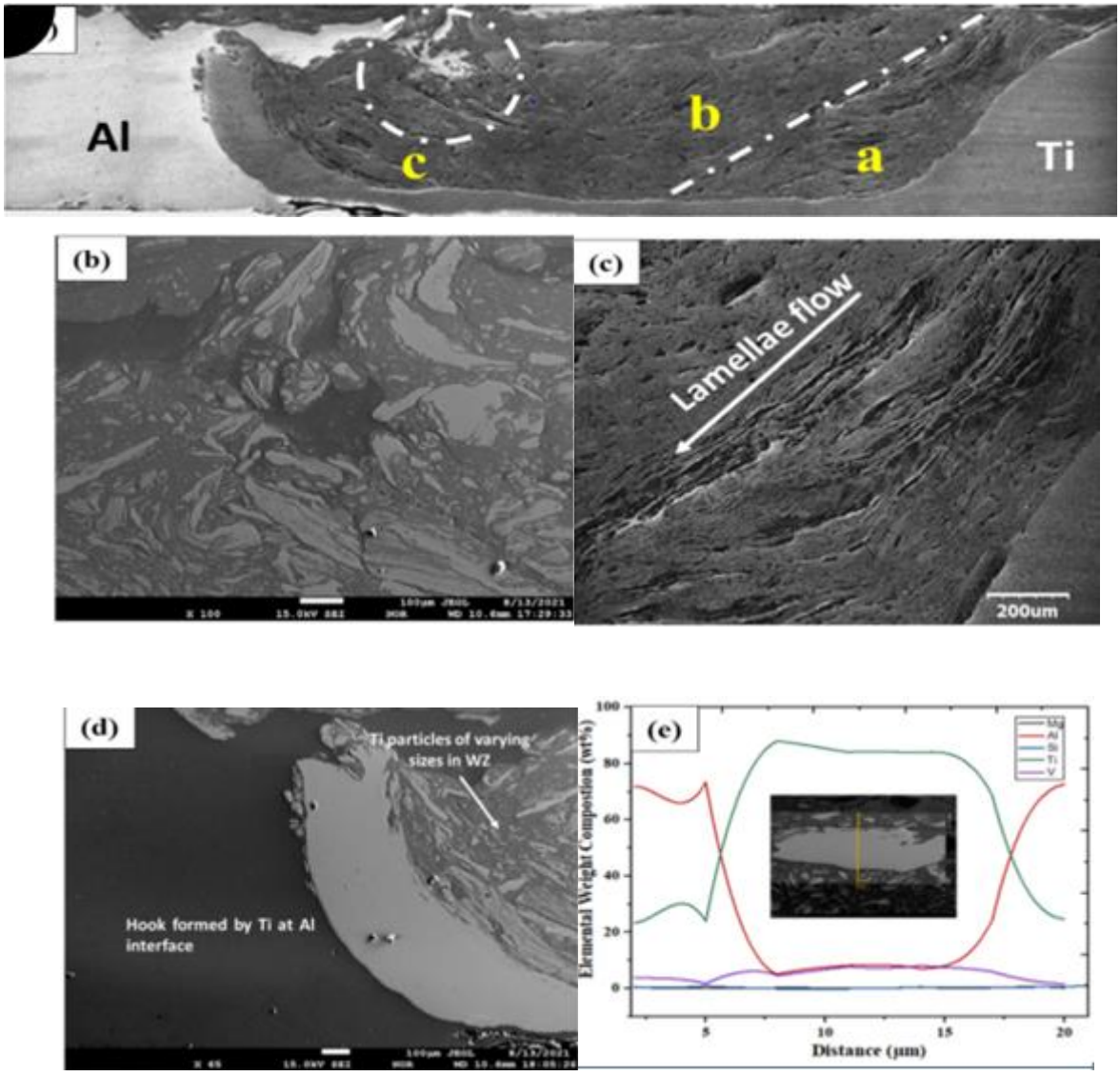

Figure 2.8 :(a) Macrograph of the Al-Ti joint; (b)Mechanically mixed zone; (c) Lamellae flow; (d) Hook at the Al interface; (e) EDS line scan of the Ti particle

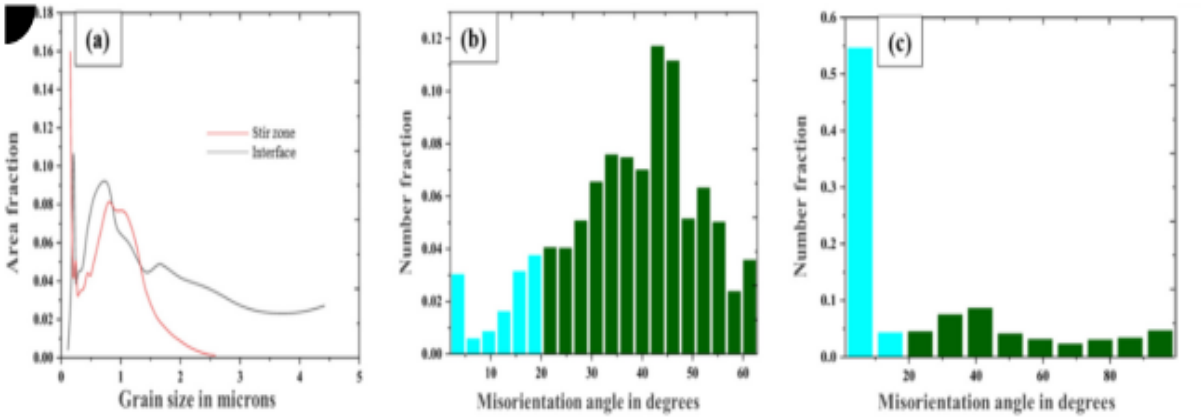

Figure 2.9: (a) Grain size distribution map; Misorientation map at (b) stir zone; (c) interface [60]

Figure 2.10 illustrates the typical microstructure of an FSW weld, which consists of four unique zones: base metal (BM), heat-affected zone (HAZ), thermomechanically affected zone (TMAZ), and weld nugget (WN). The primary cause of swirl zone formation (SWZ) during welding is thermally induced surface oxidation. The thermomechanical cycles cause the TMAZ zone to form, while the frictional heat generated by the shoulder affects the HAZ zone. The area that the pin's stirring action created is called WN. The tool's frictional heat causes the material to plastically deform and the grain boundary to slide. Overheating causes tool wear, which in turn causes the tool's material to be lost. Tool material loss will appear as an inclusion in the welded area. The tool wear tends to emerge along the weld direction in favor of feed rate, material flow, and heat transmission.

Tool wear can be reduced by preheating the workpiece [61] and by choosing the appropriate tool material for the particular workpiece. In Figs. 2.10, The optical microstructure and fundamental schematic of the FSW process are shown, accordingly. The weld zone can be subdivided into four distinct zones, as illustrated in Figure 2: the thermo-mechanically affected zone (TMAZ), the heat-affected zone (HAZ) that experiences thermal cycling, the base material zone (BM) or unaffected zone, and the stir zone (SZ) or nugget zone, where dynamic recrystallization takes place. [61].

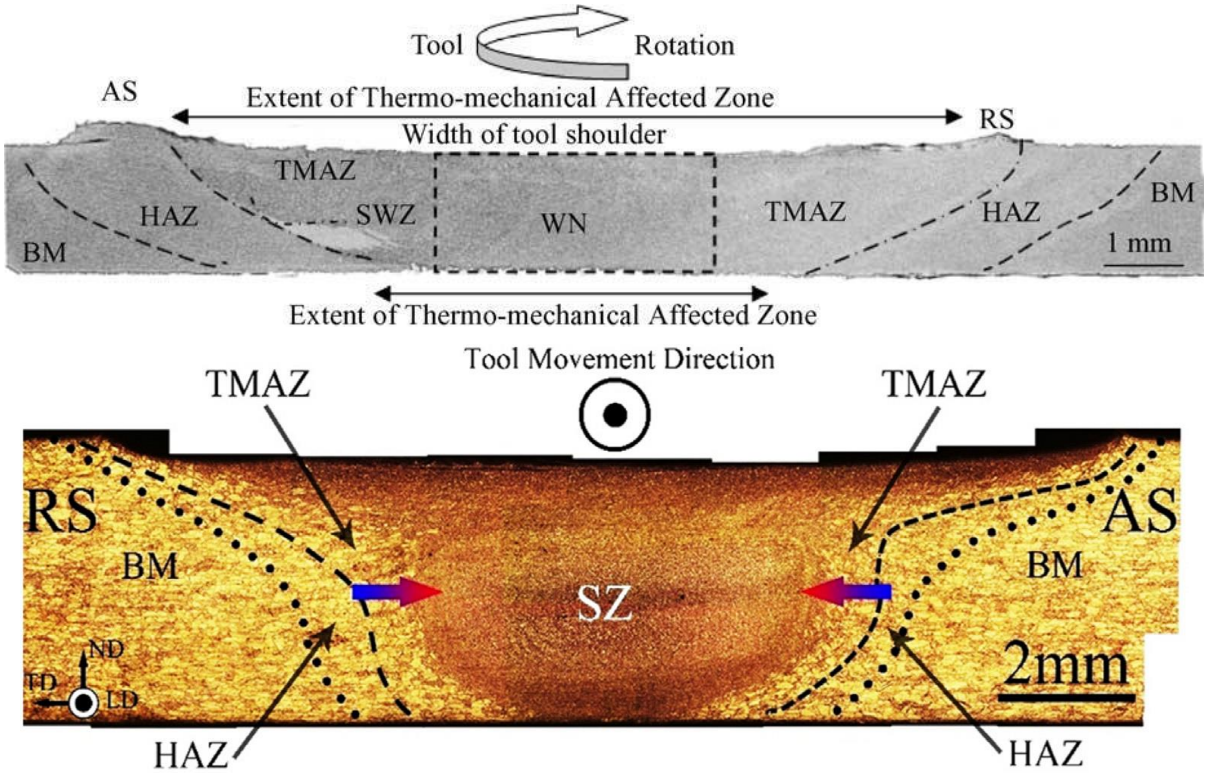

Figure 2.10: Macrostructure of a typical FSW weld [61]

2.8. Mechanical Properties of Dissimilar Ti–Al FSW System

Due to imbalances in the workpiece materials' characteristics, the mechanical properties of dissimilar Ti–Al FSW joints differ significantly from those of equivalent materials FSW systems. Tensile strength and hardness serve as indicators for the efficacy of the FSW joint. It will be possible to create welding processes for improved joint qualities by validating investigations of the welding process and microstructure characterization and demonstrating the welding mechanism through an examination of the hardness and strength distribution of Al-Ti FSW joints.

$$Tensile\ Shear\ Strength = \frac{Tensile\ Force}{Width of\ tensile\ specimen * shoulder\ width} \quad (2.1)$$

2.8.1. Tensile strength of FSW of dissimilar joints

For many applications, mechanical strength is the most important characteristic that separates a good joint from a poor one. According to theory, this is possible if the material is well blended, improved with a strong interlocking structure, has few brittle IMCs, and is defect-free [62]. Tensile shear tests were often used to assess the weld strength in lap configuration FSW. The tensile shear force per unit weld area, which is regarded as overlapping, is utilized here to take into account that the shoulder width is near to the length of the weld interface as

shown in Equation (1), despite the fact that the measurement data from each study are not standard. Regarding the first group, it's found that the Zn interlayer and no-tool penetration result in stronger joints. Weld joints with four group parameters (750 r/min or 900 r/min for the tool rotation rate, and 118 mm/min or 150 mm/min for the welding speed) were formed into standard tensile specimens before their strength was evaluated.

Three tensile specimens were cut from each parameter and the average of the strength of the three specimens was regarded as the tensile strength of weld joints, the results are seen in Table **3**.

Table 2.4 Tensile Strength of Butt Joint Ti/Al Alloy Dissimilar Materials [62]

Sample number	**Rotational speed RPM**	**Welding speed mm/min**	**Average tensile strength Mpa**
1	750	118	-
2	750	150	16.4
3	950	118	131.1
4	950	150	96.4

Table 2.4 shows that the lowest tensile strength is achieved at 750 r/min tool rotation rate and 118 mm/min welding speed. Two specimens broke when clamped in the tensile testing machine, suggesting that titanium and aluminum mix poorly at these conditions.

it is consistent with the morphology observed from weld cross-section. When the rotational speed is 950r/min and welding speed is 118 mm/min, the strength of the joint is 131MP which is the highest, but it is still far below the strength(314MPa) of LF6 aluminum alloy base material and the strength(600MPa) of TC1 titanium alloy base material. So about the FSW of Titanium and Aluminum dissimilar materials, further measures (such as the design of the stirring head, adding the middle materials, etc. are taken to improve the strength of the joint and then it is possible to carry out the applications of engineering.[62]

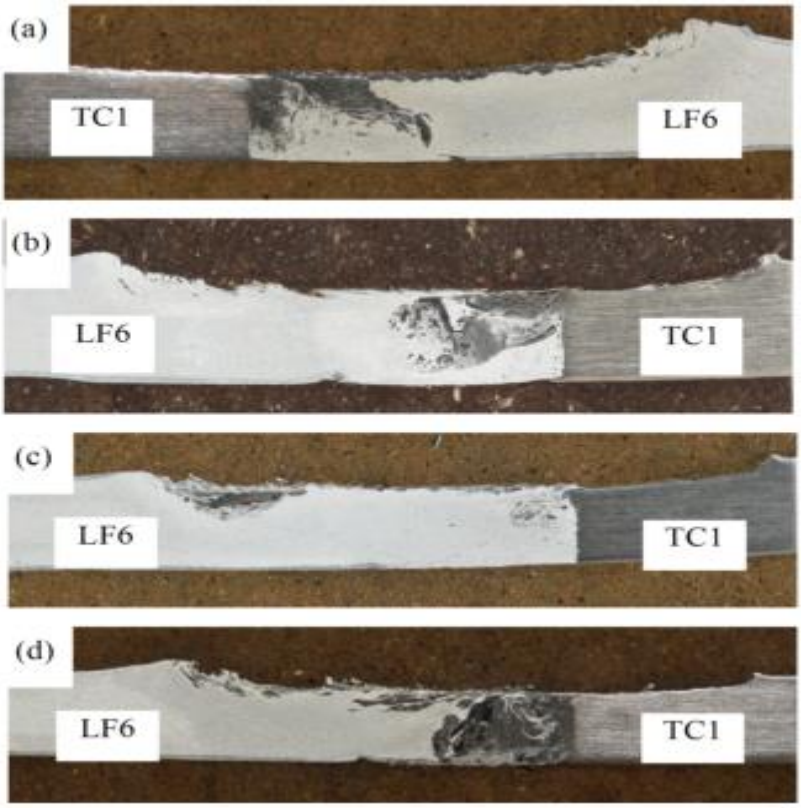

Figure 2.11 : (6). The macroscopic morphology of the cross-section of the butt joint: (a) n=750r/min, v=118mm/min; (b) n=750r/min,v=150mm/min; (c) n=950r/min,v=118mm/min; (d)n=950r/min, v=150mm/min.[62]

2.8.2 Hardness of FSW of Al-Ti Dissimilar Joints

The results obtained from the analysis of the hardness of the weldments are shown in Figure2.12. As can be observed, in all the weldments, the stirred zone exhibits hardness higher than the heat-affected zone and the base metal has the lowest hardness. This can be attributed to two reasons. Firstly, plastic deformation occurred in the stirred zone and the heat-affected zone, and secondly, the structure of the stirred area is finer than that of the base metal due to dynamic recrystallization in this area. The results showed 360 HV10 hardness in the joint area, which means that the hardness in the area of the titanium base metal and aluminum is increased by 6% and 20%, respectively. The increase in hardness has been reported by other researchers as well. For example, Kitamura showed that smaller particles increase the strength of the structure, and that hardness is also directly associated with strength, and as the grains have smaller size in the stirred zone the hardness of the stirred zone increases [63]. Hua also showed that a mixture of aluminum and titanium is formed in the stirred zone so that the mixed zone is composed of an intermetallic compound and this

increases the hardness. He also reported that hardness in the area reached 502 HV10 [63]. On the titanium side, the minimum hardness, namely 280 HV10, is related to the heat-affected zone, which is due to the effect of annealing that leads to softening of this area compared with the base metal [63].

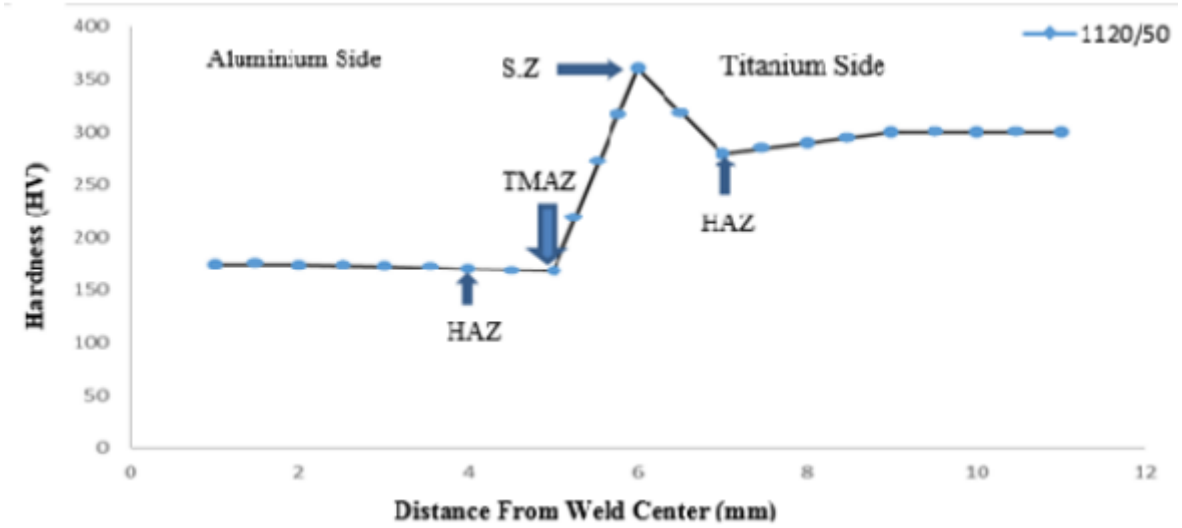

Figure 2.12 Hardness profiles with distances from the weld to the base metal of titanium and 7075 aluminum [64]

2.9. Literature Summary

In the literature, review many Authors assess process parameter tool materials and geometry of friction stir welding for aluminium and titanium metals. FSW is the most promising technique for joining different metals together. The FSW of Ti-Al dissimilar materials has been investigated by a number of researchers, with particular attention paid to numerical simulations, the welding process, joint microstructure, joint mechanical properties, and material flow pattern. The fundamental step in the FSW process that controls the performance and formation of welding joints is the welding process.

The literatures that is currently available indicates that the research being done on the FSW process of Ti and Al dissimilar materials may be clasified into four main areas: the investigation of mechanical properties, the study of Ti/Al configuration, the study of process parameters, and the selection of welding parameters.

Table 2.5 Literature Summary

Sr. no.	Author (year)	Substrate material	Parameters selected for study	Conclusion
1	Chen	Titanium to Aluminium	The rotational speed of 1500 rpm and the traverse speed of 90 mm·min-1.	Mechanical properties were derived from the intermetallic compounds. The authors found that the fracture strength of all joints was lower than the fracture strength of the base metal, and in all joints, fracture occurred at the interface of the parts welded.
2	Desler	2024 aluminium alloy and titanium	rotation speed of 800 rpm and a traverse speed of 80 mm·min-1	The stirred zone was a mixture of a recrystallization layer of aluminum and titanium particles. The tensile strength was 73% higher than that of the aluminum 2024 base metal. This can be attributed to the formation of an aluminium-titanium compound in the weld area
3	Bang	Aluminium 6061 and titanium		All joints had less strength than the base metal because the probe tip was in an area that could not perform the stirring operation effectively.
4	Sadeghi	aluminium 5083 and commercially pure titanium	rotation speed of 1120 mm·min-and a traverse speed of 150 mm·min-1	The effect of the friction stir welding process carried out at a constant rotational speed of 1120 rpm and a traverse speed of 50 mm·min-1 on hardness, tensile strength, and microstructure
5	Reshad K., Seighalani, M.K. Givi Besharati, Nasiri A.M., and Bahemmat P., (2009)	Pure Titanium	Tool Material, Geometry, and Tilt Angle	Using a high-speed steel (HSS) tool for FSW of titanium will result in complete failure of the pin and severe wear of the shoulder nose because of heat generation from friction between the tool and the base metal. -Using brittle WC as a pin material for FSW of the Ti-CP and because of high wear and stress concentrations developing on the root of the pins threads Macro structural analysis of the welded joints shows that
6	Arora A. & Mehta M. & De A. & DebRoy T. , (2009)	L80 steel and AA7075 alloy	Load bearing capacity of tool pin	A three-dimensional heat transfer and visco-plastic model is used to compute the influence of pin length and diameter on traverse force during FSW. The total traverse force increases significantly with an increase in pin length
7	*Elangovan K. , Balasubramanian V.* , (2008)	AA2219 aluminium alloy	Tool pin profile and welding speed	square pin profiled tool produced defect-free FSP region, irrespective of welding speeds. - the joints fabricated at a welding speed of 0.76mm/s showed superior tensile properties, irrespective of tool pin profiles. -the joint fabricated using a square pin profiled tool at a welding speed of

				0.76mm/s exhibited maximum tensile strength, higher hardness, and finer grains in the FSP region.
8	Arora A., Deb A. and DebRoy T.. (2011	AA6061 aluminum Alloys	Tool shoulder diameter	For different shoulder diameters, the two components of the torque are employed to calculate the ideal tool geometry. The sticking torque, MT, rises, reaches a maximum, and then falls as the shoulder diameter grows. Examining this behavior reveals that the value of the sticking torque is influenced by two primary elements. First, as the temperature rises, the material's strength declines because the shoulder diameter grows. Secondly, as shoulder diameter grows, so does the region over which the torque is imparted.
9	Cao X., Jahazi M.. (2011)	AZ31B-H24 magnesium alloy	Tool rotational speed and probe length	As the tool's rotational speed increases, the tensile shear load initially rises but then falls. Shear strength rises as probe length and bottom sheet penetration depth increase.
10	J. Rodriguez and A. J. Ramirez*	mild steel Ni-based	welding speed, rotational speed	FSW was successfully and repeatedly used to produce consolidated and defect-free dissimilar butt joints of 6.6 mm thick plates of mild steel and Ni-based alloy 625. Welded joints free of wormhole defects were produced using an axial offset of .1.63 mm; however, they presented interfaces that were not completely stirred at the joint root (faying surface). Smaller axial offsets (0.5 and 0.0 mm) exhibited wormholes on the advancing side. For the joints produced without tool axial offset (0 mm), reductions in the rotational speed decreased the size of the wormhole defects.
11	Buffa et al	Aluminum alloy	temperature distribution, hydrostatic stress distribution, strain rate, vertical, and advancing forces	The results allow finding optimal tool geometry and advancing speed to improve the nugget integrity of welded aluminum alloys.
12	Barnes et al	X65 pipeline steel	wear behavior of PCBN	There were some tungsten-rich bands visible at SZ for the welds made with W-Re tools. Additionally, the number and size of tungsten-rich bands increase in proportion to the ratio of rotational speed to traversal speed.
13	Chen et al.	316L stainless steel	wear behavior of PCBN	Compared to the tool with a spiral probe, the one with a chamfer probe shows superior wear resistance. The tool wear resistance is enhanced by the small pitch screw tool shoulder.

2.10. Literature Gaps

- The majority of earlier research focused on a small number of factors, including traverse speed, tool pin profile, axial force, and rotating speed. This demonstrates unequivocally that additional research on other factors is necessary as the studies conducted in the field of FSW process parameter improvement were restricted. This is the reason this research will look more closely at and assess the improvement of FSW process parameters.
- It is evident that not much research has been conducted in many developing nations about the optimization of FSW. As a result, this work will significantly advance the few studies conducted in impoverished nations like Ethiopia. This research will therefore examine and assess the enhancement of FSW process parameters on commercially pure titanium and dissimilar Al6061 titanium.

CHAPTER THREE

3. Research Methods & Materials

3.1 Research Methodology

This chapter presents the method employed, to achieve the research objective mentioned in Chapter One.

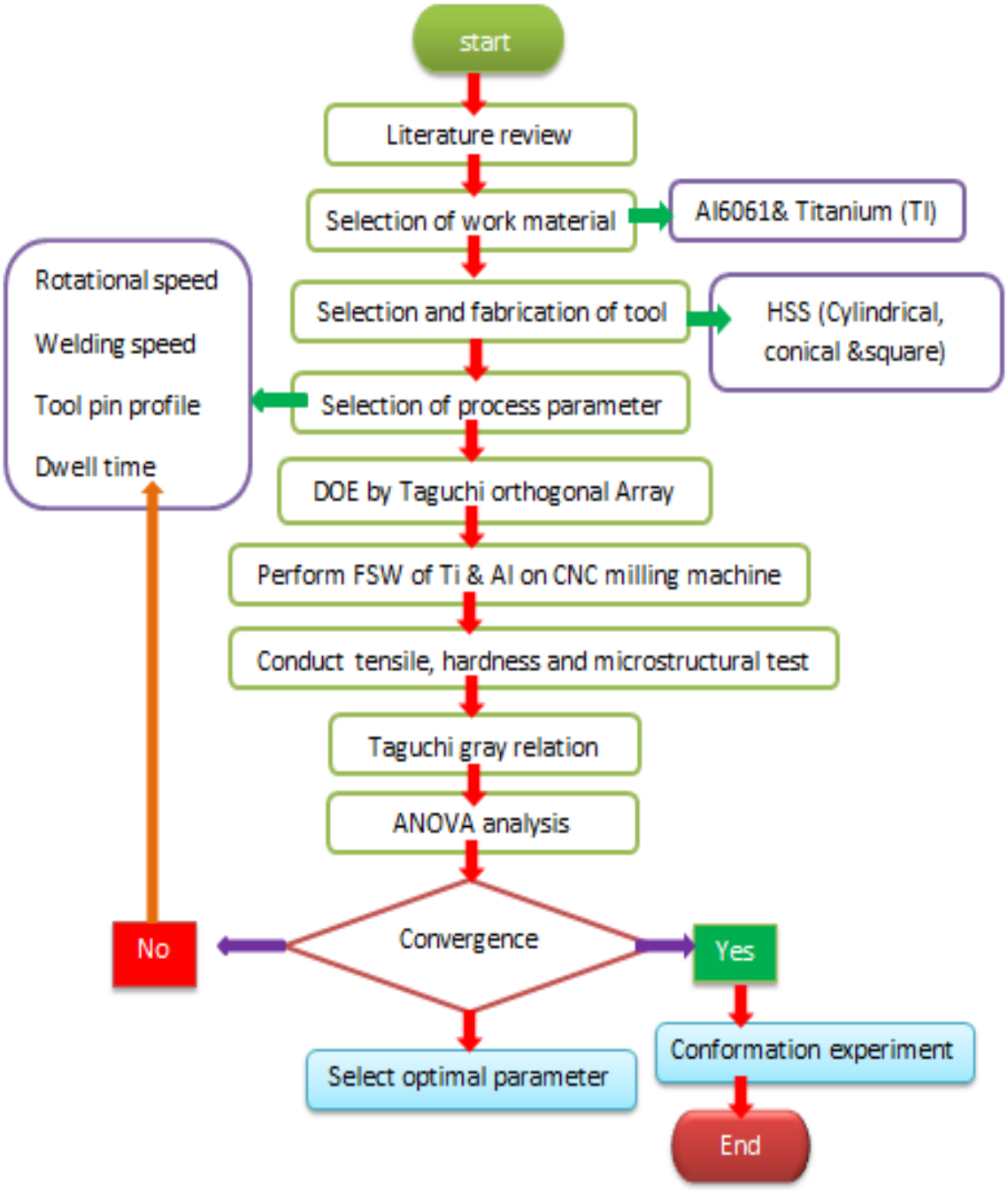

Figure 3.1: the schematic diagram of the framework of the applied Methodologies:

Literature Review: this was done by collecting and studying different articles, journals, and books concerning the friction stir welding process for dissimilar metals, especially on optimization of welding parameters, tool material, tool geometry and analysis of welding defect, microstructure, mechanical property and electrical property of friction stir welded Al6061 and commercially pure Ti metals.

3.2 Material Used and Equipment

In this paper tow, the base materials used for welding purposes are commercially pure titanium and aluminum 6061 alloys. Their property and chemical compositions are discussed below.

3.2.1 Titanium

The atomic number of the silvery-white metal titanium is 22. This metal has a high strength-to-weight ratio and is biocompatible, lightweight, ductile, robust, and resistant to corrosion. The ninth most common element on Earth is titanium. It is frequently found in sand, clay, and rocks. The two main commercial minerals that are used to extract and purify titanium are rutile and ilmenite.[67] Titanium, and mainly its alloys, are today often selected for their remarkable mechanical properties, low density, and good corrosion resistance. A comparison of material properties between titanium and some commonly used metals is shown in Table B.1. Because of its relatively high price, titanium remains a metal whose use is selective. Pure titanium undergoes an allotropic transformation at 882°C from the body-centered cubic (BCC) β phase at high temperature to the pseudo-compact hexagonal α phase at lower temperature. This temperature is also referred to as the "β transit", which can be written as Tβ. Figure B.1 shows a representation of both these lattices. The lattice parameters of α and β phases, at room temperature, are • Hexagonal phase α: c = 0.468nm and a = 0.295nm. These lattice parameters give a c/a ratio of 1.587, lower than the ideal ratio of 1.633 for a compact hexagonal lattice. Figure B.1(a) also shows the planes of maximum density: the basal plane (0002), one of the three prismatic $\{10\bar{1}0\}$ planes, and one of the six pyramidal $\{10\bar{1}1\}$ planes. The directions a1, a2, and a3 are the directions of maximum density $< 11\bar{2}0 >$. • β centred cubic phase: a = 0.332nm with the crystallographic planes of maximum density {110} and the four directions < 111 >. Titanium is rarely used in its pure form. Several titanium alloys exist: Ti17, Ti40, Ti3Al2.5, or Ti5Al2.5Sn, depending on the intended use. The most commonly produced and used titanium alloy is Ti-6Al-4V.

Titanium is classified into alpha-alloys, beta-alloys, and alpha-beta alloys. Alloys made solely of oxygen, titanium alpha alloys are frequently combined with additional metals like vanadium, molybdenum, and aluminum. These metals are added to help achieve desired qualities like increased strength, resistance to corrosion, and decreased weight. Commercial and aerospace applications, power plant condensers, desalination plants, maritime applications, architectural items, medical implants like joint replacement devices, and consumer goods like golf clubs and bicycle frames are among the common uses of titanium and its alloys. For this paper commercial pure titanium grade one type is used [67].

Chemical composition

Table 3.1 Titanium chemical composition

Type	N	C	H	Fe	O
ASTM Grade 1	0.03	0.08	0.015	0.20	0.18

Mechanical Properties

Table 3.2 Titanium mechanical property

Young's modulus (GPa)	0.2% Yield strength (MPa)	Tensile strength (MPa)	Elongation (%)
103	170	240	25

Titanium has a specific gravity of 4.54, a melting point of 1660 +/- 10°C, a boiling point of 3287°C, and a valence of 2, 3, or 4. Shiny white, pure titanium has excellent strength, low density, and resistance to corrosion. Most organic acids, wet chlorine gas, diluted sulfuric and hydrochloric acids, and chloride solutions are all substances that it is resistant to. Titanium can only be ductile in an oxygen-free environment. The only element that burns in nitrogen is titanium, which burns in the atmosphere.

Titanium is a dimorphic metal; around 880°C, it gradually transforms from its hexagonal a form to its cubic b form. At red heat temperatures, the metal mixes with oxygen; at 550°C, it combines with chlorine. Titanium weighs 45% less than steel but has the same strength. Despite being twice as strong as aluminum, the metal weighs 60% more.

Table 3.3 Physical properties of titanium

	Density	Strength	Color	Ductility	Durability
Cp – Ti	4.506 g/cm3	240 MPa	silvery-white	25%	High

Chemical properties of titanium are listed below:

1 Oxidation Potential: Because of its electron configuration and status as a transition metal, titanium has an oxidation potential. Titanium is not found in nature in its pure form due to its high oxidation potential; instead, it is found in the form of oxides in rocks and minerals.

2 Ability to create Alloys: Because of its small atomic size and transition metal status, titanium can readily create alloys with other metals and elements. There are numerous titanium alloys available.

3 Reactivity: At high temperatures, titanium is reactive to halogens and acids but completely inert to bases.

4 Corrosion Resistance: Titanium is inherently resistant to corrosion due to its tendency to react with nitrogen and oxygen. The oxides that form on the surface of titanium protect the underlying material from corrosive chemicals.

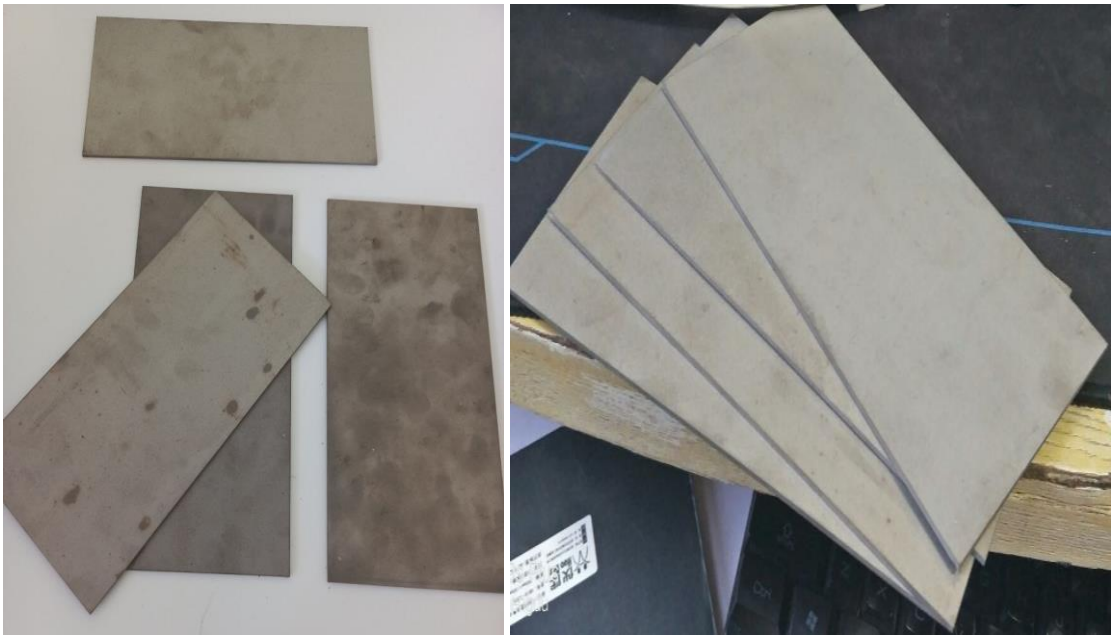

Figure 3.2: Commercial pure titanium Gr-1

3.2.2Aluminum 6061

Magnesium and silicon are the main alloying constituents of aluminum 6061 alloy (Unified Numbering System (UNS) designation A96061), which is an aluminum alloy precipitation-hardened via precipitation. It was developed in 1935 under the name "Alloy 61S".[2] It is

highly frequently extruded, has good mechanical qualities, and is weldable (being second only to 6063 in popularity).[3] It is among the most widely used aluminum alloys for everyday applications [68].

Pre-tempered grades like 6061-O (annealed), tempered grades like 6061-T6 (solutionized and artificially aged), and 6061-T651 (solutionized, stress-relieved stretched and artificially aged) are the most prevalent grades available.

Chemical composition 6061 Aluminium alloy composition by mass

Table 3.4 Chemical composition 6061 Aluminum

Constituent Element	**Si**	**Fe**	**Cu**	**Mn**	**Mg**	**Cr**	**Zn**	**Na**	**Ti**	**Al**
Standard value	0.4-0.8	≤0.7	0.15-0.4	≤0.15	0.8-1.2	0.04-0.35	≤0.25	-	≤015	
Measured value	0.625	0.498	0.256	0.109	1.068	0.116	0.115	0	0.026	97.15

Physical Properties of 6061 Aluminum

The 6xxx aluminum alloys, which include the compositions that use silicon and magnesium as the main alloying ingredients, include type 6061 aluminum. The basic aluminum's level of impurity control is indicated by the second digit. A "0" for this second digit means that the majority of the alloy is commercial aluminum with its current levels of impurities; therefore, tightening controls doesn't need to be done with special attention. Note that this is not the case with 1xxx aluminum alloys. The third and fourth digits are just designations for specific alloys. Type 6061 aluminum has the following nominal composition: 97.9% Al, 0.6% Si, 1.0% Mg, 0.2% Cr, and 0.28% Cu. The aluminum alloy 6061 has a density of 2.7 g/cm3 (0.0975 lb/in3). The aluminum alloy 6061 is easily produced, heat-treatable, weldable, and corrosion-resistant [68].

Mechanical Properties

Depending on how the 6061 aluminum alloy is heat treated or strengthened during the tempering process, its mechanical properties change. The strength ratings for this alloy will be derived from 6061-T6, or T6 tempered 6061 aluminum alloy, which is a typical temper for aluminum plate and bar stock in order to simplify this article. Table 1 contains these numbers, which indicate the alloy's stiffness, or resistance to deformation. This alloy is a

versatile industrial material since it is generally simple to combine via welding and readily deforms into most desired shapes.

Yield strength and ultimate strength are two critical components to take into account while analyzing mechanical qualities. The maximum stress required to cause an elastic deformation of the item under a specific loading arrangement (tension, compression, twisting, etc.) is described by the yield strength. Conversely, the ultimate strength indicates the highest stress a material can bear before breaking (going through permanent, plastic deformation). According to industry standard design procedures, the yield strength is the most significant design restriction for static applications; nevertheless, for some applications, the ultimate strength may be helpful.

Table 3.5 Summary of mechanical properties for 6061 aluminum alloy

Mechanical Properties	**Standard**	**Measured**
Ultimate Tensile Strength	≥290 MPa	310MPa
Tensile Yield Strength	≥240MPa	246 MPa
Elongation	≥9	14

Corrosion Resistance

The 6061 aluminum alloy turns into an oxide layer in the presence of air or water, making it inert to substances that would otherwise corrode the metal underneath. Although atmospheric and/or aqueous conditions affect corrosion resistance, corrosive effects in air and water are often insignificant at room temperature. It is significant to note that 6061 has a somewhat lower corrosion resistance than other alloy types (such 5052 aluminum alloy, which includes no copper) because of its copper presence. There might be some corrosive effects, such pitting, when in contact with alkaline soil, however this is mostly depending on the soil. Ammonia and ammonium hydroxide, as well as strong nitric acid, are very effective at corroding 6061. By completely covering the alloy in a protective layer, which 6061 alloy reacts well to, the corrosive effects can be eliminated [69].

Figure 3.3 Aluminum 6061

Table 3.6 Materials used to perform the FSW process of dissimilar material joining

No.	Materials	Purpose	Specification
1	Aluminium alloy sheet	The base material to be weld	Aluminium alloy 6061 3mm thickness
2.	Titanium sheet	The base material to be weld	Commercial pure titanium 3mm thickness.
3.	Fixture	Holding the welded material properly on the milling machine during the welding process	$200mm \times 150mm \times 50mm$ Mild steel
4.	HSS tool	To perform the welding activity by generating heat during the process and plasticized materials	18mm shoulder diameter, 2.5mm probe length, and 3.5mm (inner) and 5mm (outer) pin/probe diameter
5.	Expandable collate	To hold the FSW tool during welding	With a collates diameter of 18mm

3.3. Experimental Machines and Setups

3.3.1. Welding Machine

In Ethiopia, the FSW machine is not available in any of the manufacturing industries and scholarly universities. Hence, this study used the XHS7145 Computer Numerical Controlled (CNC) 3-axis milling machine as an FSW machine the machine specifications are depicted below the table:

Table 3.7 Technical specification of CNC milling machine

No	Part Name	Unit	Specification
1	Table working surface	mm	800 X 450
2	Max. Spindle Speed	Rpm	8,000
3	Spindle Motor	HP, KW	7.4, 5.5
4	CNC Controller	Type	Fanuc-0i MD
5	Tool Shank	Type	MAS-403 BT-40 Opt.: CAT-40

Figure 3.4 CNC milling machine with mounted fixture for FSW

3.4. Design of Fixture

Backing plates are required to resist the normal forces employed in FSW, as well as provide a stiff object to clamp the plates or sheets to be welded Material diffusivity of the backing plate material is a major element for conducting a proper FSW process [37]. In FSW, a fixture is

typically the most intricate and important part of the welding procedure. The workpieces need to be fastened to a smooth, strong backing plate so they can withstand the side and perpendicular forces that form while welding. The workpieces are often lifted and pushed apart by these pressures. The purpose of fixtures is to constrain the workpieces and prevent them from disengaging. To guarantee that the workpieces are held in place during the welding process, the fixtures that hold the materials to the backing plate should be placed as close to the joint as feasible.

3.4.1. Material for Fixtures

Proper selection of tool traverse and rotational speeds is important for heat generation, and the forces applied to the tool should be minimized to provide material flow around the tool pin. However, selecting the proper material for fixture development is good for getting defect-free FSW joints [70]. Materials such as mild steel, stainless steel, aluminum alloys, pure copper, medium carbon steel, etc. can be used as a backing plate.

During the FSW process, mild steel material is used due to its high strength and toughness [70], this material is used for the manufacturing of fixtures, backing plates, top plates, side supports, front support plate spacer (adjuster), and bottom plates.

3.4.2. Bottom backing plate

In FSW, fixtures are typically the most difficult and important part of the welding procedure. For the work parts to withstand the side and perpendicular forces that arise during the welding process, they must be clamped to a smooth, strong backing plate. The work parts are often pushed and lifted apart by these forces. The backing is placed under workpieces mainly for protection and the stability of blank/workpieces.

3.4.3. Top plate/ Clamp

The top backing plate usually adjusts plate thickness in different dimensions and holds the workpiece rigidly in the right position during the welding process by using tightening bots. The dimension of the top plate depends on the backing plate dimension. There are two top backing plates were welded on both the right and left side of the side supporter backing plate to fix and provide rigidity of the sheet/plate during the welding process.

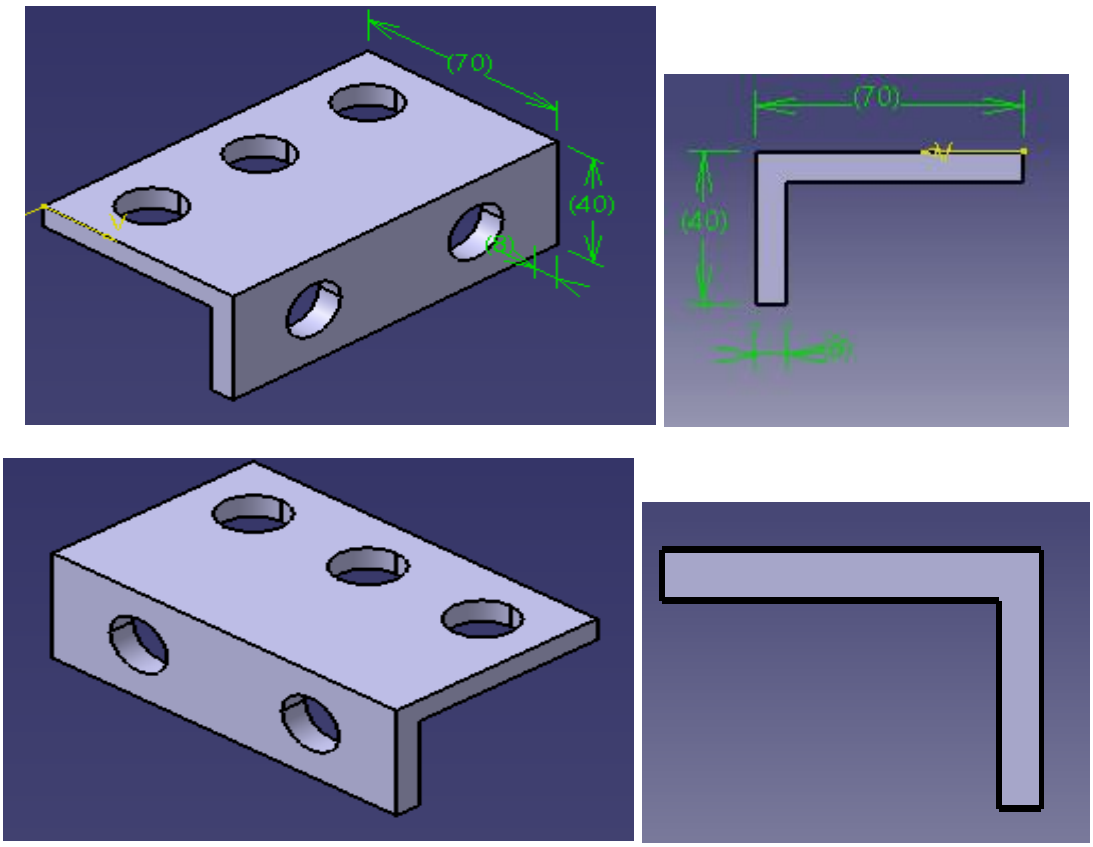

Figure 3.5: Dimensions of clamp (left side) & 3D model of Top plate/ clamp (right side)

3.4.4 Spacer (side adjuster) Plate

The side adjuster plate in this work adjusts the width of sheet/plate to be weld and additionally hold the sheet/plate to be weld against both vertical force and transverse force during plunging and welding time. The side adjuster is moveable and placed between the workpiece and the side support plate. It can be used to adjust the workpiece according to the appropriate welding position.

3.4.5 Front Supporter plate

This is required to prevent workpieces from moving longitudinally. Furthermore, it aids in maintaining the fixture's axial force and deflection, rotational force, and separation, all of which help to keep the workpiece from buckling as a result of thermal expansion [26]. The Front Support Plate serves as a locator and is used to secure the workpiece in accordance with welding instructions. It is welded to the bottom backing plate, side, and top plates.

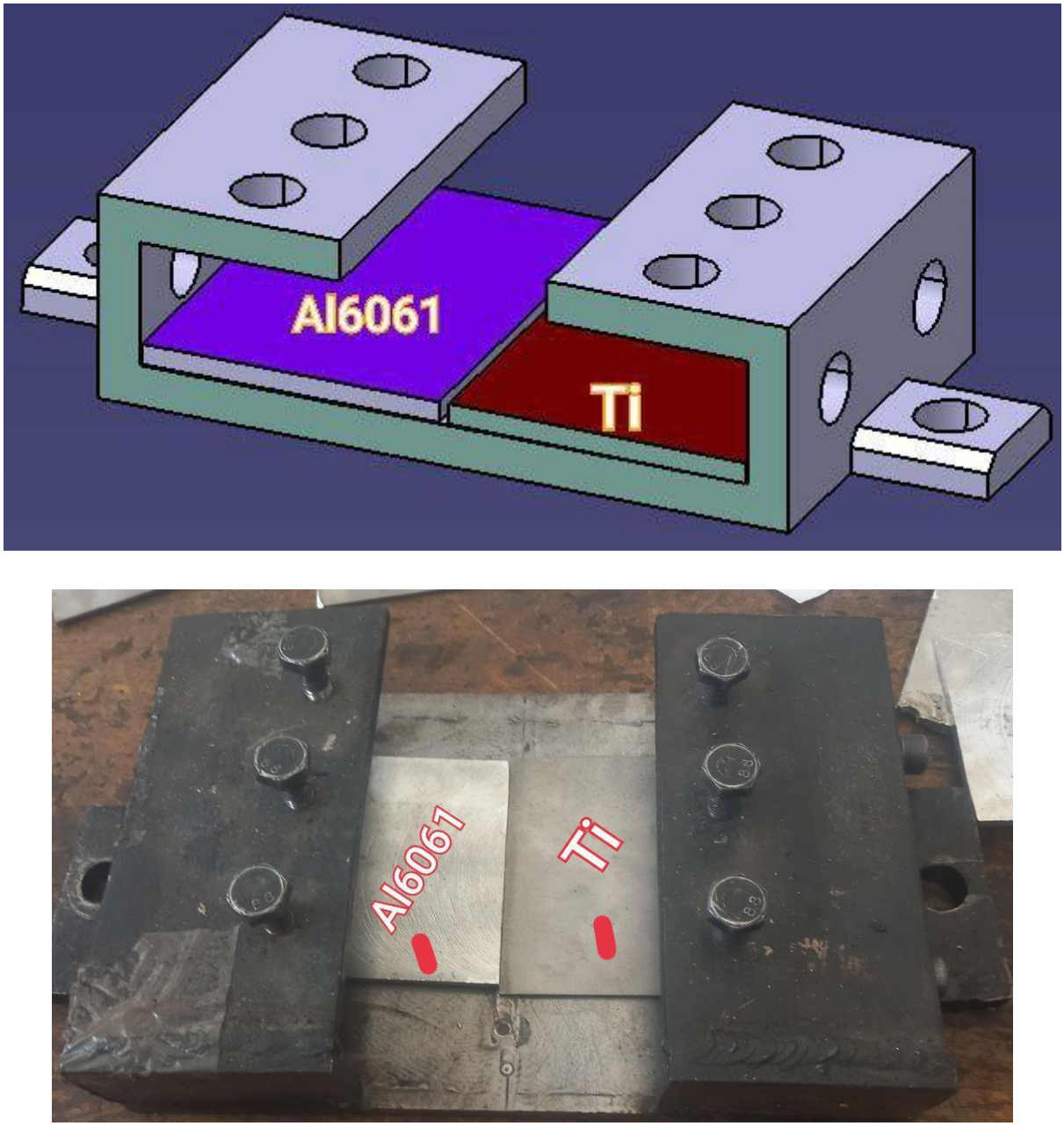

Figure3.6 Welding material Al6061 & Ti and fixture mounted on CNC milling machine

3.5. Design and fabrication of tool

A good tool may increase the maximum welding speed as well as the quality of the weld, so tool design is very important. At the welding temperature, the tool material must be robust, durable, hard, and wear-resistant enough. In order to reduce heat loss and thermal damage to the machinery further up the drive train, it should also have low thermal conductivity and good resistance to oxidation. It has been demonstrated that significant gains in productivity and quality can be achieved through advances in tool design. To improve the penetration depth and, consequently, the plate thicknesses that may be successfully welded, TWI has

created tools expressly for this purpose. An illustration of this is the "whorl" design, which enhances the downward flow of material by using a variable pitch thread or a tapered pin with re-entrant characteristics. Most tools have a concave shoulder profile, which keeps material from extruding out of the shoulder's sides, serves as an escape volume for material displaced by the pin, and maintains downward pressure for proper forging of the material behind the tool. When looking for commercially viable instruments for the welding of hard materials, material selection, design, and cost are crucial factors to take into account. Understanding the implications of the composition, structure, characteristics, and geometry of tool materials on their cost, durability, and performance is still being worked on. Tool designs are heavily influenced by the aluminum alloy sheet metal thickness. The instrument is made up of a shoulder and a pin/probe [70].

3.5. 1 Pin/probe of tool

The pin of the tool is part of the tool extruding from part of the tool's contracting surface. It can be threaded or non-threaded and is responsible for generating a mechanical mixing process in plasticized material. Only a fraction of the total heat is generated by the pin or probe of the tool. The pin or probe diameter (T) also depends on the thickness of sheet metal [29].

$$T = 0.8t + 2.2 \text{ mm} \quad (3.1)$$

Where T represents pin diameters and t represents the thickness of sheet metal

t =3mm, T= 0.8 *3 +2.2mm= 4.6mm

3.5.2 Shoulder of tool

The shoulder of the tool is the cylindrical surface responsible for generating the frictional heat [29].

Shoulder diameter (D) also depends on the thickness of sheet metal.

$$D = 2.2\ t + 7.3 \text{ mm} \quad (3.2)$$

Where D represents shoulder diameter and t is the thickness of sheet metal

t =3mm , D= 2.2*3+7.3mm= 13.9mm

The tool is prepared for the FSW process on the lathe machine. HSS alloy was employed in this experiment as the welding tool material. It is extremely hard, has outstanding wear resistance, and is more resilient. One can design and fabricate a simple attachment on the lathe tool post to handle or clamp the hand grinder on the lathe machine to grind square HSS tool material into a circular or round shape, as shown in Figure 3.8.

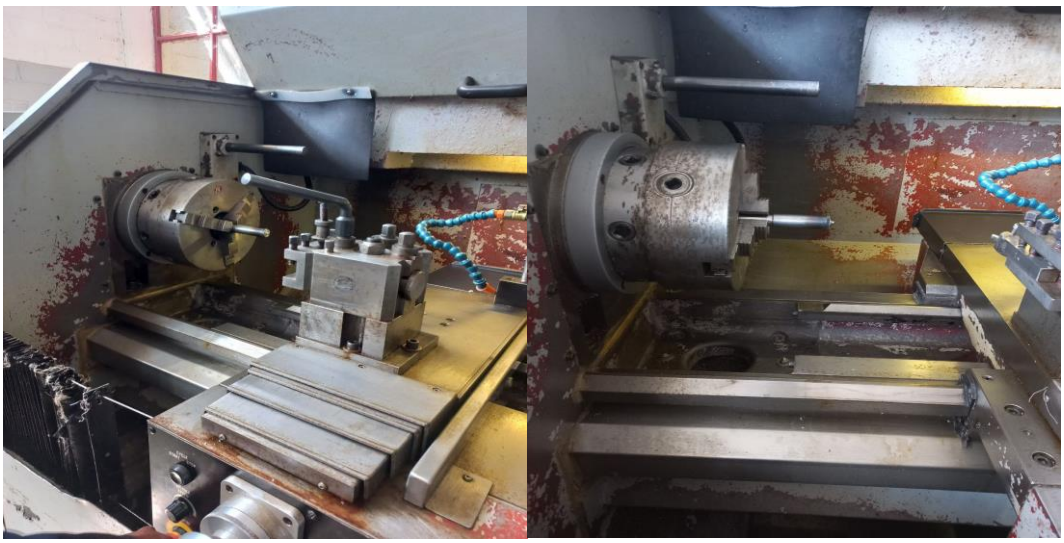

Figure 3.7: a) HSS tool preparation on lathe machine

The FSW tools that are used to perform all the welds are fabricated with the help of additional attachments on the lathe machine with dimensions, based on a different review of literatures, on the tool shown in Table 3.3. This tool consists of two main components: shoulder and pin, which are shown in Figure 3.9.

Table 3.8 Dimensions of the tool

Tool material	**Tool profile**	**Probe diameter (mm)**	**Pin length (mm)**	**Shoulder Diameter (mm)**
High Speed Steel	Cylindrical	4.6mm	2.5	13.9
	Conical	4.6		
	Square	4.6 mm		

Figure 3.8: HSS prepared tool for FSW

3.6. Welding specimen preparation

The target material, an AA 6061 and Ti plate with a butt joint structure, was chosen because it is most commonly utilized in the aerospace, automotive, and marine industries. Every specimen has its dimensions trimmed to 100 × 60 × 3 mm. Furthermore, a mechanical test was prepared in accordance with ASTM E8 following the welding of the specimen. The XHS7145 CNC machining center was used to carry out the experiment.

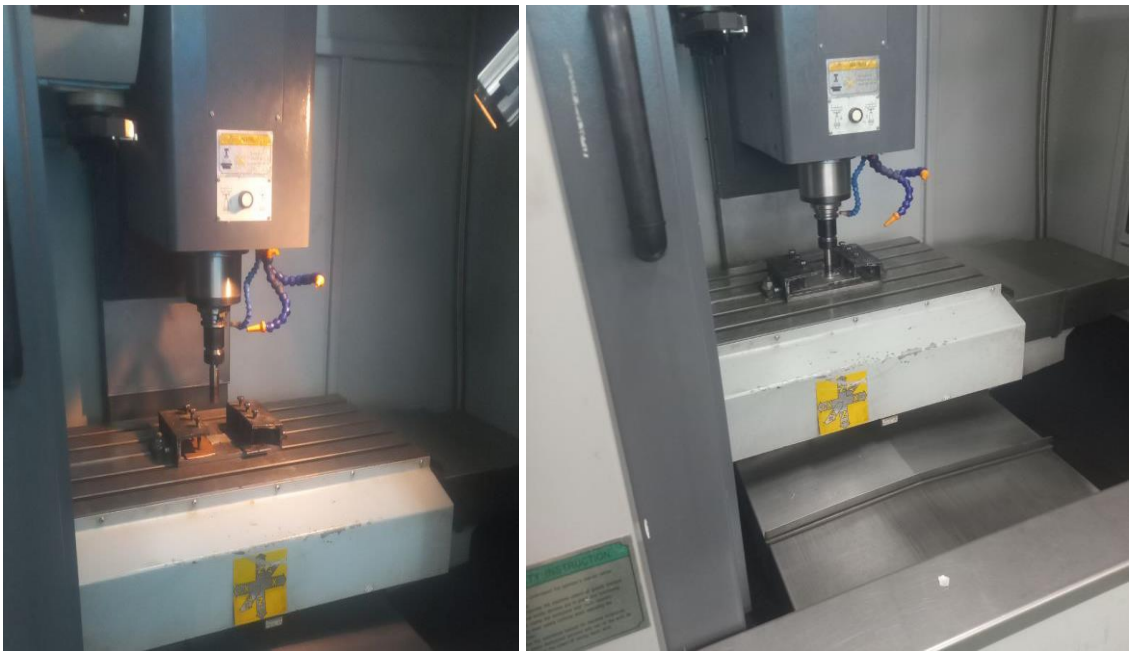

Figure 3.9 Setup for FSW on CNC milling machine

3.6.1 Approaches to the Milling Operation Design

Following the steps that are involved in Taguchi's Method, a series of experiments are to be conducted. In this thesis, FSW of dissimilar metals of aluminum 6061 and titanium using a

CNC milling machine at different parameters has been carried out. The procedures are as follows

3.7. Design of Experiment (DOE)

In this research, Taguchi orthogonal array methods were employed to design experimental runs for friction stir welding of dissimilar titanium and aluminum 6061 alloy metal. A Taguchi method was developed by Dr. Genichi Taguchi, who is a Japanese engineer [71]. Taguchi methods are a power tool for improving the production rate and product qualities with minimum production cost and processing times in machining operations. Taguchi method uses a special design of orthogonal arrays (OA) to study the entire parameter space with only a minimum number of experimental runs. OA provides a set of well-balanced (minimum) experiments with optimum settings of control parameters [71].

Generally, a process to be optimized has several control factors that have a direct impact on the target or desired value of the quality responses. The optimization then involves determining the best control factor or input parameter levels to achieve the targeted output response values.

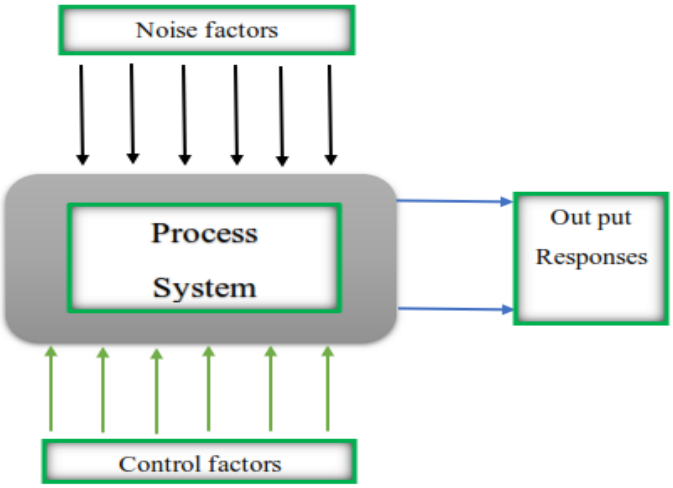

Figure 3.10: shows the designations models of Taguchi methods [71].

Designs of experiments have those Advantages

- ✓ Minimize the number of experimental runs
- ✓ Identify optimum values of parameters
- ✓ Assessment of experimental error can be made
- ✓ Qualitative estimation of parameters can be made
- ✓ Inference regarding the effect of parameters on the characteristics of the process can be made.[71]

Step 1: Identification of main functions and their side effects

The main function of this study is friction stir welding of dissimilar titanium and aluminum 6061 metals by using a CNC milling machine. by considering different welding parameters the welding is performed then the result could be evaluated on mechanical test and microstructural tests.

Step 2: Identify variables

Friction stir welding has main independent variables that are used to control the FSW process. those are:-

- welding speed,
- the tool's rotational speed,
- the pin profile of the tool,
- Dwell time
- Tool design

A. Tool rotation and Transverse speed

Two critical factors for FSW are the tool traverse speed (n, mm/min) along the joint line and the tool rotation rate (v, rpm) in either a clockwise or counterclockwise orientation. The tool's motion creates frictional heat inside the workpieces, which extrudes the surrounding softened plasticized material and forges it into place to create a flawless, solid-state connection. Heat is produced at the shoulder/work-piece interface and, to a lesser extent, at the pin/work-piece contact surfaces when the tool (rotates and) moves along the butting surfaces due to the dissipation of frictional energy. The type of alloy, rotational speed, penetration depth, and joint type are some of the variables that affect the welding speed. Increased tool rotation rates cause greater temperatures due to increased friction heating, which also intensifies material swirling and mixing. Because of the tool's rotation and traversing motion, softened material from the leading edge transfers to the trailing edge during traversing. An axial force is then applied to the trailing edge of the tool to consolidate the transferred material.[27]

B. Tool tilt and Plunge depth

In addition to the tool rotation rate and traverse speed, other important process parameters are tool tilt concerning the workpiece surface and plunge depth. A proper inclination of the spindle in the direction of trailing ensures that the tool's shoulder retains the material stirred

by the threaded pin and effectively transfers material from the pin's front to back. The tool is often identified by a tiny tilt angle (θ), and the blank material is locally backwardly extruded up to the tool's shoulder as it is inserted into the sheets. Furthermore, good welds with smooth tool shoulders depend on the pin's plunge depth—also known as the goal depth into the workpieces [29].

C. Tool Design

Heat generation, plastic flow, power consumption, and the consistency of the welded junction are all impacted by tool design. Because they have an impact on heat generation and the flow of plastic material, tool geometry factors including probe length, shape, and shoulder size are critical. An essential component of this welding procedure is the instrument. It is made up of a pin and a shoulder. The pin profile is essential to material flow, which in turn controls the FSW process's welding speed. The majority of the heat is produced by the shoulder, which also keeps the plasticized material from fleeing the workpiece. The material flow is influenced by both the tool pin and the shoulder.

The virtually spherical flow contours and well-defined weld nuggets that distinguish friction stir welds are contingent upon the process circumstances, welding parameters, and tool design employed [27, 29].

Step 3: Identify the objective function to be optimized

In the Taguchi method, the term signal represents the mean or desired value for the quality responses and term noise represents the undesirable value (standard deviation) for the responses [70]. The Taguchi approach uses a log function of the desired output as the objective function for optimization, classifying optimization problems into three categories based on the nature of the problem [71].

These are:

1. Smaller-the-Better,
2. Larger-the-Better and
3. Nominal-the-Best.

Signal-to-noise ratios (S/N) are log functions of desired output responses, serve as objective functions for optimization, and help in data analysis and prediction of optimum results.

In this study, surface roughness and material removal rates are the output responses to be optimized. Surface roughness and material removal rates have conflicting objectives in the

machining of materials. The objectives of surface roughness are decreasing the values of roughness as much as possible to improve the quality of machined products, while the objectives of material removal rates are to increase as much as possible to raise the production rates by minimizing processing times.

Therefore, the appropriate Taguchi signals to noise (S/N) ratios for surface roughness are smaller the better.

Mathematically, it is expressed as shown in equation 3.11.

(S/N = -10log10 (MSD)).

- $For\ smaller\ is\ better$: $MSD = (y1\ 2 + y2\ 2 + \cdots)/n$ (3.3)
- $For\ biger\ is\ better$: $MSD = (1/y1\ 2 + 1/y2\ 2 + \cdots)/n$ (3.4)
- $For\ nominal\ is\ best$: $MSD = [(y1 - y0\ )\ 2 + (y2 - y0\ )\ 2 + \cdots]/n$ (3.5)

In addition to the design of an experiment, Taguchi's approach prescribes analysis methods to Identify the influences of the factors and their interactions (main/interaction effects analysis) Determine the best mix of relevant factors by ranking them according to how much of an impact each has on the response variable's variability (typically accomplished using ANOVA). This combination might be more than what can be tested according to the OA.

It is typically necessary and best practice to conduct a confirmation experiment once the ideal condition has been identified and predicted performance has been estimated [72].

Step 4: Identify the levels of machining parameters

Table 3.9 lists the FSW parameters and their corresponding levels. The rotational speed(1100, 1400, 1600) rpm , transvers speed(50,60,80)mm/min, tool pin profile(cylindrical, rectangular, conical) and dwell (5,10,15) sec. which is analogous to some of the previous values found in the kinds of literature.

Table 3.9 Selecting process parameters and their values

Process parameter	**Level 1**	**Level 2**	**Level 3**
Rotational speed	1100 r/min	1400 r/min	1600 r/min
Transverse speed	50 m/min	60 m/min	80 m/min
Tool pin profile	Cylindrical	rectangular	Conical
Dwell time	5 sec	10 sec	15 sec

Step 5: Select a suitable Orthogonal Array and construct the Matrix

The selection of a suitable Orthogonal array (OA) is an important task in the Taguchi method. Orthogonal arrays are a special standard experimental design that requires the minimum number of experimental runs to find the main factor effects on output responses. The minimum number of experimental trials required in an orthogonal array is given by [72]:

$$Nmin = 1 + F(L - 1) \quad (3.6)$$

Where N_{min} is the number of experiments to be conducted, F is the number of control factors, and L is the number of levels, In this study, the number of control factors (F) was equal to four namely Rotational speed, Transverse speed, Tool pin profile and dwell time and each control factors have three levels, L= 3.

Therefore, $N_{min} = 1 + 4\ (3-1) = 9$

The standard of OA types is tabulated in Table 3.6 below. L9 orthogonal array types are appropriate for four factors, and three level parameters.

Table 3.10 Standards of design of experiments [64]

Levels factors	Number of experimental runs	Orthogonal array types
2^3	4	L_4
2^7	8	L_8
2^5		
2^3		
3^4	9	L_9
3^3		
4^5	16	L_{16}
2^{15}		
$2^1 \times 3^7$	18	L_{18}
$2^2 \times 3^6$		
3^7		
$2^1 \times 3^6$		
$2^1 \times 3^4$		
$2^1 \times 3^3$		
3^3	27	L_{27}

Therefore, L9 (3^4) was selected in this study to construct the matrix. The most suitable orthogonal array for experimentation is L9 array as shown in Table 3.10

3.7.1 Taguchi design using Minitab

Taguchi design of experiment L9 orthogonal array also analyze through Minitab 21.2 software as follows:

1. Open Minitab 20. Software > choose Stat > DOE > Taguchi > Create Taguchi Design > select type of design and number of factor > ok
2. Choose Designs > L9 then click ok
3. Choose Factors > edit the name of the factors and give level values > ok
4. Click ok then Taguchi design is created and number of welds to be fabricated are known

Taguchi Design

WORKSHEET 1

Taguchi Design

Design Summary

Taguchi Array	L9(3^4)
Factors:	4
Runs:	9

Columns of L9(3^4) array: 1 2 3 4

	C1	C2	C3-T	C4
	Rotational speed	Welding speed	Tool pin profile	Dwell time
1	1100	50	Conical	5
2	1100	60	square	10
3	1100	80	Cylinderic	15
4	1400	50	square	15
5	1400	60	Cylinderic	5
6	1400	80	Conical	10
7	1600	50	Cylinderic	10
8	1600	60	Conical	15
9	1600	80	square	5

Figure 3.11: Taguchi orthogonal array

3.8. Mechanical Testing and Microstructure Examination

3.8.1 Tensile Test

A tensile test is a fundamental mechanical test in which a well-prepared specimen is loaded within controlled conditions while the applied load and the specimen's elongation are measured. The sample dimensions of 100 mm x 10 mm x 3 mm used depend on standard and machine capacity as shown in Figure 3.12. The samples were prepared to the proper dimensions required for the test, according to ASTM E-04 standards [73]. This experiment aims to gather information about each experiment's result to get the optimum UTS. As shown in Figure 3.13, The UTM consists of a 150 mm displacement crosshead with a 50 KN maximum piston stroke and a 6 mm/sec speed.

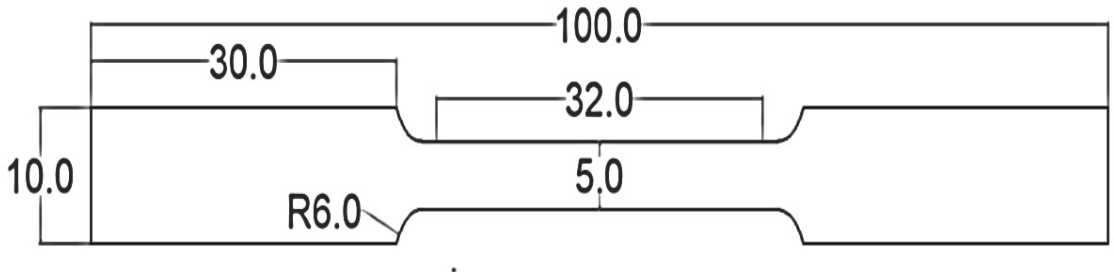

Figure 3.12:-tensile test specimen dimension

Tensile testing is one of the most fundamental tests for engineering and provides valuable information about a material and its associated properties. The sample dimensions were 100 mm × 10 mm × 3 mm depending on standard and machine capacity. The samples were already machined to the proper dimensions required for the test, according to ASTM E8-40 standards. Three samples of each experiment were tested in the Kinston load frame, and the data was gathered into an Excel spreadsheet. The purpose of this experiment was to gather information about each experiment result to get optimum UTS, so that important mechanical properties could be determined. Each specimen was measured with the calipers to determine the diameter of the cross-section. Once the tensile test was finished, the gage length—typically 32.00 mm was established and scribed onto the specimen to allow for the measurement of the separation between the two markings. To make sure the software only recorded the tensile load delivered to the specimen, the load cell was reset to zero. The specimen was evenly spaced between the two clamps when it was placed into the Instron load

frame's jaws. In order to verify that the transverse extensometer was spanning the entire diameter of the specimen and that the axial extensometer was accurately set when attaching it to the gage, the axial and transverse extensometers were attached to the reduced gage section of the specimen. Better data are produced as a result of this precaution, which also keeps the extensometers safe.

Figure 3.13: Tensile test machine

Figure 3.14: prepared tensile test specimen and after tensile test

3.8.2 Hardness Test

Hardness is a material's ability to withstand plastic deformation; typically as determined by penetration. It wasn't an essential characteristic of the substance. This property's value was determined by a defined dimension procedure; hence the hardness value will vary according to the hardness method applied. A specially formed indenter that is noticeably harder than the test sample is used in all hardness tests. With a particular force, this indenter was pressed into the sample's exterior. To get a hardness value, the indent's size or depths are measured. Because hardness measures are quick and regarded as Tobe non-destructive tests when the marks or indentations they generate are in low-stress locations, they were widely utilized for the quality control of materials [74]. There are various ways to measure hardness; Brinell, Vickers, and Rockwell hardness tests are commonly employed. Vickers' hardness test was utilized in this experiment to gauge the sample's extrusion properties. The size of an imprint left by a pyramid-shaped diamond indenter under load is used in the Vickers hardness test to quantify a material's hardness. A calibrated microscope was used to measure the size of the impression made when the diamond was placed onto the material at a measuring range of up to about 10 Kgf (kilogram-force).The Vickers hardness number (HV) was calculated using the following formula:

HV = constant * test force/surface area of indentation.

$$= 0.102*2F\ (\sin 1360\ /2)/d1d2 \tag{3.7}$$

Where; F is indentation forces and d1d2 represents indentation area.

The Vickers hardness should be stated as 400 HV/10, indicating that 10 kg of force was used to achieve a Vickers hardness of 400. One of the key benefits of the Vickers hardness test is that very exact readings can be obtained, and all metal types and surface treatments are tested using the same kind of indenter.From ten samples for each test, 10 mm × 10 mm × 2 mm specimens were cut at the cross section for microstructural study and macro-hardness measurement from each sample. Before macro hardness, measurement welded sample mounted and ground with 400, 800, 1200, and 2000 grit size sandpaper and polished by diamond suspension. Macro-hardness was measured with Vickers micro-hardness tester HVS-50 machines just after the microstructural test by using both 5Kgf and 10Kgf.

Figure 3.15 Vickers hardness testing machine

3.4.3 Microstructure Observation

Microstructure observation is used to determine grain size, shape, and distribution of various phases and inclusions which is important as these affect the mechanical properties of the metal. This process follows some procedures to observe the structures. The specimen preparation of the sample to examine the microstructure was cutting off the specimen, grinding, polishing, etching, and observing the microstructure by optical microscopy.

Determining grain size, shape, and distribution of various phases and inclusions was important as these affect the mechanical properties of the metal. The microstructure would expose the mechanical and thermal treatment of the metal, and it may be possible to predict its behavior under a given set of conditions. The procedure of specimen preparation metallographic test was as follows.

3.4.3.1 Cut Specimen from the Sample

The first step of any microstructural test is to; cut the specimen from the sample accurately to the required testing size. For this work, nine samples were selected to examine microstructures which is seven from the welded sample, and two samples from Al6061 and Ti sheet metal were selected to examine microstructure for each test. Then two-centimetre length specimen was cut from each sample by using a consumable high-speed rotating disc abrasive cutter.

3.4.3.2 Mounting the specimen

The second step of specimen preparation was mounting specimens for microstructural analysis. Specimens cut from each sample were fixed in a holder to be managed easily during polishing, which is necessary to examine the microstructure. The RB 206 Metpress-A machine using MC-PRC (phenolic resin conductive powder), did the mounting operation. The maximum heating temperature was 2500C and took 1020 seconds to 17 minutes (i.e., 300 sec for heating time, 300-sec holding time, and 420 sec for cooling time) for each sample. The machine consists of an upper ram, a lower ram, and a heating part that is cooled by water controlled by a solenoid valve. A small piece of the specimen was increased into a 32 mm diameter pellet before grinding and polishing.

Figure 3.16 Hot mounting press (RB 206 Met press-A)

3.4.3.3 Grinding of Specimen

After a mounting operation, two grinding processes were applied to each specimen. The first one was a rough grinding using silicon carbide paper and the second one intermediate grinding process using an RB 204 Metpol-II machine. The specimen was ground by the same method and procedure. Firstly, the specimen was ground with 400 grit size silicon carbide paper for about two minutes. Again grinded by the following carbide papers 800, 1200, and 2000 grit size respectively. After each step of grinding dust particles are washed by water and removed by compressor. The rough grinding of the sample was continued until the surface is flat and free from nicks, burrs, etc.

3.4.3.4 Polishing of specimen

The attention used in the previous grinding operation phase is a major factor in the success of fine polishing. The Vickers hardness should be stated as 400 HV/10, indicating that 10 kg of force was used to achieve a Vickers hardness of 400. One of the key benefits of the Vickers hardness test is that very exact readings can be obtained, and all metal types and surface treatments are tested using the same kind of indenter. In this step of specimen preparation, the specialized liquid spray on the surface of the polishing cloth was diamond suspension liquid used as spray form. Ten specimens of a sample of each test were polished four times before the etching. In each of the polishing steps, the specimen is washed with water and dried using the pressurized compressor. The process continued up to four times until the specimen was free from any scratches and a shine surface was obtained.

3.4.3.5 Etching

The last stage of specimen preparation was etching, which allowed the sample to display several structural features of the metal. This was achieved by exposing the polished surface to chemical action using the proper reagent. 25 ml of hydrochloric acid, 25 ml of nitric acid, 25 ml of methanol, and one droplet of hydrogen fluoride mixture were used to etch all of the samples. Every sample was etched for a length of 30 seconds. Subsequently, the specimen's glossy surface is placed on the optical microscopy table to analyze its microstructure characteristics. There were five magnification ranges available for optical microscopy: 50×, 100×, 200×, 500×, and 1000×. The area under scan measures 104 mm by 102 mm. qualities of the microstructure as measured using a 20 micrometer label.

Figure 3.16: Optical Microscopy

3.9. Methods

3.9.1 Determination of Working Limits of Parameters

A popular statistical method for identifying process attributes that are statistically significant and affect the study's outcome is the Analysis of Variance, or ANOVA [75]. ANOVA is a tool used by many researchers to identify the factors that impact the study response percentage. Consequently, the current investigation analyzed and determined the most crucial process factors that improved the study's response. Pareto principles are used to choose and calculate parameters that were obtained from a previous similar study that looked at the average proportion of contribution across twelve article periodicals. A fishbone diagram is another tool used to identify the underlying causes of the specified parameters. There is also an assessment of the magnitude of RPM levels from earlier, related investigations. The choice is based on highly or frequently used magnitudes for different aluminum alloys by scholars. Based on magnitudes that are remarkably close to the chosen RPM magnitudes, the remaining magnitude levels are picked.

Table 3.11 Parameters with its contribution to the response of mechanical properties of FSW joint

No	Parameter with % contribution								Ref.
	TS	TRS	TPS	TPP	PD	TTA	AL	ERROR	
1	3.47	3.04		26.56	8.94			57.99	[76]
2	40.5	18.13			25.84			15.25	[77]
3	36.64	55.18				5.63		2.54	[78]
4	5.37	85.1	4.01					5.52	[79]
5	48.7	15.13	27.48					8.52	[80]
6	33	41					21	5	[81]
7	12.69	57.56				22.97		6.77	[82]
8	13.5	67.2				15		4.3	[83]
9	31.05	44.33		19.55				5.06	[84]
10		77.17	6.89	15.85				0.09	[85]
Average	24.99111	46.384	12.79333	20.65333	17.39	14.53333	21		

** TS – Traverse speed; TRS – Tool Rotational Speed; TPP Tool pin profile; TSD – Tool Shoulder diameter; PD – Plunge Depth; TTA – Tool Tilt Angle; AL - Axial load; D/d - Shoulder diameter-to-pin diameter ratio

Based on the table (3.11) results to identify the vital parameters from the trivial ones, the Pareto principles are used. The Pareto diagram essentially states that 80% of quality problems in the product or service are caused by 20% of the problems in the production or service processes.

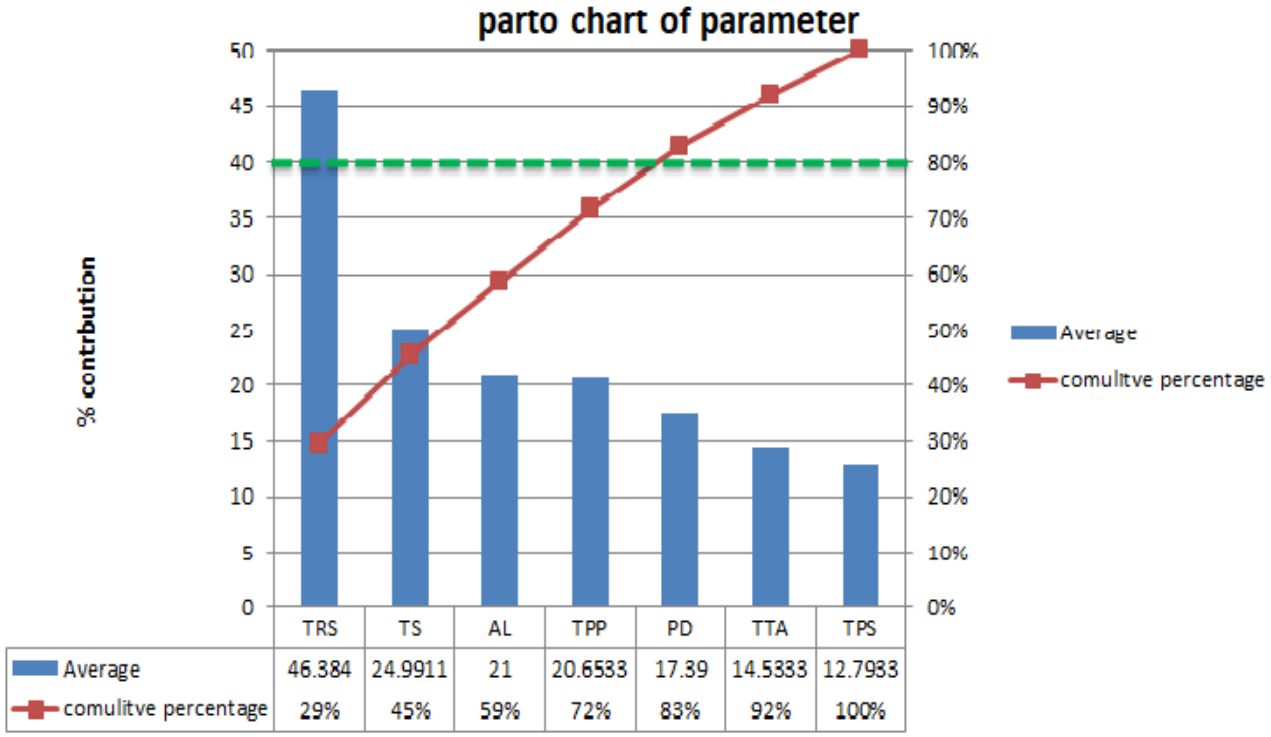

Figure 3.17 Parto chart of parameter

Based on the Pareto diagram, the first four parameters out of seven consist of 80% of the total parameters, namely: tool rotational speed, tool traverse speed, tool pin profiles, and axial load, which are the most vital parameters. However, axial load is not possible to control on a 3-axis CNC machine. Instead of axial load, consider plunge depth as a process parameter because plunge depth is directly proportional to axial load. When increasing plunge depth, the axial force also increases and generates high heat. This high amount of heat affects grain growth in the nugget zone. Low plunge depth decreases the axial load, which leads to low heat supply and improper material flow. Therefore, for producing a good quality weld, adequate plunge depth and forging pressure are required for deep penetration. To achieve the downward pressure, set an adequate plunge depth for the tool to fully penetrate.

3.9.2 Determination of Working Limits of levels

To select the appropriate rotational and traverse speeds for the target materials of AA 6061 and pure Ti , a review of the existing literature that is like this study was conducted, and the levels were chosen based on their frequency. i.e., which level magnitudes scholars frequently use, and the level magnitudes that impart the highest response value are selected.

3.9.2.1 Determination of RPM levels

The selection of tool rotational speeds selected from different scholars as shown in the table 3.12.

Table 3.12 Selections of tool rotational speed

No	Title	Material	Initial RPM	Optimized RPM	Result	Refer
1	Study on the Joining of Titanium and Aluminum Dissimilar Alloys by Friction Stir Welding	TC1 Ti alloy and LF6 Al alloy	750, 950, 1500	950	131MPa	[13]
2	Using a biogeography-based optimization algorithm, multi-objective optimization of the Friction Stir Welding process parameters of AA6061-T6 and AA7075-T6	AA6061-T6 and AA7075-T6	800, 1000, 1200, 1400 and 1600	1200	T.S. = 256 MPa H.S. = 71.5 HV	[86]
3	Impact of welding speed on filler-induced FSW AA6082 and AA5052 junctions' mechanical characteristics and corrosion resistance rates	AA6082 and AA5052	1150	1150	177 Mpa 93 Hv	[87]
4	Influence of FSW Parameters on Dissimilar Joints AA6061-T6 and AA5052-H32	AA5052- H32 and AA6061-T6	800, 950, 1100	1100	181 MPa 90 HV	[88]
5	Friction Stir Welding of aluminum 6061-T6 in presence of water cooling: analyzing mechanical properties and residual stress distribution	6061-T6	600, 1000 and 1400	1400	T.S. = 251 MPa H.S. = 98 Hv	
6	Hybrid technique for multi-objective optimization of friction stir welding process parameters for connecting dissimilar aluminum alloys AA5083 and AA6063	AA5083 And AA6063	700, 900 and 1100	900	T.S. = 161.2 MPa H.S. = 85.25 Hv	
7	Dissimilar FSW of thick plate AA5052- AA6061 aluminum alloys: effects of material positioning and tool eccentricity	5052-H32 and 6061 – T6	1120	1120	215Mpa 70 HV	
8	Examining the Effects of Welding Parameters on the Microstructure and Mechanical Properties of the Dissimilar Al Alloy Welded Joints, FSW 5052 and 6061	5052-H32 and 6061 – T6 5mm	900, 1100	1100	165.84MPa 70 HV	

9	Response Surface Methodology (RSM) optimization of friction stir welding settings for aluminum alloys AA6061 and AA7039	AA 6061 and AA 7039	760, 800, 900, 1000 and 1040	900	T.S. = 175 MPa H.S. = 79.3 Hv	
10	Modeling and optimization of Friction Stir Welding on AA6061 Alloy	AA 6061	800, 950, 1100, 1250 and 1400	1100	143.5 Mpa 95.53 Hv	
11	Process parameter optimization for friction stir welding using the Taguchi method to combine A6061 and A6082 alloys	A6061 and A6082	900, 1550, 2200	1550	267.74 MPa and 80.55 HRB	
12	Investigation of welding parameter dependent microstructure and mechanical properties in friction stir welded pure Ti joints	Cp-Ti plates	200	200(300mm/min)	190Hv	
13	Selection of best process parameters for friction stir welded dissimilar Al-Cu alloy: a novel MCDM amalgamated MORSM approach	AA6061-T6 and pure copper	800, 1200, 1600, 1800	1600	121.512Mpa, 105.35Hv	[47]
14	Simulation and Adjustment of Friction Stir Welding Process Settings for Differing Aluminum Alloys	aluminum alloy of 6061 and 2024	1500, 1700, 1900	1700	182.8Mpa	[55]
15	Design and Fabrication of Friction Stir Welding Setup on Conventional Milling Machine to Join and Characterize AA 6023- T6 alloy sheet	Aluminum alloy 6023 T6	1250,1600, 2000	2000	194.67 MPa and 53.63 HV	
16	Using Taguchi and Grey Relational Analysis, Multi-Objective Process Parameter Optimization of Friction Stir Welding on 6061 Aluminum Alloy	6061 AA	900, 1200, 1400	1400	256 MPa	[66]
17	Experimental Investigation of Aluminum Alloy and Polymer Joints Made by Friction Stir Welding Process	AA6023 and HDPE sheets	850, 1000, 1250	1250	1.96 MPa	[89]
18	Optimizing procedure settings for Friction Stir Welding of two different aluminum alloys (AA5052–H32 and AA6061–T6)	AA6061–T6 and AA5052–H32	900, 1100, 1400	1400	183.04Mpa	[70]

The magnitude of parameters is selected based on the frequency of the scholars most used.

Table 3.13 shows the parameters selected for this thesis work.

RPM	Tensile Test	Hardness	Frequency	Rank
200		190Hv	1X	
900	T.S. = 175 MPa	H.S. = 79.3 Hv	2X	2
	T.S. = 161.2 MPa	H.S. = 85.25 Hv		
950	131MPa		1X	
1100	181 MPa	90 HV	3X	1
	165.84M Pa	70 HV		
	143.5 Mpa	95.53 Hv		
1120	215Mpa	70 HV	1X	3
1150	177 Mpa	93 Hv	1X	
1200	T.S. = 256 MPa	H.S. = 71.5 HV	1X	
1250	1.96 MPa	83.4Hv	1X	
1400	T.S. = 251 Mpa	H.S. = 98 Hv	3X	1
	256 MPa	55.6Hv		
	183.04Mpa	76.40 HV		
1550	267.74 MPa	80.55 HRB	1X	3
1600	121.512Mpa	105.35Hv	1X	
1700	182.8Mpa		1X	
2000	194.67 Mpa	53.63 HV	1X	

Based on the above table it is possible to select 1100, 1400 or 1600 rpm as the rotational speed magnitude for welding of dissimilar AA6061 and pure-Ti materials. The first magnitude gap is not equal to the second and third. The reason for this is that most scholars achieve maximum tensile strength at a rotational speed of 1100 rpm and achieve maximum tensile strength at 1400 rpm or 1600 rpm

3.9.2.2 Determination of Traverse speed levels

The selection of level magnitudes of traverse speed is based on the selected mm/min magnitudes.

Table 3.14 Selection of Transverse Speed

	Titel	Material	Initial traverse speed	Optimized traverse speed	Result
1	Study on the Joining of Titanium and Aluminum Dissimilar Alloys by Friction Stir Welding	TC1 Ti alloy and LF6 Al alloy	60,95,118,150	150	131MPa
2	Using a biogeography-based optimization algorithm, multi-objective optimization of the Friction Stir Welding process parameters of AA6061-T6 and AA7075-T6	AA6061-T6 and AA7075-T6	150, 160	150	T.S. = 256 MPa H.S. = 71.5 HV
3	Impact of welding speed on filler-induced FSW AA6082 and AA5052 junctions' mechanical characteristics and corrosion resistance rates	AA6082 and AA5052	40,60,80	80	177 Mpa 93 Hv
4	Influence of FSW Parameters on Dissimilar Joints AA6061-T6 and AA5052-H32	AA5052-H32 and AA6061- T6	40,60,80	60	181 MPa 90 HV
5	Friction Stir Welding of aluminum 6061-T6 in presence of water cooling: analyzing mechanical properties and residual stress distribution	6061-T6	20, 50, 80	50	T.S. = 251 MPa H.S. = 98 Hv
6	Hybrid technique for multi-objective optimization of friction stir welding process parameters for connecting dissimilar aluminum alloys AA5083 and AA6063	AA5083 And AA6063	40,60,80	60	T.S. = 161.2 MPa H.S. = 85.25 Hv
7	Dissimilar FSW of thick plate AA5052- AA6061 aluminum alloys: effects of material positioning and tool eccentricity	5052-H32 and 6061 – T6	50,70,90	90	215Mpa 70 HV

8	Examining the Effects of Welding Parameters on the Microstructure and Mechanical Properties of the Dissimilar Al Alloy Welded Joints, FSW 5052 and 6061	5052-H32 and 6061 – T6 5mm	28	28	165.84M Pa 70 HV
9	Modeling and optimization of Friction Stir Welding on AA6061 Alloy	AA 6061	30,60,90	60	143.5 Mpa 95.53 Hv
10	Process parameter optimization for friction stir welding using the Taguchi method to combine A6061 and A6082 alloys	A6061 and A6082	46,56,80	80	267.74 MPa and 80.55 HRB
11	Investigation of welding parameter dependent microstructure and mechanical properties in friction stir welded pure Ti joints	Cp-Ti plates	50,150,200, 300	200	190Hv
12	Simulation and Adjustment of Friction Stir Welding Process Settings for Differing Aluminum Alloys	aluminum alloy of 6061 and 2024	30,60,90	60	182.8Mpa
13	Design and Fabrication of Friction Stir Welding Setup on Conventional Milling Machine to Join and Characterize AA 6023- T6 alloy sheet	Aluminum alloy 6023 T6	12.5, 25, 50	12.5	194.67 MPa and 53.63 HV
14	Multi-Objective Process Parameters Optimization of Friction Stir Welding on 6061 Aluminum Alloy using Taguchi and Grey Relational Analysis	6061 AA	37.5, 42.5,47.5	37.5	256 MPa
15	Experimental Investigation of Aluminum Alloy and Polymer Joints Made by Friction Stir Welding Process	AA6023 and HDPE sheets	40, 50, 63	50	1.96 MPa
16	Optimizing procedure settings for Friction Stir Welding of two different aluminum alloys (AA5052–H32 and AA6061–T6)	AA6061–T6 and AA5052–H32	40,50,60	40	183.04Mpa

Table 3.15: Selected traverse speed

transferred speed (mm/min)	Tensile Test	Hardness	Frequency	Rank
12.5	267.74 MPa	80.55 HRB	1X	3
28	215Mpa	70 HV	1X	3
37.5	121.512Mpa	105.35Hv	1X	3
40	194.67 Mpa	53.63 HV	1X	3
50	181 MPa	90 HV	2X	2
	182.8Mpa			
60	131MPa		4X	1
	165.84M Pa	70 HV		
	T.S. = 256 MPa	H.S. = 71.5 HV		
	183.04Mpa	76.40 HV		
80	T.S. = 161.2 MPa	H.S. = 85.25 Hv	2X	2
	1.96 MPa	83.4Hv		
90	143.5 Mpa	95.53 Hv	1X	3
150		190Hv	2X	2
	T.S. = 175 MPa	H.S. = 79.3 Hv		
200	T.S. = 251 Mpa	H.S. = 98 Hv	1X	3

Table 3.16 Summary of Selected speed of tool rotation and transfer or welding speed

Rotational Speed (rpm)	Traverse speed (mm/min)
1100	50
1400	60
16000	80

3.10. Optimization Techniques

Numerous academic fields employ optimization techniques to identify solutions that maximize or minimize certain study criteria, such as minimizing expenses in the creation of a thing or service, maximizing revenues, minimizing the amount of raw materials needed to make a good, or maximizing production..There are many methods for optimization of process parameters for different type's materials, which are listed below;

- Nature algorithm
- Taguchi and Grey relational analysis
- Genetic algorithm
- Tabu search
- Ant colony algorithm etc

3.10.1. Taguchi method

The Taguchi method is a methodical approach to applying experimental technique design in order to create and enhance product quality. Process parameter optimization holds the key to achieving outstanding quality in the Taguchi technique without increasing costs. The Taguchi method evaluates the data using signal-to-noise (S/N), a statistical performance metric. Using the Taguchi approach, there are three ways to calculate the S/N ratio: larger is better, nominal is best, and smaller is better. However, selecting the appropriate S/N ratio calls for some process comprehension, real world experience, and aptitude. Since the goal of this research is to determine which higher hardness and tensile strength are associated with better welding performance, a larger is better S/N ratio was chosen. This was computed using the following equation [47].

$$S\,N\,(\eta) = -10\,\log\,10\,1\,n\,\sum\,1\,y\,2\,ijk\,n\,i=1 \qquad (3.8)$$

Where n is the number of replications and yijk is the response value of the ith performance characteristic in the jth experiment during the kth trial.

3.10.2 Grey relational analysis

Grey relational analysis (GRA) is a model of grey system theory. It was developed by Deng Julong of Huazhong University of Science and Technology. Grey relational analysis (GRA) or Grey analysis is a technique by measure the degree of estimate among sequences relating to the grey relational grade (GRG). It consists of four steps: first, the input data must be

normalized; then, the deviation sequence must be calculated; next, the grey relational coefficient must be estimated; and last, the grey relational grade (GRG) must be estimated using the weights. The AHP approach and the CRITIC method can also be used to compute the weights.GRA uses a specific concept of information, defining situations with no information as black, and those with perfect information as white. The steps in Grey relational analysis include normalizing the data, determining the deviation sequence, and estimating the Grey relational Coefficient (GRC). Grey relational grade is a commonly used metric in grey relational analysis to quantify the degree of link between sequences. Grey relational analysis has been used by several scholars to optimize the control parameters with multi-responses through grey relational grade[70]. The Grey relational analysis is widely used to combine all the considered performance characteristics into a One of the drawbacks of the Taguchi method is used to optimize only a single parameter (i.e., Mono-objective optimization). The combination of Taguchi with a grey relational analysis method can optimize multiple parameters easily and effectively [70]. GRA is a useful technique for multi-response condition optimization. This analytical technique was employed to resolve the complex relationships between the multiple-objective replies [48]. In order to determine grey relational coefficients and grey relational grades, grey relational analysis uses data normalization. It examines the ideal configuration and uses ANOVA to calculate the ideal grey relational grade estimate. One value that can be utilized in optimization issues as the only characteristic.

3.10.2.1 Data normalization In GRA method

Based on the response values' intended nature, there are three forms of normalization for response values. The lowest values of the objective function are anticipated in the initial normalization, which follows the maxim "the smaller the better." The second approach, where the objective function has average values, is "nominal the better." The third one is ‘higher the better’ where highest values of the results are expected. Assembling a comparable sequence that is distinct from the original sequence begins with normalizing the data. The normalization of the experimental data is represented as the interval between zero and one. When the target's directions in the sequence diverge or the arrangement scatter range is excessively wide, the procedure is required [48]. The following equation [70] predicts the properties that normalization will scale the response into an appropriate range, so if the reaction is to be enhanced, larger is preferable.

$$Xi(k) = \frac{Xi\,°(k) - \min Xi°\,(k)}{\max Xi°\,(k) - \min Xi°\,(k)} \quad (3.9)$$

Where

The reference sequence is Xi0 (k).

The sequence following data pre-processing (comparability sequence) is xi*(k).

The biggest value in the reference sequence is max xi0 (k).

The smallest value in the reference sequence is min xi0 (k), where i = 1, 2, m and k = 1, 2..., n represent the number of experiments and experimental data, respectively.

3.10.2.2 Deviation sequences and grey relational coefficients Calculation (GRC)

The next step is to take the normalized data and use the following calculation to get the gray relationship coefficient, ξi (k). The GRC is used to describe the correlation between the comparability sequence and the reference sequence. The GRC (ξ) is calculated in order to integrate the data derived from equations [66].

$$\Delta 0\ i(k) = \|xo * (k) - xi *(k)\|$$

$$(\Delta\min(k) + \xi\Delta\max(k)\ )/(\Delta 0i(k) + \xi\Delta\ \max(k)\ ) = \xi(xo\ *(k) - xi\ *\ (k)\ ). \quad (3.11)$$

Prior to computing the GRC, it is crucial to compute the deviation sequences, where ξ is the differentiating coefficient and Δ0i(k) is the deviation sequence of the comparability sequence (xi ∗(k) and reference sequence (xo ∗(k). The deviation sequences are computed using an equation.

3.10.2.3 Grey relational grades (GRG) calculation

Following a grey relational generation of the discrete sequence, the correlation between the measurement spaces factor and the target sequence is measured using the grey relational degree. To find the gray relation coefficient ξi (k), use the following formula.The GRG represents the degree of correlation between the comparability sequence and the reference sequence. The GRG is a weighted average of the multi-objective GRC [70]. This equation can be used to compute it.

$$\gamma i(x0\ *, x1\ *) = \sum_{i=1}^{n} wi\xi\ \left(x0\ *\ (k), x1\ *\ (k)\right) \quad (3.12)$$

where φi(x0 ∗, x1 ∗) is the GRG for the ith experiment, wi is the weighting value of the ith performance characteristic, and n is the number of performance characteristics.

CHAPTER FOUR

4. RESULT AND DISCUSSION

4.1. Introduction

The overall results of the trials using the relational analysis approach of Taguchi and Grey are provided in this section. The experiment sought to ascertain the ideal aluminum sheets for titanium and 6061 in terms of hardness and tensile strength response. The optimal condition, which shows the common influence trend of each parameter, is found by looking at the primary effects of the parameters. The main statistical technique for evaluating the experiment results is the analysis of variance (ANOVA), which calculates each parameter's percentage contribution with a given degree of confidence. Through an analysis of the main effects plots based on the experimental data gathered, this study aims to investigate the optimization of FSW parameters on the chosen quality criteria. The optimal state for every quality attribute has been identified by S/N data analysis.

4.2 Experimental results and discussions

The tests are conducted to determine how process variables affected the output response characteristics of hardness and tensile strength was displayed in Table 4.1. A number of welding tests were conducted to determine the impact of welding parameters on the tensile strength and hardness of pure Ti and AA 6061 materials. The data were subjected to statistical analysis using MINITAB 20 software packages. Several welding tests were conducted to look into how welding factors affected the hardness and tensile strength of the weld material. The experimental results for the hardness and tensile strength of weld materials with varying process parameters are shown in Table 4.1.

Table 4.1 Experimental result

Sample No.	Rotational speed(rpm)	Welding speed (mm/min)	Tool pin Shape	Dwell time	Ultimate Tensile Strength (MPa)	Hardness value (HV)
1	1100	50	Conical	5	181	78.4
2	1100	60	square	10	176	84.3
3	1100	80	Cylindrical	15	196.6	75.4
4	1400	50	square	15	194.1	69.1
5	1400	60	Cylindrical	5	188.3	72.3
6	1400	80	Conical	10	189.2	66.8
7	1600	50	Cylindrical is	10	142	81.3
8	1600	60	Conical	15	135.1	76.8
9	1600	80	square	5	98.4	83.9

4.2.1 Tensile strength

The most stress a material can withstand when stretched or pulled before failing or breaking is referred to as its highest tensile strength. The test for different FS welded Al6061 and CpTi was carried out at room temperature. The greatest tensile strength observed was 196.6MPa using a cylindrical pin profile tool with a rotation speed of 1100 rpm, a traverse speed of 80 mm/min, and a dwell period of 15 seconds. As a result, a minimum tensile strength value of 98.4 MPa was obtained using the rectangular tool pin profile at 1600 rpm rotational speed, 80 mm/min traversal speed, and 5-second dwell time. while employing commercial pure titanium (cpTi), the FSW weld joint's tensile strength is 81.91%; while using AA6061 individually, it is 63.42%. The weld joint's ultimate tensile strength of 196.6 MPa indicates that it has an 81.91% weld joint efficiency to the weak base metal at 1100 rpm, traverse speed of 80 mm/min, and dwell duration of 15 seconds. Because of the lower thickness brought on by the tool's forging action, fractures have happened inside the weld line in certain joints.The outcome demonstrates that when the tool's traverse speed, dwell time, and rotational speed increase, sufficient heat is produced to connect the base metal. Conversely, when the tool's traverse speed, dwell time, and rotational speed drop. Tensile testing was performed on the

received and welded samples in accordance with the ASTM E8 standard, utilizing various process settings[73]. The tensile test was carried out with a UTM apparatus; the method of friction stir welding has demonstrated the importance of tool shape, rotating speed, dwell time, and traverse speed. The most important factor is tool shape; rectangular tools have greater UTS values than conical and cylindrical tools.

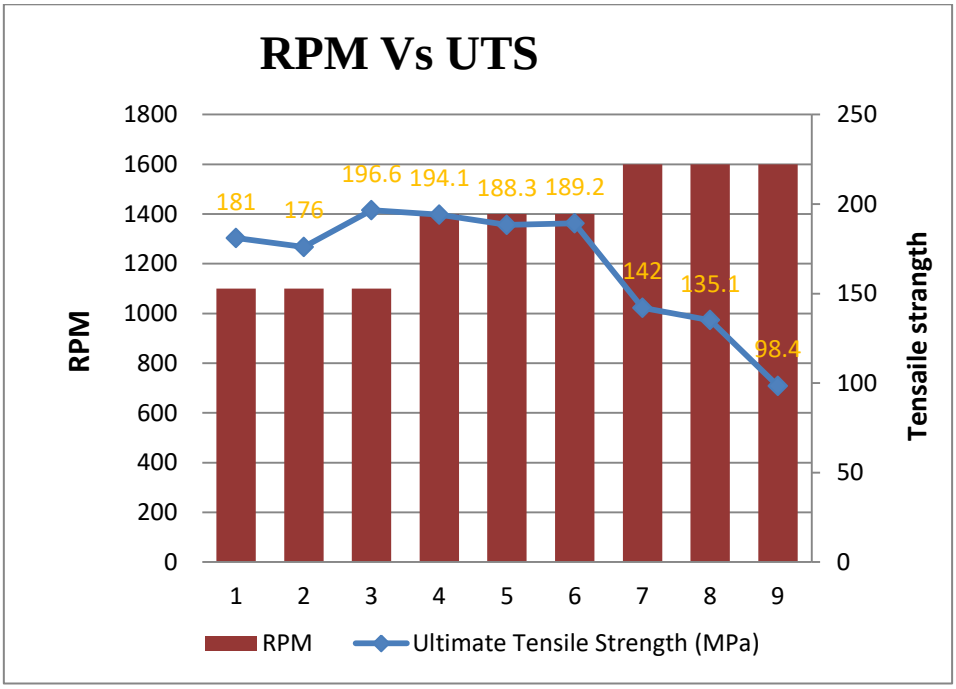

Figure 4.1: Rotational speed Vs. Tensile strength

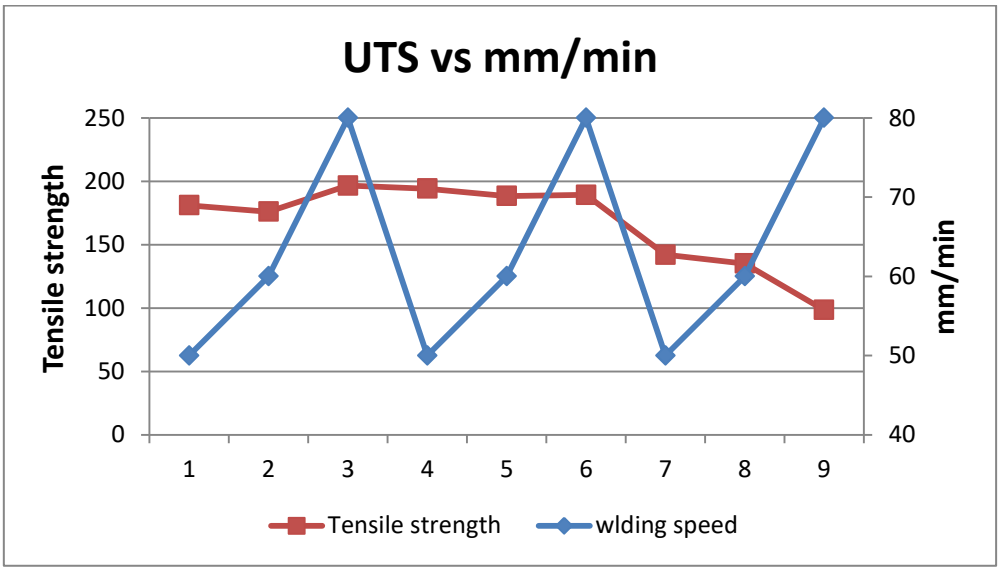

Figure 4.2: Transfer speed Vs. tensile strength

4.2.2. Hardness

The joint's hardness was measured three times at the nugget zone. The higher hardness value of 84.3HV was attained with a square tool pin profile, a dwell period of 10 seconds, a traversal speed of 60 mm/min, and a rotation speed of 1100 rpm. Additionally, with the lowest hardness value of 66.8HV, a conical tool pin profile with a dwell time of 10 seconds, a traverse speed of 60 Mm/min, and a rotational speed of 1400 rpm were measured. Combining a conical tool pin with a 10-second dwell duration at a slower rotational speed yields the highest hardness.

The rotational speed with a combination of traverse speed, tool shape and dwell time contributes a extraordinary impact on the hardness of the joint.

As shown in the figure 4.2 below, the rotational speed of 1100 rpm imparts the maximum hardness for the dissimilar FS welding of AA6061 and Titanium. This is because of the hardness of the joint, which was depended on the amount of heat that develops during the stirring process.

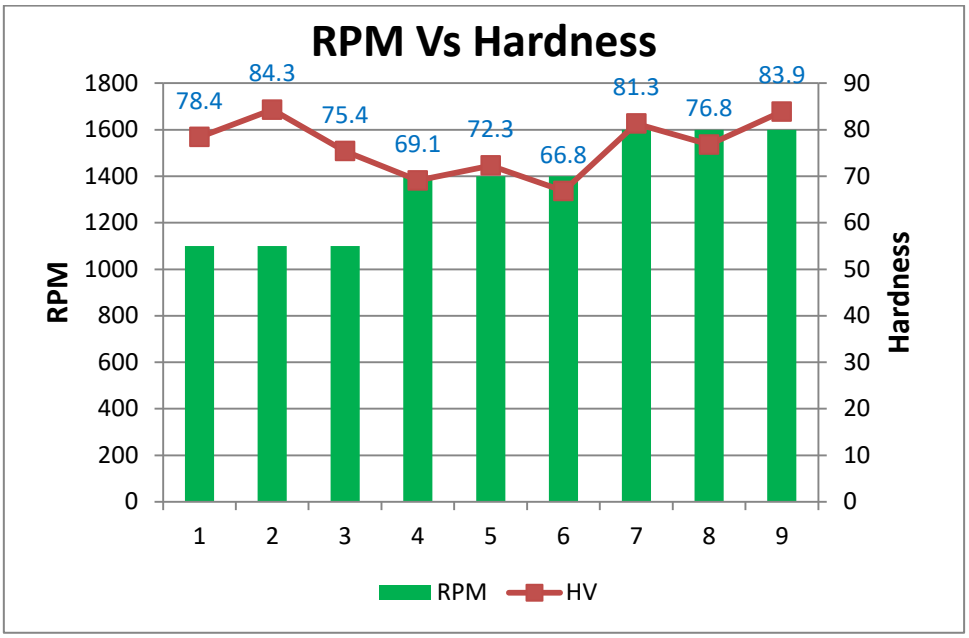

Figure 4.3: Rotational speed's Vs. hardness

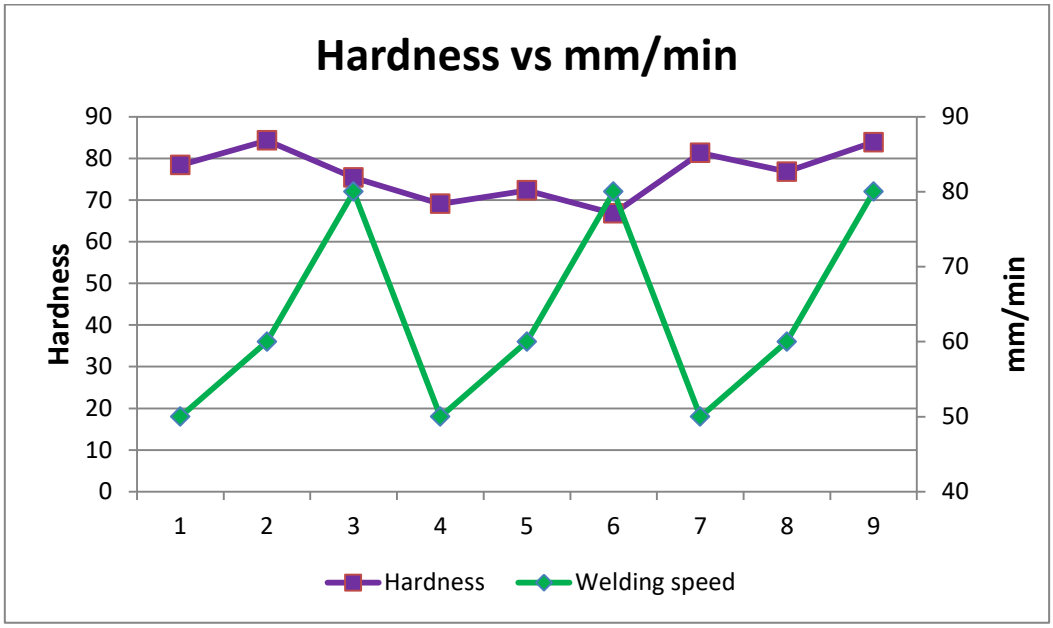

Figure 4.4: Transfer speed Vs. hardness

4.2.3 Process Parameters effect on Microscopic Test

Friction stir welding has four distinct regions of metallographic properties, such as the stir zone or nugget zone (SZ), the Thermo-mechanical heat affected zone (TMAZ), the heat affected zone (HAZ), and base metal. Recrystallization of grains occurs due to high deformations during tool moves in the regions. In the stir zone, small-sized grains or fine grains are formed due to recrystallization. In TMAZ, the shape and size of the grains changed. The region after TMAZ is a heat-affected zone, in this region precipitation that impacts the properties of this zone. Microstructural and physical properties are not changed in the last region, which is the base metal [60]. Figure 4.5 shows optical microscopy images of stir or welding zone of nine samples.

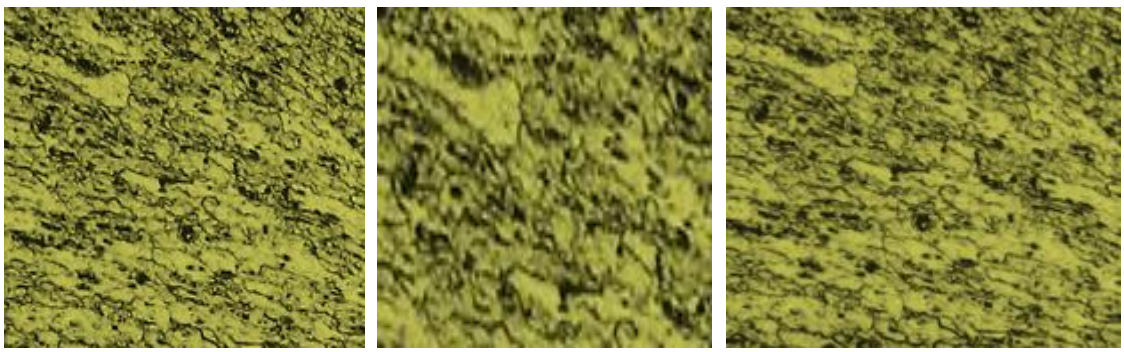

Sample1 Sample 2 Sample 3

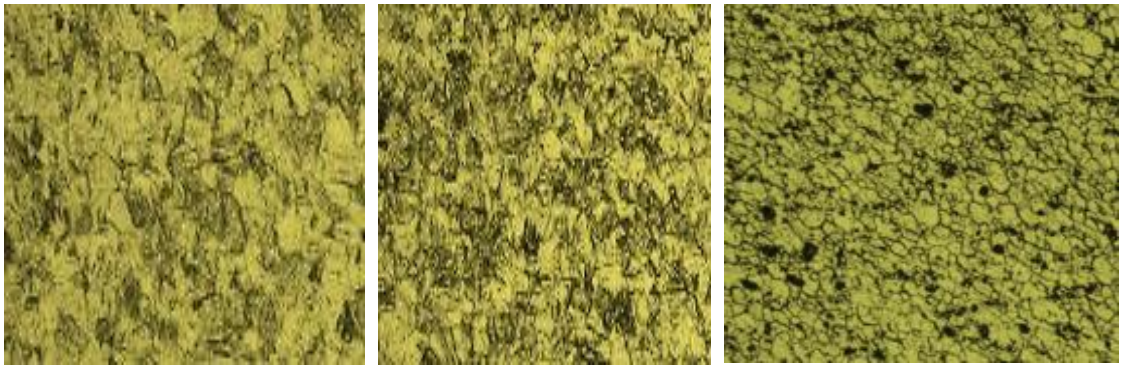

Sample 4 Sample 5 Sample 6

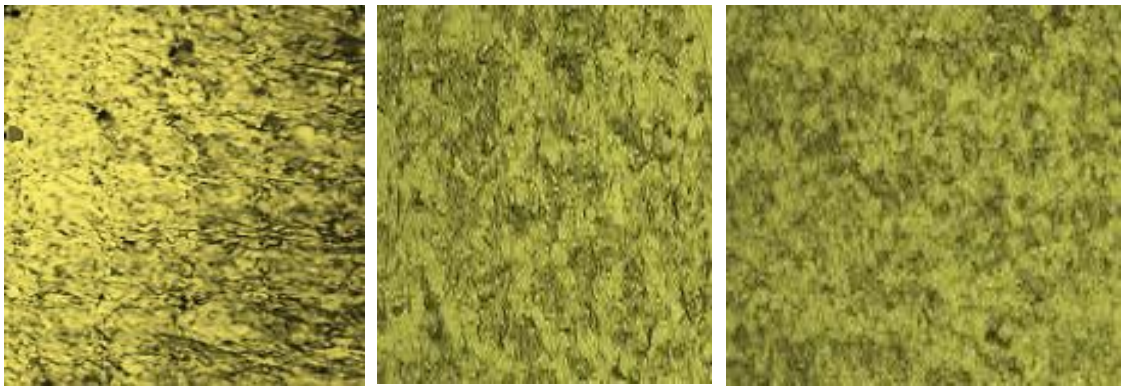

Sample 7 Sample 8 Sample 9

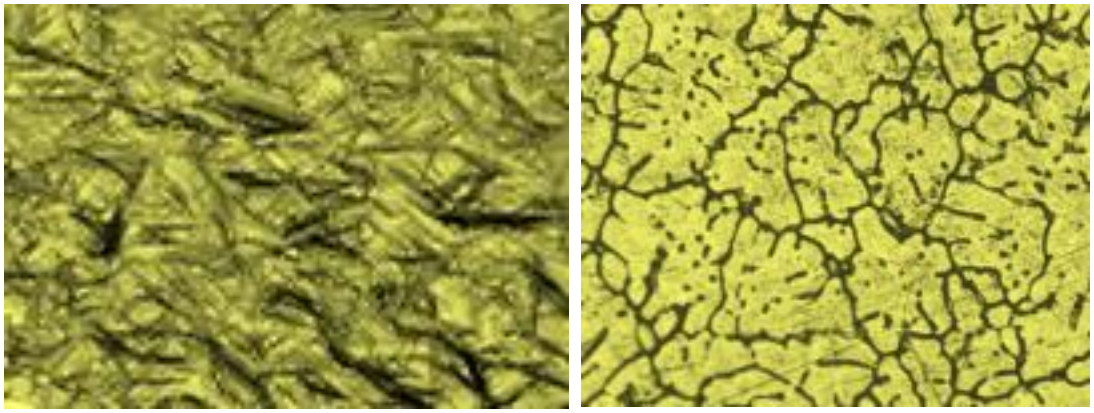

Titanium Al6061

Figure 4.5 Base metals (Ti & Al6061) and nine samples stir zone optical microscope images

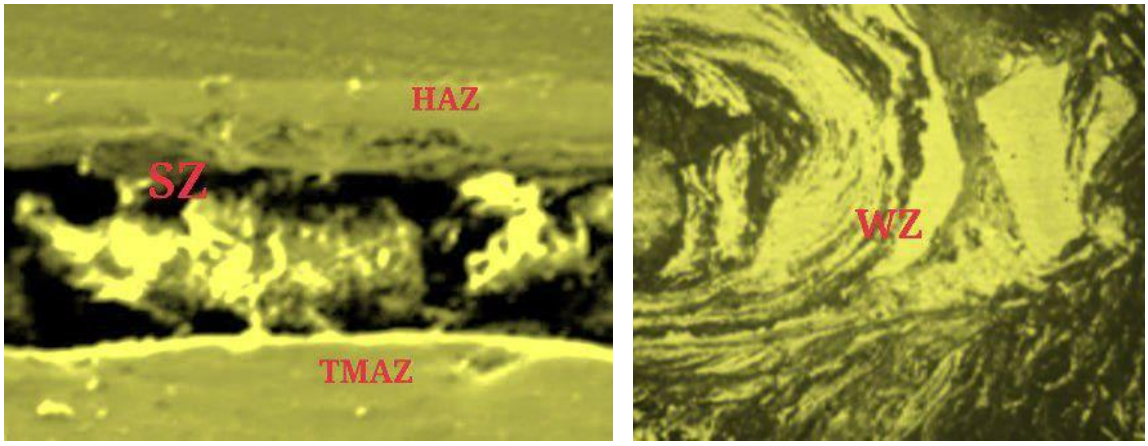

Figure 4.6 optical microscope images on welding area

4.3 Effect of welding parameters on the joint quality

The impact of welding parameters on the dissimilar FSW of cpTi and AA6061metals joint strength is displayed in table 4.5 below.

No.	Process parameters	Mechanical property	Welding Joint	Observation
1	1100rpm,50mm/min Cylindrical,5sec	UTS=181Mpa , HV=78.4		Cavity
2	1100rpm,60mm/min rectangular,10sec	UTS=176 Mpa, HV=84.3		Defect free
3	1100rpm,80mm/min conical,15sec	UTS=196.6Mpa, HV=75.4		Defect free

4	1400rpm,50mm/min Rectangular ,15sec	UTS=194.1 Mpa, HV=69.1		Joint area deformation
5	1400rpm,60mm/min Conical ,5sec	UTS=188.3 Mpa, HV=72.3	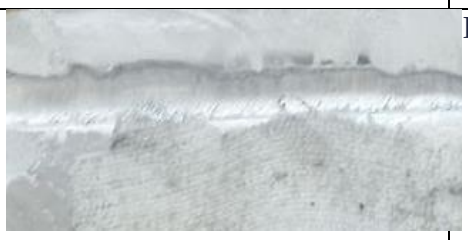	Defect free
6	1400rpm,80mm/min Cylindrical,10sec	UTS=189.2 Mpa, HV=66.8		Cavity
7	1600rpm,50mm/min conical,10sec	UTS=142 Mpa, HV=81.3		Flash
8	1600rpm,60mm/min Cylindrical,15sec	UTS=135.1 Mpa, HV=76.8		Cavity
9	1600rpm,80mm/min Rectangular ,5sec	UTS=98.4 Mpa, HV=83.9		Joint area deformation

Figure 4.7 Impact of traverse speed and RPM on joint strength

4.4. Taguchi-based grey analysis

Using the Taguchi approach, there are three ways to calculate the signal-to-noise (S/N) ratio: larger is better, nominal is best, and smaller is better. However, selecting the appropriate S/N ratio calls for some process comprehension, real world experience, and aptitude. The goal of this research is to determine which increased tensile strength and hardness levels translate into improved welding performance. Larger is better S/N ratio was therefore chosen. Equation 4.3was used for the calculation.

$$(S/N = -10\log10\ (MSD)), \tag{4.3}$$

$$For\ bigger\ is\ better: MSD = (1/y1\ 2 + 1/y2\ 2 + \cdots)/n \tag{4.4}$$

Table 4.2 provides the S/N ratio results as well as the results of UTS, Hv, and their S/N ratios.

Table 4.2: Results of UTS, Hv, and their S/N ratios in experiments

Sample No.	Ultimate tensile strength(MPa)	Hardness (HV)	S/N UTS	S/N HV
1	181	78.4	45.1535715	37.8863213
2	176	84.3	44.91025336	38.5165515
3	196.6	75.4	45.87167027	37.5474269
4	194.1	69.1	45.76051071	36.789561
5	188.3	72.3	45.4970064	37.182766
6	189.2	66.8	45.53842264	36.4955293
7	142	81.3	43.04576689	38.2018109
8	135.1	76.8	42.61310698	37.7072244
9	98.4	83.9	39.85990197	38.4752392

4.5. Grey relational analysis

The Taguchi method's use to optimize just one parameter (also known as mono-objective optimization) is one of its shortcomings. Taguchi in conjunction with a gray relational analysis approach allows for the simple and efficient optimization of several parameters [90]. GRA, or grey relational analysis, is a useful technique for multi-response condition optimization. This analytical technique was employed to resolve the complex relationships between the multiple-objective answers. To optimize numerous responses, GRA offers seven stages [91]. The following procedures were followed in this study:

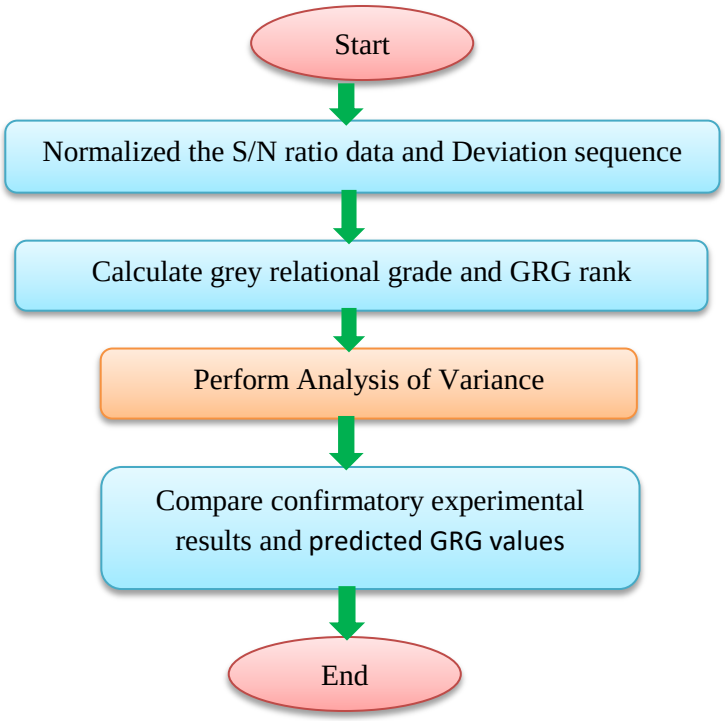

Figure 4.6 Steps of Grey relational analysis to optimize multiple responses

Normalization of response values are divided into three types according to expected nature of the response values. The lowest values of the objective function are anticipated in the initial normalization, which follows the maxim "the smaller the better." The second is "nominal the better," in which average values are found for the objective function. The third one is 'higher the better' where highest values of the results are expected. The first step in obtaining a comparable sequence that modifies the original sequence is normalization of the data.

$$(\Delta\min(k) + \xi\Delta\max(k))/(\Delta 0i(k) + \xi\Delta\max(k)) = \xi(xo^{*}(k) - xi^{*}(k)). \quad (4.5)$$

Prior to computing the GRC, it is crucial to compute the deviation sequences, where ξ is the differentiating coefficient and Δ0i(k) is the deviation sequence of the comparability sequence (xi ∗(k) and reference sequence (xo ∗(k). The value of ξ is 0.5[66].

Table 4.3 Normalization of data and succession of deviations

Step 1: Data normalized			**Step 2: Deviation sequence**	
Sample No.	**UTS**	**HV**	**UTS**	**HV**
1	0.880551	0.311837	0.119449	0.688163
2	0.840078	0	0.159922	1
3	1	0.479522	0	0.520478
4	0.98151	0.854513	0.01849	0.145487
5	0.937678	0.659956	0.062322	0.340044
6	0.944567	1	0.055433	0
7	0.529938	0.155733	0.470062	0.844267
8	0.457969	0.400454	0.542031	0.599546
9	0	0.020441	1	0.979559

4.5.1. Calculation of grey relational grades

The degree of correlation between the comparability and reference sequences is indicated by the grey relational grade. A weighted average of the multi-objective grey relational coefficients is the grey relational grade [90].

$$(x0*, x1*) = 1\ n \sum(x0*(k), xi*(k))\ n\ i{=}1 \tag{4.6}$$

where n is the number of performance characteristics, wi is the weighting value of the i th performance characteristic, and γi($x0*, x1*$) is the GRG for the i th experiment.

Table 4.4: Grey Relation Coefficient and Grey Relation Grade result

Step 3: Grey relational coefficient			Step 4: Grey relational grade with rank	
Sample No.	**UTS**	**HV**	**GRD**	**Rank**
1	0.80716916	0.42081781	0.61399348	5
2	0.75766475	0.333333333	0.54549904	6
3	1	0.489966454	0.74498323	3
4	0.96433814	0.774609393	0.86947377	2
5	0.88917067	0.595206845	0.74218876	4
6	0.90019932	1	0.95009966	1
7	0.51543101	0.371950017	0.44369051	8
8	0.47983229	0.454733268	0.46728278	7
9	0.33333333	0.337938598	0.33563597	9
GRD mine			0.6347608	

4.5.2 Establishing the ideal value for every parameter

The response table for the grey relational analysis is determined using the main effect analysis of GRG, as shown in table 4.9, which shows the average of each response characteristic for each factor level. The delta static is the highest minus the lowest average of each element. Minitab ranks the optimal parameters according to delta values: rank 1 indicates the highest delta value, rank 2 indicates the second delta value, and so on. These ranks indicate the relative importance of each factor to the answer. The mean response is the average value of the performance characteristic for each parameter at different levels.

Table 4.5 S/N Ratios response table

Level	Rotational speed	Welding speed	Tool pin profile	Dwell time
1	-4.019	-4.170	-3.763	-5.436
2	-1.416	-4.821	-5.321	-4.256
3	-7.716	-4.161	-4.068	-3.460
Delta	6.300	0.659	1.557	1.976
Rank	1	4	3	2

Table 4.6 Response Table for Means

Level	Rotational speed A	Welding speed B	Tool pin profile C	Dwell time D
1	0.6348	0.6424	0.6771*	0.5639
2	0.8539*	0.5850	0.5835	0.6464
3	0.4155	0.6769*	0.6436	0.6939*
Delta	0.4384	0.0919	0.0936	0.1300
Rank	1	4	3	2

* Indicates the optimum value in each parameter

Figure 4. 7: Grey Relational Grade's Main effects

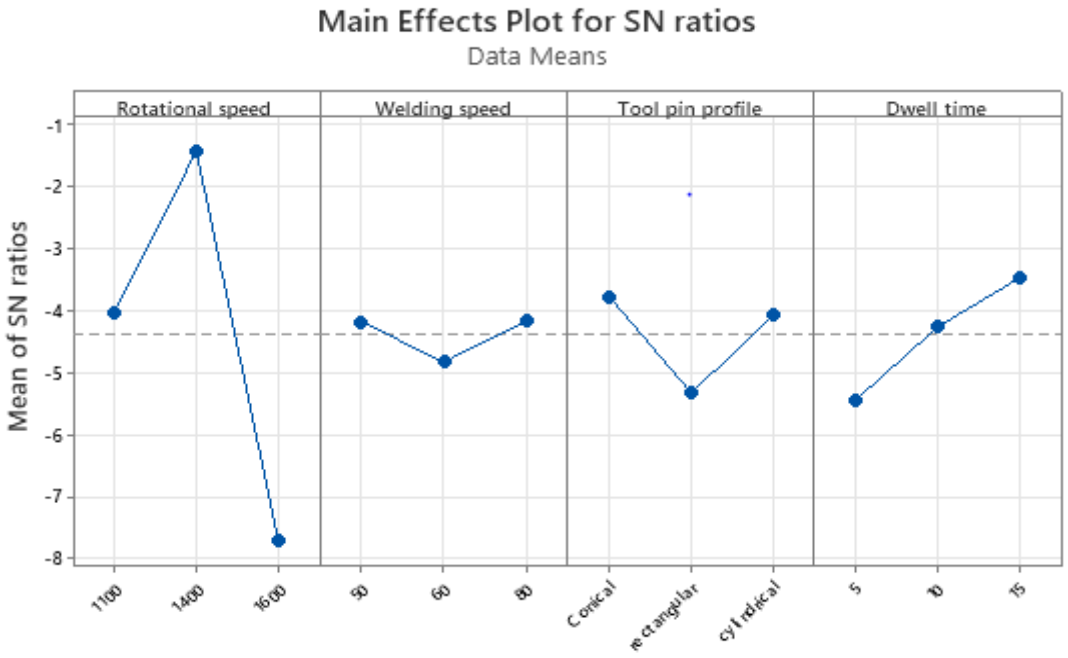

Figure 4. 8: Main effects plots for SN ratios

4.6 Performing Analysis of Variance (ANOVA)

The purpose of the Analysis of Variance (ANOVA) was to identify important parameters. The findings of the ANOVA were utilized to determine how the factors affected the grey relational grade. A factor or parameter is deemed significant if its P-value falls below 0.05 at a 95% confidence level and its F-value in the ANOVA table is higher than its F-value reading from a standard table [82]. The performance characteristics are analyzed using statistical software that includes an ANOVA analysis tool to identify which parameter has a significant impact. Table 4.7 lists the ANOVA results for the grey relationship grades.

Table 4.7: ANOVA results for a grey relational grade (GRG)

Source	DF	Seq SS	Contribution	Adj SS	Adj MS	F-Value	P-Value
Dwell time	1	0.025340	7.44%	0.025340	0.025340	41.36	0.098
Rotational speed	2	0.288271	84.62%	0.288271	0.144136	235.23	0.046
Welding speed	2	0.012934	3.80%	0.012934	0.006467	10.55	0.213
Tool pin profile	2	0.013492	3.96%	0.013492	0.006746	11.01	0.208
Error	1	0.000613	0.18%	0.000613	0.000613		
Total	8	0.340650	100.00%				

*DF-Degree of Freedom; SS-Sum of Square; MS-Mean Square; PC- Percentage contribution

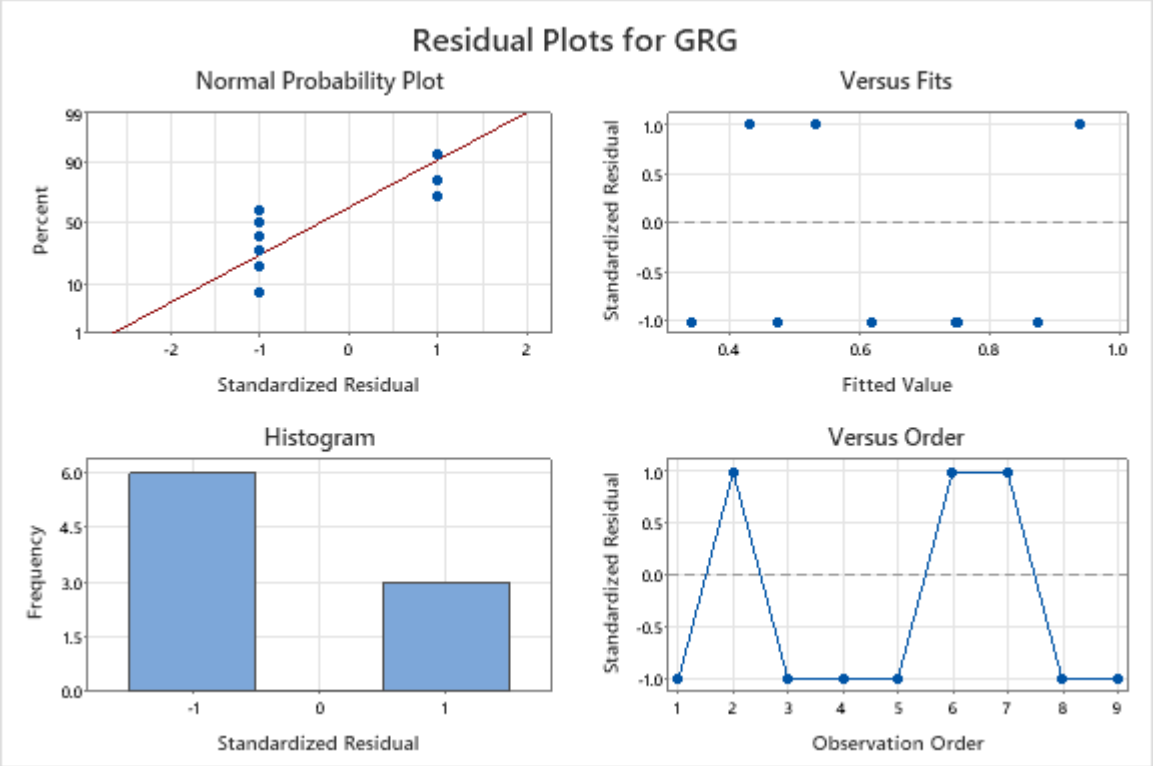

Figure 4.9 Regression Analysis: GRG versus Rotational speed, Welding speed, Dwell time, Tool pin profile

As shown in pie plot below the contribution of welding parameters are rotational speed 84.62%, welding speed 3.80%, tool pin profile 3.96%, and dwell time 7.44% contribution based on ANOVA result.

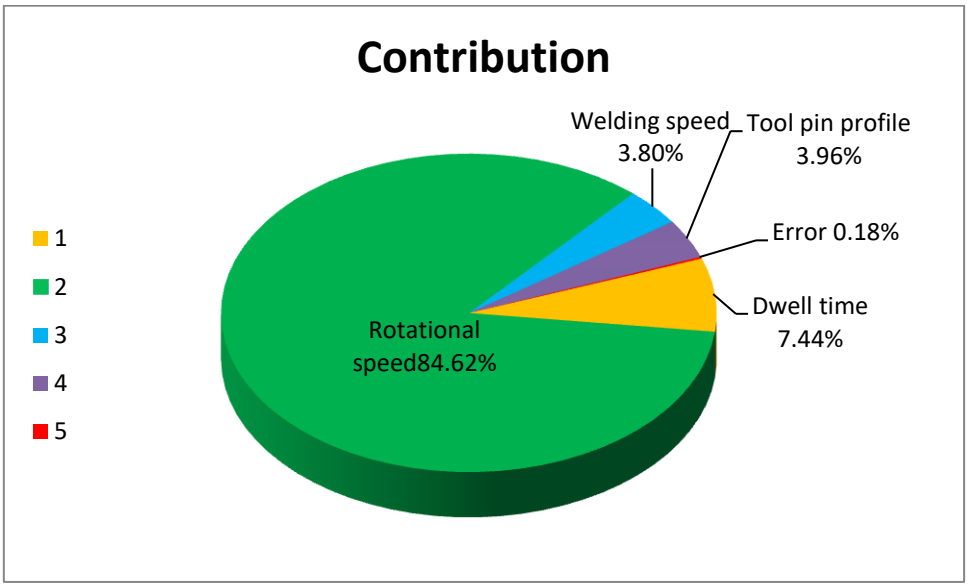

Figure 4.10: Contribution of each welding parameters in ANOVA

4.7 Interactions plot of GRG

The combined effect of all parameters considered in the thesis as shown in Figure 4. 11. The tool rotation and transverse rate affect the grain size and quality of the weld. An increase in rotational speed decreased strength, while an increase in transverse speed increase welds strength.

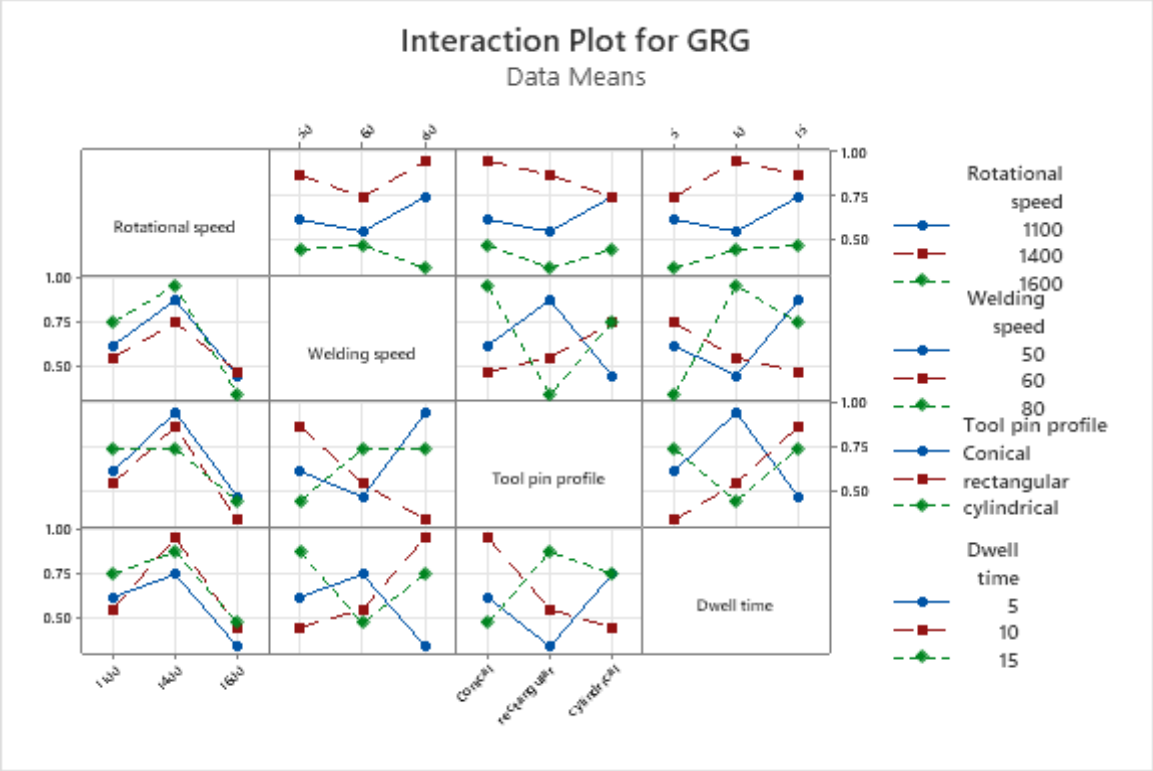

Figure 4.11 Interaction Plot for GRG

4.8 Confirmation Test

Verifying the projected outcome versus the experimental result was the last phase, which was carried out once the ideal combination of process parameters and their levels was discovered. There is no need for a confirmation test if the ideal set of parameters and their values coincidentally matches one of the OA's trials. Through confirmation experimental runs, Verification has been done on the outcomes attained at the ideal process parameter setting.For each quality parameter (tensile strength and hardness), three confirmation experiments were conducted in order to obtain the average values. The expected mean value of GRG at the ideal degree of parameter adjustment was determined using equation (4.6). To validate the estimated values for multi-response optimization at the optimal level of parameter setting, confirmation experimental results were employed. The response variable

averages have to fall inside the 95% confidence interval (CI) that was determined by the confirmation experiments.

μA1B2 = ΄GRG + (A1 - ΄GRG) + (B2 - ΄GRG) = A1 + B2 – ΄GRG (4.7)

In the scenario when GRG represents the grey relational grade = 0.6881 overall mean, GRG is equivalent to that value. The mean values of the grey relational grade with optimally set parameters are A1, B1, C3 and D3.

μA1B2=0.6348+(0.8539-0.6348)+(0.6769-0.6348)+(0.6771-0.6348)+(0.6939-0.6348)

= 0.9974

The following formula is used to estimate the expected mean of the grey relationship grade in the confirmation test: The following formula is used to determine the confidence interval for the expected mean on a confirmation run.

$$CI = \mu \pm \sqrt{F\alpha; (1; fe) * Ve(\frac{1}{neff} + \frac{1}{r})} \quad (4.8)$$

In the Appendices 8 F-Table, Ff_0; (1, fe) = F0.05; (1, 1) = 161.45

Error DOF = 1, fe = Error, and α = Risk.

Table 4.7: Error adjusted mean square (Ve) = 0.000613

In the confirmation experiment, nine replications make up the effective number of replications, or neff R. In addition, the effective number of replications (neff) is determined by using

$$Neff = \frac{Tn}{1} + Ts \quad (4.9)$$

Neff= 9/(1+2)= 3

Therefore, CI is calculated

$$CI = 0.9974 \pm \sqrt{161.45 * 0.000613(1/3 + 1/9)}$$

CI= 0.9974± 0.2097

Consequently, for confirmation experiments, the expected mean's 95% confirmation interval and predicted confidence interval are as follows: (μ – CI) < μ < (μ + CI)

(0.9974 - 0.2097) < 0.9974< (0.9974 + 0.2097)

0.7877< 0.9974< 1.2071

The mean GRG confirmation result is between 0.7877 and 1.2071 based on the confidence interval analysis at 95% of the confidence level. If there is a high degree of correlation between the observed and anticipated GRG values for each of the performance parameters, then the optimal condition will be effective. The expected results were verified three times under ideal circumstances to test the theory. For the conformation test experiment, the gray relational grade is 0.7550, falling within the 95% confidence level range.

Table 4.8: Confirmation test

Optimal Combination	The response of quality characteristics				
A2B3C1D3	UTS(MPa)	UTS S/N	Hardness (Hv)	Hardness S/N	GRG
Replication 1	196.41	74.51	45.8633	37.4443	0.752454
Replication 1	196.80	73.24	45.8805	37.2950	0.776605
Replication 1	195.98	69.80	45.8442	36.8771	0.854931
Average					0.7947

Table 4.9 result confirmation test

Optimal parameter setting	Predicted optimal value (GRG)	Predicted confidence intervals at 95% confidence level	Actual value (Avg. of 3 confirmation test)
A2B3C1D3	0.9974	0.7877< 0.9974< 1.2071	0.7947

The experiment is therefore the safest, according to the findings of the confirmatory experiment testing.

CHAPTER FIVE

5. CONCLUSION AND RECOMMENDATIONS

5.1. Conclusion

This study used friction stir welding to butt weld a joint made of commercially pure titanium alloy and 6061 aluminum alloy, with a thickness of 3 mm. The welding parameters used were rotational speed (1100, 1400, 1600 rpm), traverse or welding speed (50, 60, 80 mm$^{\rightarrow}$min-1), tool pin profile (square, conical, cylindrical), and dwell time (5, 10, 15) seconds. Numbers of experiments is determining by Taguchi's optimization technique and it has led to the development of a sound weld with enhanced mechanical properties. The evaluation of hardness and microstructure was performing by using scanning optical microscopy. In the stirred zone, the weld microstructure contains three areas: the aluminium base metal, the titanium base metal, and a mechanical mixture of aluminium and titanium. The titanium joint area only contained the stirred zone and the heat-affected zones, but the aluminum side's joint area comprised the stirred zone, the thermo-mechanically affected zone, and the heat-affected zone. The maximum hardness was achieve in the stirred zone with a value of 84.3 HV. because of plastic deformation that occurs in this zone ,as well as because of titanium aluminium intermetallic compounds. This can be attributing to severe plastic deformation and formation of intermetallic compounds of titanium and aluminium in this area. The joints have the potential to withstand significant plastic deformation and achieve a tensile strength of 196.6 MPa, which is equivalent to 63.41% of the strength of aluminum base metal. The outcomes of Taguchi Grey relational analysis may be widely implemented to determine the most crucial element and utilized to optimize the weld process's process parameters. Testing was done to determine the best possible combination of parameters and how they would affect the tensile strength and hardness of the welded joints.

The tool rotating speed of 1100 rpm, the welding speed of 80 mm/min, the cylindrical tool pin, and the 15-second dwell time profiles are the optimal independent process parameters to maximize the tensile strength and hardness of the welded joints, according to the tensile and hardness results. The tool pin profile contributed more than the combined amount of the tool rotational speed and the weld traverse speed, according to an analysis of variance (ANOVA) used to determine the percentage contribution of different FSW process parameters.

The results of the experiment and ANOVA indicate that the hardness of the stir zone, the creation of defects, and the tensile strength of the 6061 AA and titanium materials that are friction stir welded are significantly influenced by the rotating speed, traverse speed, tool shape, and dwell time. The percentage contribution of process parameters to joint efficiency, as determined by the ANOVA findings

- Tool rotational speed contributes 84.62%,
- Tool pin profile has a higher impact of 3.96%.
- The contribution of the traverse speed effect is 3.8%,
- While the dwell time is 7.44%.

The greatest tensile strength of the joint, which was manufactured using a cylindrical tool pin at 1100 rpm, 80 mm/min, and a dwell period of 15 seconds, was 196.6 MPa, or 63.41% with Al6061 and 81.91% with Cp-Ti, regardless of the foundation material.
When compared to other pin profiles, the square pin profile displayed finer and more equal grains, according to microstructural analyses. Low material stirring causes crack flaws in the microstructure at high rotating speeds. Because of its pulsing stirring action, the cylindrical tool yields superior microstructure and mechanical qualities than the rectangular and conical tools combined.

In summary, distinct process factors yield varying outcomes, and a blend of regulated and unregulated parameters yields noteworthy outcomes. The hardness and tensile strength of the welding material Al6061 & Titanium were found to be more significantly impacted by the parameters of rotational speed, traverse speed, tool shape, and dwell duration.

5.2. Recommendations

- Some parameters like tool tilt angle and axial load are not controlled in 3 axis CNC milling machines therefor to get more investigation result on mechanical property and defect free weld it better to use friction stir welding machine or 5 axis CNC milling machine.
- The use of various shoulders diameters and having different shoulder features on the tool help to get an adequate temperature and stirring process. It is worth to mention that a laboratory instrument is a problem that, needs to be addressed.
- A few CNC milling are functional and are available from all corners of the country. As well, it is difficult to get a friction stir welding machine; SEM for microstructure

analysis.so, higher institution should think importing those machines for further study in this area.

5.3 Future work

- Further research work is to be incorporate temperature measurements and measurement of the forces acting during the process.
- The research work is performed for butt welding configurations, but it can be applied for lap welding and T welding.
- Utilization of tools that have features on the shoulder and the pin will improve the adequacy of heat during the stirring process

REFERENCE

[1]. *Asadi, Mohammad Kazem Besharati Givi and Parviz. 2014.* Advances in Friction Stir Welding. Woodhead Publishing. 2014. Advances in Friction Stir Welding and Processing. london: Woodhead Publishing.

[2] Pedro M. G. P. Moreira • Lucas F. M. da Silva Paulo M. S. T. de Castro *Structural Connections for Lightweight Metallic Structures*

[3]. *Preetish Sinha, S. Muthukumaran, S.K. Mukherjee.* Analysis of first mode of metal transfer in friction stir welded plates by image processing technique. journal of materials processing technology 197 (2008) 17–21.

[4]. *S. Muthukumaran & Kumar Pallav & Vikas Kumar Pandey & S. K. Mukherjee*. A study on electromagnetic property during friction stir weld failure. International journal of Advanced Manufacturing Technology (2008) 36:249–253.

[5]. *Moataz M. Attallah, Hanadi G. Salem.* Friction stir welding parameters: a tool for controlling abnormal grain growth during subsequent heat treatment. Materials Science and Engineering A 391 (2005) 51–59

[5]. *Thomas WM, Johnson KI, Wiesner CS.* Friction stir welding-recent developments in tool and process technologies. Adv Eng Mater 2003;5:485–90.

[6] *Gurunath Shindeaa, Sameer Gajghateb , Dr.P.S.Dabeer, Dr.C.Y. SeemikeriGurunath Shinde /* Materials Today: Proceedings 4 (2017) 8901–8910

[7] *A. Saravana Sundar, T. Vishnu Vardhan, Adepu Kumar*/ Microstructural characterization of aluminium-titanium friction stir welds/ Department of Mechanical Engineering, National Institute of Technology, Warangal 506004, India

[8] *Ulrike Dressler, Gerhard Biallas [1], Ulises Alfaro Mercado*/Friction stir welding of titanium alloy TiAl6V4 to aluminium alloy AA2024-T3/German Aerospace Center, Institute of Materials Research, Linder Höhe, 51147 Köln, Germany

[9]. *L.V. Kamble, S.N. Soman, P.K. Brahmankar,* Effect of Tool Design and Process Variables on Mechanical Properties and Microstructure of AA6101-T6 Alloy Welded by Friction Stir Welding, IOSR Journal of Mechanical and Civil Engineering (IOSR-JMCE) ISSN(e) : 2278-1684, ISSN(p) : 2320–334X, Pp.30-35.

[10] *Taher A. Shehabeldeen, Yajun Yin , Xiaoyuan Ji , Xu Shen , Zhipeng Zhang , Jianxin Zhou* Investigation of the microstructure, mechanical properties and fracture mechanisms of dissimilar friction stir welded aluminium/titanium joints

[11] *KUMAR, S., KUMAR, S. & KUMAR, A. 2013.* Microstructure and Percentage Elongation Analysis for Friction Stir Welding of Joining A6061 and A6082 alloys.

[12] *CamG, Ipekoglu G, Tarik Serindag H.* Effects of use of higher strength interlayer and external cooling on properties of friction stir welded AA6061-T6 joints. Sci Technol Weld Join 2014;19:715e20.

[13]Y. *Chen, C. Liu, G. Liu,* Study on the joining of Titanium and Aluminum dissimilar alloys by friction stir welding, Open Mater. Sci. J. 5 (1) (2011) 256–261

[13] *Ng, M.N.Y. S, M.A. A.,* Reviews on aluminum alloy series and its applications, Acad. J. Sci. Res. 5 (2017) 708–716. https://doi.org/10.15413/ajsr.2017.0724.

[14] *Heidarzadeh A, Mironov S, Kaibyshev R, C¸ am G, Simar A, Gerlich A, et al.* Friction stir welding/processing of metals and alloys: a comprehensive review on microstructural evolution. Prog Mater Sci 2021;117:100752.

[15] *KHAN, N. Z., SIDDIQUEE, A. N., KHAN, Z. A. & SHIHAB, S. K. 2015b.* Investigations on tunneling and kissing bond defects in FSW joints for dissimilar aluminum alloys. Journal of Alloys and Compounds, 648, 360-367.

[16] *Verma M, Ahmed S, Saha P.* Challenges, process requisites/inputs, mechanics and weld performance of dissimilar micro-friction stir welding (dissimilar mFSW): a comprehensive review. J Manuf Process 2021;68:249e76.

[17] *ROY, R. K. 2010.* A PRIMER ON THE TAGUCHI METHOD, United States of America.

[18] *NOURANI, M., MILANI, A. S. & YANNACOPOULOS, S. 2011*. Taguchi optimization of process parameters in friction stir welding of 6061 aluminum alloy: A review and case study. Engineering, 3, 144.

[19]. *Wei, Y.N.; Li, H.; Xiao, P.; Luo, Y.G.; Qu, H.T.; Liang, S.H.* Research Progress of Friction StirWelding Technology and Microstructure of Copper/Aluminum Joint. Hot Work. Technol. **2020**, 49, 1–5. (In Chinese)

[20]. *Mishra, R.S.; Mahoney, M.W.* Friction stir welding and processing. ASM International 2007, 1 368. doi: 10.1361=fswp2007

[21]. *Akinlabi, E.T.; Els-Botes A.; McGrath, P.J.* Effect of travel speed on joint properties of dissimilar metal friction stir welds. In Proceedings of 2nd International Conference on Advances in Engineering and Technology (AET), Uganda,2011.

[22]. *Fotouhi, Y.; Rasaee, S.; Askari, A.; Bisadi,* H. Effect of transverse speed of the tool on microstructure and mechanical properties in dissimilar butt friction stir welding of Al5083– copper sheets. Engineering Solid Mechanics 2014, 2 (3), 239– 246.

[23]. *Muthua, M.F.X.; Jayabalan,* V. Tool travel speed effects on the microstructure of friction stir welded aluminum–copper joints. Journal of Materials Processing Technology 2015, 217, 105–113.

[24]. *Zadeh, A.A. Saeid, T.; Sazgari,* B. Microstructural and mechanical properties of friction stir welded aluminum=copper lap joints. Journal of Alloys and Compounds 2008, 460, 535–538.

[25] *Galvao, I.; Oliveira, J.C.; Loureiro, A.; Rodrigues, D.M.* Formation and distribution of brittle structures in friction stir welding of aluminium and copper: influence of process parameters Science and Technology of Welding and Joining 2011, 16 (8), 681–689.

[26]. *Esmaeili, A.; Zareie Rajani, H.R.; Sharbati, M.; Besharati Givi, M.K.; Shamanian, M.* The role of rotation speed on intermetallic compounds formation and mechanical behaviour of friction stir welded brass=aluminum 1050 couple. Intermetallics 2011, 19 (11), 1711–1719.

[27]. *Xue, P.; Ni, D.R.; Wang, D.; Xiao, B.L.; Ma, Z.Y.* Effect of friction stir welding parameters on the microstructure and mechanical properties of the dissimilar Al–Cu joints. Materials Science and Engineering A 2011, 528, 4683–4689.

[28] *Bisadi, H.; Tavakoli, A.; Sangsaraki,M.T.; Sangsaraki, K.T.* The influences of rotational and welding speed on microstructures and mechanical properties of friction stir welded Al5083 and commercially pure copper sheets lap joints. Materials and Design 2013, 43, 80–88.

[29] *HUSSAIN, M. A., KHAN, N. Z., SIDDIQUEE, A. N. & KHAN, Z. A. 2018.* Effect Of Different Tool Pin Profiles On The Joint Quality Of Friction Stir Welded AA 6063. Materials Today: Proceedings, 5, 4175-4182.

[30] *ELANGOVAN, K. & BALASUBRAMANIAN, V. 2008*. Influences of tool pin profile and tool shoulder diameter on the formation of friction stir processing zone in AA6061 aluminium alloy. Materials & design, 29, 362-373.

[31] A.S Vagh and S. N. Pandya, Influence Of Process Parameters On The Mechanical Properties Of Friction Stir Welded AA 2014-T6 Alloy Using Taguchi Orthogonal Array, International Journal of Engineering Sciences & Emerging Technologies,

[32]. *Mishra, R.S.; Mahoney, M.W.* Friction stir welding and processing.ASM International 2007,1–368

[33]. *Akbari, M.; Abdi Behnagh, R.; Dadvand,* A. Effect of material position on friction stir lap welding of Al to Cu. Science and Technology of Welding and Joining 2012, 17 (7), 581–588

[34] *RAJAKUMAR, S., MURALIDHARAN, C. & BALASUBRAMANIAN, V. 2011*. Influence of friction stir welding process and tool parameters on strength properties of AA7075-T6 aluminium alloy joints. Materials & Design, 32, 535-549.

[35] *SEVVEL, P. & JAIGANESH, V. 2017*. Effects of axial force on the mechanical properties of AZ80A Mg alloy during friction stir welding. Materials Today: Proceedings, 4, 1312-1320.

[36] *LAKSHMINARAYANAN, A. & BALASUBRAMANIAN, V. 2008.* Process parameters optimization for friction stir welding of RDE-40 aluminium alloy using Taguchi technique. Transactions of Nonferrous Metals Society of China, 18, 548-554.

[37]. *Galvao, I.; Loureiro, A.; Verdera, D.; Gesto, D.; Rodrigues.D.M.* Influence of tool offsetting on the structure and morphology of dissimilar aluminum to copper friction stir welds. Metallurgical and Materials Transactions: A 2012, 43 (13), 5096–5105.

[38]. *Firouzdor, V.; Kou, S. Al-to-Cu Friction Stir Lap Welding.* Metallurgical and Materials Transactions A 2012, 43 (1), 303–315.

[39] *Saravana Sundar, T. Vishnu Vardhan, Adepu Kumar* Microstructural characterization of aluminium-titanium friction stir welds Department of Mechanical Engineering, National Institute of Technology, Warangal 506004, India

[40] *Huseyin Uzun, Claudio Dalle Donne, Alberto Argagnotto, Tommaso Ghidini and Carla Gambaro. 2005.* "Friction stir welding of dissimilar Al 6013-T4 To X5CrNi18-10 stainless steel." Materials and Design 26: 41–46.

[41] *Mukuna P. Mubiayi. Member, IAENG and Esther T. Akinlabi, Member, IAENG. 2013.* "Friction Stir Welding of Dissimilar Materials between Aluminium Alloys and Copper - an overview." Proceedings of the World Congress on Engineering. London.

[42] Experimental Investigation of Aluminum Alloy and Polymer Joints Made by Friction Stir Welding Process, *by Redwan Kedir*

[43]*Joon-Tae Yooa, Jong-HoonYoona, Kyung-Ju Mina and Ho-Sung Lee. 2015.* "Effect of Friction Stir Welding Process Parameters on Mechanical Properties and Macro Structure of Al-Li alloy." Procedia Manufacturing 2: 325 – 330.

[44]*Francesco Lambiase, Alfonso Paoletti, Valentino Grossia and Antoniomaria Di Ilio. 2017.* "Friction assisted joining of aluminum and PVC sheets." Journal of Manufacturing Processes 29: 221–231.

[45] *Prabhu Subramanya, Murthy Amar, Shettigar Arun, Herbert Mervin and Rao Shrikantha. 2018.* "Friction stir welding of Aluminium matrix composites – A Review." MATEC Web of Conferences .

[46]*Yongxian Huang, Xiangchen Meng, Yuming Xie, Long Wan, Zongliang Lv, Jian Cao, Jicai Feng. 2018.* "Friction stir welding/processing of polymers and polymer matrix." Composites 235–257.

[47]. *Rai, R.; De, A.; Bhadeshia, H.K.D.H.; Debroy,* T. Review: friction stir welding tools. Science and Technology of Welding and Joining 2011, 16 (4), 325–342.

[48]. *Mishra, R.S.; Mahoney, M.W.* Friction stir welding and processing. ASM International 2007, 1–368

[49]. *Mehta, K.P.; Badheka, V.J.* A Review on Dissimilar Friction StirWelding of Copper to Aluminum: Process, Properties and Variants.Mater. Manuf. Processes **2016**, 31, 233–254.

[50].*SAUMIL K.JOSHI, J. D. G. 2015.* Influence of Tool Shoulder Geometry on Friction Stir Welding: A Literature Review. IJRSI, III, 261-264.

[51]. *Esmaeili, A.; Besharati Givia, M.K.; Zareie Rajanib, H.R.* A metallurgical and mechanical study on dissimilar friction stir welding of aluminum 1050 to brass (CuZn30). Materials Science and Engineering: A 2011, 528 (22–23), 7093–7102.

[52]. *Agrarwal, P.; Nageswaran, P.; Arivazhagan, N.; Ramkumar, K.D.* Development of friction stir welded butt joints of AA6063 aluminum alloy and pure copper. In Proceeding of International Conference on Advanced Research in Mechanical Engineering(ICARME-2012), Trivendum, India, 2012. 46–50.

[53]. *Girard, M.; Huneau, B.; Genevois, C.; Sauvage, X.; Racineux, G.* Friction stir diffusion bonding of dissimilar metals. Science and Technology of Welding and Joining 2010, 15 (8), 661–665.

[54]. *Genevois, C.; Girard, M.; Huneau, B.; Sauvage, X.; Racineux, G.* Interfacial reaction during friction stir welding of Al and Cu. Metallurgical and Materials Transactions A 2011, 42 (8), 2290–2295.

[55]. *Nandan, R.; DebRoy, T.; Bhadeshia, H.K.D.H.* Recent advances in friction-stir welding – process, weldment structure and properties. Progress in Materials Science 2008, 53 (6), 980–1023.

[56]. *Mishra, R.S.; Ma, Z.Y.* Friction stir welding and processing. Materials Science and Engineering 2005, 50 (1–2),

[57]. *RGalvao, I.; Leal, R.M.; Loureiro,* A.; Rodrigues, D.M. Material flow in heterogeneous friction stir welding of aluminium and copper thin sheets. Science and Technology of Welding and Joining 2010, 15 (8), 654–660.

[58] *Singh K, Singh G, Singh H*. Review on friction stir welding of magnesium alloys. J Magnes Alloy 2018;6:399e416

[59] *NOOR ZAMAN KHAN, A. N. S. A. Z. A. K. 2017.* Friction Stir Welding: Dissimilar Aluminium Alloys, CRC Press

[60] Interfacial Microstructure and Mechanical Properties of Dissimilar Friction Stir Welds between 6061-T6 Aluminum and Ti-6%Al-4%V Alloys* Ki-Sang Bang1;2, Kwang-Jin Lee1, Han-Sur Bang2 and Hee-Sun Bang

[61] *Heidarzadeh A, Mironov S, Kaibyshev R, C¸ am G, Simar A, Gerlich A, et al.* Friction stir welding/processing of metals and alloys: a comprehensive review on microstructural evolution. Prog Mater Sci 2021;117:100752.

[62]Study on the Joining of Titanium and Aluminum Dissimilar Alloys by Friction Stir Welding Yuhua Chen, Changhua Liu and Geping Liu

[63] *Hua, CY., Qua, N., Ming, KL.,"* Interface characteristic of friction stir welding lap joints of Ti/Al dissimilar alloys", Transactions of Nonferrous Metals Society of China, 2, 299-304 (2011)

[64]Mojtaba Sadeghi- Ghoghery Masoud Kasiri- Asgarani Kamran Amini Friction Stir Welding Of Dissimilar Joints between Commercially Pure Titanium Alloy and 7075 Aluminium Alloy

[65]*SACHIN JAMBHALE, S. K. A. S. K. 2015*. Effect of Process Parameters & Tool Geometries on Properties of Friction Stir Spot Welds: A Review. Universal Journal of Engineering Science, 3, 6-11.

[66] Multi-Objective Process Parameters Optimization of Friction Stir Welding on 6061 Aluminum Alloy using Taguchi and Grey Relational Analysis Messele, Eyob

[67] https://www.xometry.com/resources/materials/titanium

[68] https://en.wikipedia.org/wiki/6061_al

[69] https://www.thomasnet.com/articles/metals-metal-products/6061-aluminum/

[70]Optimization of process parameters in FSW of dissimilar aluminum alloys (AA6061–T6 and AA5052–H32) *By: Wondu Tesfaye Heramo*

[71] N. Semioshkina and G. Voigt, "An overview on Taguchi Method," J. Radiat. Res., vol. 47 Suppl A, no. 2, pp. A95–A100, 2006,: http://www.ncbi.nlm.nih.gov/pubmed/19879888.

[72]A Primer on the Taguchi Method 2 nd edition Author: Ranjit K. Roy Publisher/Year: Society of Manufacturing Engineers/2010

[73] *ASTM E8, ASTM E8/E8M* standard test methods for tension testing of metallic materials 1, Annu. B. ASTM Stand. 4. (2010) 1–27. https://doi.org/10.1520/E0008.

[74] ASTM E92-82, Standard Test Method for Vickers Hardness of Metallic Materials, ASTM Int. 82 (2004) 1–9.

[75]*C.DEVANATHAN, A. M., A.SURESH BABU 2013.* Optimization Of Process Parameters In Friction Stir Welding Of AL 6063. International Journal of Design and Manufacturing Technology (IJDMT), 4, 42-48.

[76] *P.K. Sahu, S. Pal*, Multi-response optimization of process parameters in friction stir welded AM20 magnesium alloy by Taguchi grey relational analysis, J. Magnes. Alloy. 3 (2015) 36–46.

[77] *K. Manigandan, S. Subramaniam*, Multi-response optimization of friction stir corner welding of dissimilar thickness AA5086 and AA6061 aluminum alloys by Taguchi grey relational analysis, Proc. Inst. Mech. Eng. Part C J. Mech. Eng. Sci. 233 (2019) 3733– 3742

[78] *J. Kundu, H. Singh*, Friction stir welding: multi-response optimisation using Taguchibased GRA, Prod. Manuf. Res. 4 (2016) 228–241.

[79] *K. Palani, C. Elanchezhian*, Multi response Optimization of Friction stir welding process parameters in dissimilar alloys using Grey relational analysis, IOP Conf. Ser. Mater. Sci. Eng. 390 (2018) 1–9. https://doi.org/10.1088/1757-899X/390/1/012061.

[80] Ş. Kasman, Optimisation of dissimilar friction stir welding parameters with grey relational analysis, Proc. Inst. Mech. Eng. Part B J. Eng. Manuf. 227 (2013) 1317–1324.

[81]*LAKSHMINARAYANAN, A. 2009b.* Optimization of process parameters for friction stir welding of cast aluminium alloy A319 by Taguchi method. J. Mater. Sci. Mech. Eng, 25, 655-664.

[82]*ELATHARASAN, G. & KUMAR, V. S. 2013.* An experimental analysis and optimization of process parameter on friction stir welding of AA 6061-T6 aluminum alloy using RSM. Procedia Engineering, 64, 1227-1234.

[83]*D.DEVAIAH, K. K., P. LAXMINARAYANA 2016.* Optimization of Process Parameters in Friction Stir welding of dissimilar aluminium alloys (AA5083 and AA6061) Using Taguchi Technique. International Journal of Innovative Research in Science, Engineering and Technology, 5, 15303-15310.

[84]*UGRASEN, G., BHARATH, G., KUMAR, G. K., SAGAR, R., SHIVU, P. & KESHAVAMURTHY, R. 2018*. Optimization of process parameters for Al6061- Al7075 alloys in friction stir welding using Taguchi's technique. Materials Today: Proceedings, 5, 3027-3035.

[85] *KUMAR, S. R. K. R. A. P. 2016.* Optimization of Process Parameters of Friction Stirs Welding of Aluminum Alloys (6061) Using Taguchi Method. International Journal of Science and Research, 5, 1988-1994.

[86]*TAMJIDY, M., BAHARUDIN, B., PASLAR, S., MATORI, K., SULAIMAN, S. & FADAEIFARD, F. 2017*. Multi-objective optimization of friction stir welding process parameters of AA6061-T6 and AA7075-T6 using a biogeography based optimization algorithm. Materials, 10, 533.

[87] *D. Devaiah, K. Kishore, P. Laxminarayana,* Effect of Welding Speed on Mechanical Properties of Dissimilar Friction Stir Welded AA5083-H321 and AA6061-T6 Aluminum Alloys, Int. J. Adv. Eng. Res. Sci. 4 (2017) 22–28.

[88] *S. Balamurugan, K. Jayakumar, K. Subbaiah,* Influence of Friction Stir Welding Parameters on Dissimilar Joints AA6061-T6 and AA5052-H32, Arab. J. Sci. Eng. 46 Wondu Tesfaye: MSc Thesis, 2023 83 (2021) 11985–11998.

[89] *Redwan Kedir Hassen* Experimental Investigation of Aluminum Alloy and Polymer Joints Made by Friction Stir Welding Process,

[90]*SAMPATH KUMAR, R., ARUN KUMAR AND AMRISHRAJ 2016.* Optimization of process parameters during Friction Stir Welding of dissimilar aluminium alloys using Grey relational analysis. Journal of Chemical and Pharmaceutical Sciences, 9, 1647- 1653.

[91] *VIJAYAN, S., RAJU, R. & RAO, S. K. 2010.* Multiobjective optimization of friction stir welding process parameters on aluminum alloy AA 5083 using Taguchi-based grey relation analysis. Materials and Manufacturing Processes, 25, 1206-1212.

Appendices

Appendices –A procured Al6061 plate

明 泰 铝 业 产 品 质 量 证 明 书

MING TAI AL. PRODUCT QUALITY CERTIFICATE

订货单位 Customer				编 号: Serial No:	MT20041174
产品名称 Product	批 号 Lot No	合金状态 Alloy And Temper	规格（mm） Dimension		
铝板/铝带	GFC2005N60188	6061 T6	10*2000*4000		
技术标准 Technique Standard		GB/T 3880-2012	化学成分标准 Composition Standard		GB/T 3190-2008

化学成分 % Chemical Composition

元素 Element	Si	Fe	Cu	Mn	Mg	Cr	Zn	Na	Ti	Al
标准值 Standard Value	0.4-0.8	≤0.7	0.15-0.4	≤0.15	0.8-1.2	0.04-0.35	≤0.25	—	≤0.15	余量
实测值 Measured Value	0.625	0.498	0.256	0.109	1.068	0.116	0.115	0	0.026	97.15

力学性能 Mechanical Property

取样方法 Sampling Method	抗拉强度（MPa） Tensile Strength		屈服强度（MPa） Yield Strength		延伸率（%） Elongation	
横向	标准值 Standard Value	实测值 Measured Value	标准值 Standard Value	实测值 Measured Value	标准值 Standard Value	实测值 Measured Value
	≥290	323	≥240	276	≥9	14

杯凸 Cup Bulge			制耳率（%） Earing		
	标准值 Standard Value	——		标准值 Standard Value	——
	实测值 Measured Value	——		实测值 Measured Value	——

90° 折弯 90° bend	合格	其他 Others	合格
表面质量 Surface Control	合格	几何尺寸 Dimension Control	合格
综合判定 Overall Conlusion	合格		

填表人： 席国飞 审批人： 张国帅 日期： 2020年06月02日

Inspector: Approver: Date:

河南明泰铝业股份有限公司 技术质量处

地址：河南省巩义市回郭镇新310国道清中村中段 邮编：451283

电话：0371-67664998 67664621 传真：0371-67664618

Appendices: B part programs used for FSW

Test -1	Test -2	Test -3
O2121	O2121	O2121
G90 G17 G40 G94 G49 G80 ;	G90 G17 G40 G94 G49 G80 ;	G90 G17 G40 G94 G49 G80 ;
G54;	G54;	G54;
M06 T01 ;	M06 T02 ;	M06 T03 ;
M03; S1100;	M03; S1100;	M03; S1100;
G00 Z5;	G00 Z5;	G00 Z5;
G01 Z-3.5; F5;	G01 Z-3.5; F10;	G01 Z-3.5; F15;
G01 X1.3 F50;	G01 X1.3 F60;	G01 X1.3 F80;
G04 X5;	G04 X5;	G04 X5;
G01 Y-94;	G01 Y-94;	G01 Y-94;
G01 Z10;	G01 Z10;	G01 Z10;
G00 Z300;	G00 Z300;	G00 Z300;
Y108;	Y108;	Y108;
M05;	M05;	M05;
M30;	M30;	M30;
%	%	%

Test -4	Test -5	Test -6
O2121	O2121	O2121
G90 G17 G40 G94 G49 G80 ;	G90 G17 G40 G94 G49 G80 ;	G90 G17 G40 G94 G49 G80 ;
G54;	G54;	G54;
M06 T01 ;	M06 T02 ;	M06 T03 ;
M03; S1400;	M03; S1400;	M03; S1400;
G00 Z5;	G00 Z5;	G00 Z5;
G01 Z-3.5; F5;	G01 Z-3.5; F10;	G01 Z-3.5; F15;
G01 X1.3 F50;	G01 X1.3 F60;	G01 X1.3 F80;
G04 X5;	G04 X5;	G04 X5;
G01 Y-94;	G01 Y-94;	G01 Y-94;
G01 Z10;	G01 Z10;	G01 Z10;
G00 Z300;	G00 Z300;	G00 Z300;
Y108;	Y108;	Y108;
M05;	M05;	M05;
M30;	M30;	M30;
%	%	%

Test -7	Test -8	Test -9
O2121	O2121	O2121
G90 G17 G40 G94 G49 G80 ;	G90 G17 G40 G94 G49 G80 ;	G90 G17 G40 G94 G49 G80 ;
G54;	G54;	G54;
M06 T01 ;	M06 T02 ;	M06 T03 ;
M03; S1600;	M03; S1600;	M03; S1600;
G00 Z5;	G00 Z5;	G00 Z5;
G01 Z-3.5; F5;	G01 Z-3.5; F10;	G01 Z-3.5; F15;
G01 X1.3 F50;	G01 X1.3 F60;	G01 X1.3 F80;
G04 X5;	G04 X5;	G04 X5;
G01 Y-94;	G01 Y-94;	G01 Y-94;
G01 Z10;	G01 Z10;	G01 Z10;
G00 Z300;	G00 Z300;	G00 Z300;
Y108;	Y108;	Y108;
M05;	M05;	M05;
M30;	M30;	M30;
%	%	%

Appendices C: Tensile Test Results

number of experiment	Trial 1	Trial 2	Trial 3	average
1	177	187	179	181
2	175	179	174	176
3	191	203	196	196.6
4	191.3	195.3	195.4	194.1
5	186.3	191.7	186.8	188.3
6	188.3	193.7	185.8	189.2
7	130.7	154.1	143.3	142
8	131.1	145.8	128.5	135.1
9	109.5	93.5	92.1	98.4

Appendices: D: F-Critical values

	DF1	α = 0.05																	
DF2	1	2	3	4	5	6	7	8	9	10	12	15	20	24	30	40	60	120	Inf
1	161.45	199.5	215.71	224.58	230.16	233.99	236.77	238.88	240.54	241.88	243.91	245.95	248.01	249.05	250.1	251.14	252.2	253.25	254.31
2	18.513	19	19.164	19.247	19.296	19.33	19.353	19.371	19.385	19.396	19.413	19.429	19.446	19.454	19.462	19.471	19.479	19.487	19.496
3	10.128	9.5521	9.2766	9.1172	9.0135	8.9406	8.8867	8.8452	8.8123	8.7855	8.7446	8.7029	8.6602	8.6385	8.6166	8.5944	8.572	8.5494	8.5264
4	7.7086	6.9443	6.5914	6.3882	6.2561	6.1631	6.0942	6.041	5.9988	5.9644	5.9117	5.8578	5.8025	5.7744	5.7459	5.717	5.6877	5.6581	5.6281
5	6.6079	5.7861	5.4095	5.1922	5.0503	4.9503	4.8759	4.8183	4.7725	4.7351	4.6777	4.6188	4.5581	4.5272	4.4957	4.4638	4.4314	4.3985	4.365
6	5.9874	5.1433	4.7571	4.5337	4.3874	4.2839	4.2067	4.1468	4.099	4.06	3.9999	3.9381	3.8742	3.8415	3.8082	3.7743	3.7398	3.7047	3.6689
7	5.5914	4.7374	4.3468	4.1203	3.9715	3.866	3.787	3.7257	3.6767	3.6365	3.5747	3.5107	3.4445	3.4105	3.3758	3.3404	3.3043	3.2674	3.2298
8	5.3177	4.459	4.0662	3.8379	3.6875	3.5806	3.5005	3.4381	3.3881	3.3472	3.2839	3.2184	3.1503	3.1152	3.0794	3.0428	3.0053	2.9669	2.9276
9	5.1174	4.2565	3.8625	3.6331	3.4817	3.3738	3.2927	3.2296	3.1789	3.1373	3.0729	3.0061	2.9365	2.9005	2.8637	2.8259	2.7872	2.7475	2.7067
10	4.9646	4.1028	3.7083	3.478	3.3258	3.2172	3.1355	3.0717	3.0204	2.9782	2.913	2.845	2.774	2.7372	2.6996	2.6609	2.6211	2.5801	2.5379
11	4.8443	3.9823	3.5874	3.3567	3.2039	3.0946	3.0123	2.948	2.8962	2.8536	2.7876	2.7186	2.6464	2.609	2.5705	2.5309	2.4901	2.448	2.4045
12	4.7472	3.8853	3.4903	3.2592	3.1059	2.9961	2.9134	2.8486	2.7964	2.7534	2.6866	2.6169	2.5436	2.5055	2.4663	2.4259	2.3842	2.341	2.2962
13	4.6672	3.8056	3.4105	3.1791	3.0254	2.9153	2.8321	2.7669	2.7144	2.671	2.6037	2.5331	2.4589	2.4202	2.3803	2.3392	2.2966	2.2524	2.2064
14	4.6001	3.7389	3.3439	3.1122	2.9582	2.8477	2.7642	2.6987	2.6458	2.6022	2.5342	2.463	2.3879	2.3487	2.3082	2.2664	2.2229	2.1778	2.1307
15	4.5431	3.6823	3.2874	3.0556	2.9013	2.7905	2.7066	2.6408	2.5876	2.5437	2.4753	2.4034	2.3275	2.2878	2.2468	2.2043	2.1601	2.1141	2.0658
16	4.494	3.6337	3.2389	3.0069	2.8524	2.7413	2.6572	2.5911	2.5377	2.4935	2.4247	2.3522	2.2756	2.2354	2.1938	2.1507	2.1058	2.0589	2.0096
17	4.4513	3.5915	3.1968	2.9647	2.81	2.6987	2.6143	2.548	2.4943	2.4499	2.3807	2.3077	2.2304	2.1898	2.1477	2.104	2.0584	2.0107	1.9604
18	4.4139	3.5546	3.1599	2.9277	2.7729	2.6613	2.5767	2.5102	2.4563	2.4117	2.3421	2.2686	2.1906	2.1497	2.1071	2.0629	2.0166	1.9681	1.9168
19	4.3807	3.5219	3.1274	2.8951	2.7401	2.6283	2.5435	2.4768	2.4227	2.3779	2.308	2.2341	2.1555	2.1141	2.0712	2.0264	1.9795	1.9302	1.878
20	4.3512	3.4928	3.0984	2.8661	2.7109	2.599	2.514	2.4471	2.3928	2.3479	2.2776	2.2033	2.1242	2.0825	2.0391	1.9938	1.9464	1.8963	1.8432
21	4.3248	3.4668	3.0725	2.8401	2.6848	2.5727	2.4876	2.4205	2.366	2.321	2.2504	2.1757	2.096	2.054	2.0102	1.9645	1.9165	1.8657	1.8117
22	4.3009	3.4434	3.0491	2.8167	2.6613	2.5491	2.4638	2.3965	2.3419	2.2967	2.2258	2.1508	2.0707	2.0283	1.9842	1.938	1.8894	1.838	1.7831
23	4.2793	3.4221	3.028	2.7955	2.64	2.5277	2.4422	2.3748	2.3201	2.2747	2.2036	2.1282	2.0476	2.005	1.9605	1.9139	1.8648	1.8128	1.757
24	4.2597	3.4028	3.0088	2.7763	2.6207	2.5082	2.4226	2.3551	2.3002	2.2547	2.1834	2.1077	2.0267	1.9838	1.939	1.892	1.8424	1.7896	1.733
25	4.2417	3.3852	2.9912	2.7587	2.603	2.4904	2.4047	2.3371	2.2821	2.2365	2.1649	2.0889	2.0075	1.9643	1.9192	1.8718	1.8217	1.7684	1.711
26	4.2252	3.369	2.9752	2.7426	2.5868	2.4741	2.3883	2.3205	2.2655	2.2197	2.1479	2.0716	1.9898	1.9464	1.901	1.8533	1.8027	1.7488	1.6906
27	4.21	3.3541	2.9604	2.7278	2.5719	2.4591	2.3732	2.3053	2.2501	2.2043	2.1323	2.0558	1.9736	1.9299	1.8842	1.8361	1.7851	1.7306	1.6717
28	4.196	3.3404	2.9467	2.7141	2.5581	2.4453	2.3593	2.2913	2.236	2.19	2.1179	2.0411	1.9586	1.9147	1.8687	1.8203	1.7689	1.7138	1.6541
29	4.183	3.3277	2.934	2.7014	2.5454	2.4324	2.3463	2.2783	2.2229	2.1768	2.1045	2.0275	1.9446	1.9005	1.8543	1.8055	1.7537	1.6981	1.6376
30	4.1709	3.3158	2.9223	2.6896	2.5336	2.4205	2.3343	2.2662	2.2107	2.1646	2.0921	2.0148	1.9317	1.8874	1.8409	1.7918	1.7396	1.6835	1.6223
40	4.0847	3.2317	2.8387	2.606	2.4495	2.3359	2.249	2.1802	2.124	2.0772	2.0035	1.9245	1.8389	1.7929	1.7444	1.6928	1.6373	1.5766	1.5089
60	4.0012	3.1504	2.7581	2.5252	2.3683	2.2541	2.1665	2.097	2.0401	1.9926	1.9174	1.8364	1.748	1.7001	1.6491	1.5943	1.5343	1.4673	1.3893
120	3.9201	3.0718	2.6802	2.4472	2.2899	2.175	2.0868	2.0164	1.9588	1.9105	1.8337	1.7505	1.6587	1.6084	1.5543	1.4952	1.429	1.3519	1.2539
Inf	3.8415	2.9957	2.6049	2.3719	2.2141	2.0986	2.0096	1.9384	1.8799	1.8307	1.7522	1.6664	1.5705	1.5173	1.4591	1.394	1.318	1.2214	1